ADVANCED ANTENNA SYSTEM

for the

DEEP SPACE INSTRUMENTATION FACILITY

Interim Report

March 10, 1961

Prepared for

JET PROPULSION LABORATORY

CALIFORNIA INSTITUTE OF TECHNOLOGY

Padadena, California

This work was performed for the Jet Propulsion Laboratory, California Institute of Technology, sponsored by the National Aeronautics and Space Administration under Contract NAS7-100.

WESTINGHOUSE ELECTRIC CORPORATION

East Pittsburgh, Pennsylvania

TABLE OF CONTENTS

Table of Contents

A. SUMMARY

A. SUMMARY

This interim report is a summary of the major study areas by Westinghouse in developing an Advanced Antenna System. Since the initial meeting and progress report at Sunnyvale, California in February, effort has been devoted to several areas of immediate primary interest to the structural design study. Among these were the selection of the primary reflector configuration to insure maximum stiffness and the finalization of the dimensions of the Cassegrain optic system. Certain aspects of our thinking on the optic system were influenced by a visit to RCA Victor, Montreal, Canada on March 2, 1961, but the effects of this meeting are not fully expressed in this report due to the timing.

Another major study effort was the development of the antenna position sensing system which incorporates a 4-axis combined Az-El and Equatorial mount on top of the ground reference tower. The hardware details of this system are yet to be worked out, but it shows excellent promise. The systems for monitoring the primary reflector shape and the position of the sub-reflector have also been worked out.

Thru analytical work and computer study, a servo drive system has been evolved which will permit accurate determination of all aspects involved in demonstrating the feasibility of the electro magnetic coupling drive system.

Further study effort will be in the direction of optimizing the drive system and evolving detail specifications for both Azimuth and Elevation systems.

Considerable effort has been expanded in study of various methods and arrangements of position sensing and coordinate conversion equipment which will be consistent with the requirements of a digital control system. A tentative functional layout has also been made of equipment required for signal processing and instrumentation.

Most of the major design concepts have been decided upon and the remainder of the study program will be devoted to detailed analysis and optimization of the various system components. Certain aspects of the system will require further study during Phase II and this will be developed in subsequent reports.

B. MICROWAVE OPTIC SYSTEM

I. INTRODUCTION

At the time of writing of this report approximately eight weeks of the total allocated time for Phase I have passed. At this, the mid-point of the study program, it is necessary to evaluate the progress to date and anticipate the scope of work which can be completed in the remaining time period. Primarily the effort to date has been devoted to considering sizes, locations, and tolerances of the major components of the microwave optics system. In attempting to establish a knowledgeable position from which to make a detailed, substantiated recommendation it is evident that much analytical work, particularly on second order effects, will remain to be completed during Phase II; and a well conceived model measurement program will be required to verify any postulated design. In fact, a continuing program in the Cassegrain optics field will yield several successive steps of worthwhile major modifications to the original system.

Time and scope of this report will not permit reproduction of all the efforts performed. We have attempted to discuss those areas believed to be particularly pertinent to an evaluation of our progress to this stage.

II. FEED SYSTEM PARAMETERS (D = 240'; F/D = .25)

The choice of the feed system parameters requires compromising a multitude of factors in order to meet the demands placed upon the feed system by the specification. The major factors to be considered are gain, sidelobe levels, structure, alignment accuracy, and operating convenience. The alignment accuracy requires a maximum rigidity in the feed support and the Cassegrain mirror support. The requirement for operating convenience can be translated into one, that the feed and receiver be readily accessible for maintainance and adjustment. The figure of merit specification requires that the receiver be located as close to the feed as possible. The requirement for changing feeds in half an hour dicates that the feed be accessible, have equipment for handling, and a convenient and accessible storage location. In addition, switching from transmit to receive in two minutes for other modes of operation than the super sensitive listening mode will require manual access to the feed to make the necessary adjustments. As a result of these considerations we feel that the feed should be located no more than 15 feet from the vertex of the main reflector and should be located in a broad support tower. Microwave optics requires that the feed approach the focus of the main reflector and gives sufficient reason for the use of a short feed tower. A longer feed tower will compromise the receiver and source system accessibility and make difficult adjustments, maintenance, and fast changes. In addition, we suspect that a longer feed tower may produce mechanical design problems.

The gain and sidelobe specifications place contradictory requirements upon the illumination pattern of the feed system. To produce high gain a nearly uniform illumination is required upon the aperture of the main reflector. The illumination must be low and smoothly tapered at the edge of the aperture to reduce the sidelobes which are caused by a rapid change in the illumination across the aperture and by diffraction from the illuminated edge of the main reflector. The uniform illumination of the main reflector aperture requires a nearly uniform illumination on the Cassegrain mirror with a consequent high edge illumination upon the mirror. The high edge illumination of the mirror produces large spillover sidelobes and large diffraction sidelobes. Increasing the size of the mirror will reduce the level of the spillover sidelobes and the diffraction lobes. A larger mirror also allows improved control of the illumination of the main reflector (i.e. higher efficiency, higher gain). As a result, we have chosen the largest possible Cassegrain mirror. The size is limited only by the combined sidelobe levels due to illumination taper and the blocking of the aperture by the mirror.

Section II.A gives a detailed consideration of the gain reduction which results from a parabolic illumination with various edge illumination levels and from the blocking of the aperture by the Cassegrain mirror. A parabolic illumination of the aperture with an 18 db edge illumination and a 24 foot diameter reflector including the blocking of the mirror produces an efficiency of -1.8 db. The sidelobe levels due to illumination taper, aperture blocking by the Cassegrain mirror, and spillover around the

Cassegrain mirror are considered in Section II.B. The sidelobes due to diffraction from the edge of the main reflector will be minimized by making the angle subtended by the Cassegrain mirror at the focal point of the main reflector less than the angle subtended by the main reflector. The edge diffraction sidelobes from the Cassegrain mirror have not been considered.

A square horn with a 5λ aperture and a 20° flare angle has been selected as a preliminary feed design. Such a feed has the desirable low noise properties. Detailed study of the source system may indicate modifications to this initial concept which will act to improve performance.

A feed system has been selected using a 24 foot Cassegrain mirror and a feed horn whose 5λ aperture is 15 feet from the vertex of the main reflector. This design will meet the 52 db sidelobe specification for sidelobes due to illumination taper, aperture blocking by the Cassegrain mirror, and spillover around the Cassegrain mirror. As discussed in Section IV.A, it is not expected that the sidelobes produced by the Cassegrain mirror support structure will meet the 52 db specification. Edge diffraction lobes or sidelobes to surface tolerances have not been considered.

The gain of the antenna is considered in detail in Section II.A, and is found to be 60.4 db. This is not a final gain calculation. The detailed feed design should increase the gain while consideration of additional degrading factors may decrease it.

A. GAIN CONSIDERATIONS

The expected gain of the antenna has been determined from the consideration of several factors which degrade the gain and one which improves it slightly. The gain of a uniformly illuminated parabolic antenna that is 240 feet in diameter is 64.9 db.

First consider the efficiency as influenced by the illumination taper and the aperture blocking by the Cassegrain mirror. Assume that the illumination is parabolic and that the relative power of the illumination at the edge of the aperture is k^2. The formula for the illumination, $f(r)$, as a function of the normalized distance from the axis, r, is the following:

$$f(r) = 1 - (1-k)r^2$$

The formula for the efficiency, , is the following:

$$\eta = \frac{\left|\int_\alpha' 2r f(r)dr\right|^2}{\int_\alpha' 2r|f(r)|^2 dr} = \frac{\left|\int_\alpha' 2r[1-(1-k)r^2]dr\right|^2}{\int_\alpha' 2r[1-(1-k)r^2]dr}$$

where is the normalized radius of the Cassegrain mirror. The formula for the efficiency η after the integration is performed is as follows:

$$\eta = \frac{\left[\frac{1+k}{2} - \alpha^2 + \frac{1}{2}(1-k)\alpha^4\right]^2}{\left[k + \frac{1}{3}(1-k) - \alpha^2 + (1-k)\alpha^4 - \frac{1}{3}(1-k)^2\alpha^6\right]}$$

The 14 db edge illumination of the mirror gives k = .2 and the 24 foot diameter of the mirror gives α = .1, so that the efficiency is .866 or -.63 db. The extra edge tapering from the small aperture angle of the mirror reduces this efficiency to .83 or -.82 db.

The next factor to be determined is normally called space attenuation and is the decrease in the illumination at the edge of the reflector with respect to the center due to the greater distance of the edge from the focal point. This factor will be termed space gain here to maintain a consistent terminology and because for the present design the factor increases the edge illumination. The space gain, G_s, is given by the following formula:

$$G_s = \left[\frac{(f+a)^2}{(2f-x_1)^2 + y_1^2}\right]\left[\frac{F}{f-a}\right]^2\left[\frac{x_1^2 + y_1^2}{x_2^2 + y_2^2}\right]$$

where

F = focal length of the main reflector,

$2f$ = focal length of the Cassegrain mirror,

a = a constant in the equation of the Cassegrain mirror such that

d = the diameter of the Cassegrain mirror,

D = the diameter of the main reflector,

(x_1, y_1) = the point where a ray intercepts the Cassegrain mirror,

and (x_2, y_2) = the point where the same ray intercepts the main reflector.

The equations for (x_1, y_1) and (x_2, y_2) are the following:

$$\left(\frac{X_1 - f}{a}\right)^2 - \frac{2}{ad} Y_1^2 = 1$$

and

$$X_2 = F - \frac{Y_2^2}{4F}$$

The following figure shows the space gain, the illumination from the feed system, and the illumination as modified by the space gain.

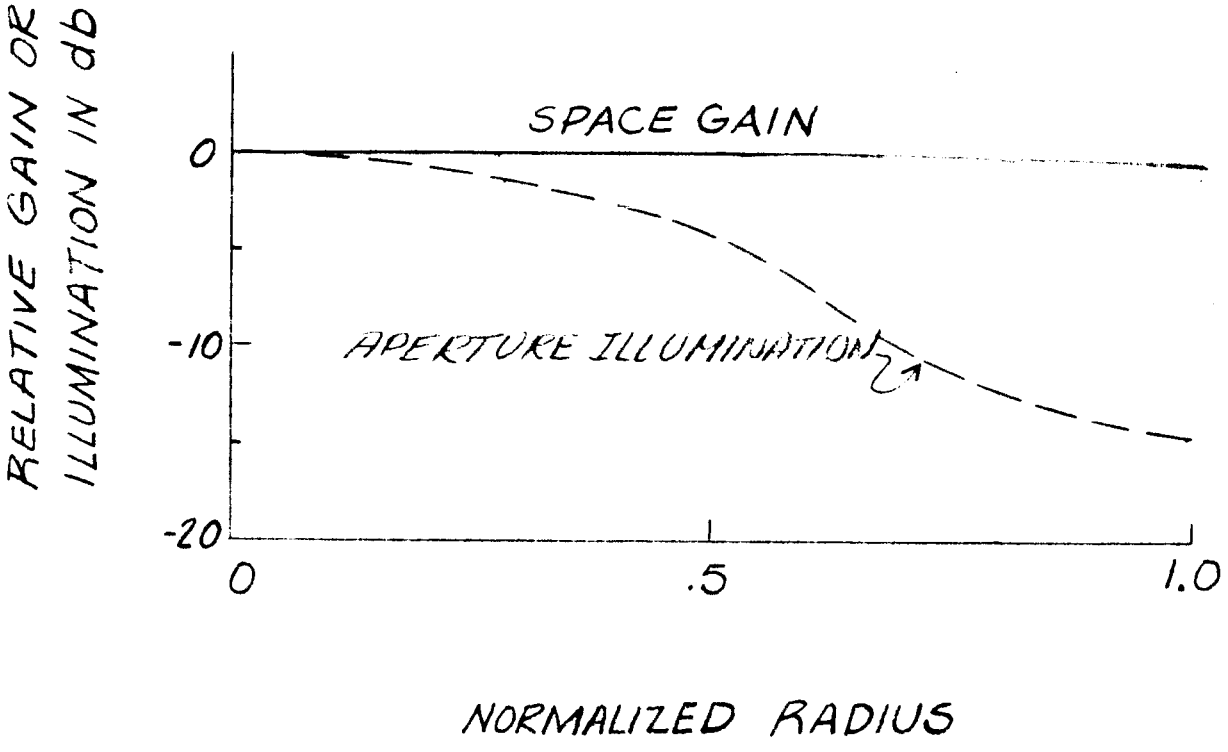

The resultant illumination closely approximates the parabolic illumination used to calculate the illumination efficiency. The large increase in slope at the edge is due to making the subtended angle of the main reflector slightly more than the subtended angle of the Cassegrain mirror at the focal point of the main reflector. This reduces the back lobe and the sidelobes.

Consider the following formula for G_s evaluated at the edge of the main reflector:

$$G_s = \frac{(F-f+a)^2}{F^2+(d/2)^2}\left(\frac{F}{f-a}\right)^2\left(\frac{d}{D}\right)^2$$

It is quite apparent from this formula that a larger Cassegrain mirror boosts the illumination near the edge of the reflector, and will allow a more nearly uniform illumination to be produced by feedhorns of conventional design. This naturally will improve the aperture efficiency.

The following table presents the gain factors considered here.

Gain Factors

64.9 db	Uniformly illuminated aperture gain
- 1.80 db	Efficiency due to illumination taper, blocking by Cassegrain mirror, and space gain.
- 1.62 db	RMS surface error
- .2 db	Cassegrain mirror defocusing
- .05 db	Horn defocusing
- .3 db	Departure of average shape of main reflector from the ideal parabolic shape.

- .5 db	Aperture blocking by Cassegrain mirror support structure
60.4 db	Resultant gain
60.9 db ± 1	Specified gain

The RCA loss for a .25 inch RMS surface error has been accepted at face value pending a detailed study of the surface tolerance problem. It is hoped that the gain loss from the aperture blocking by the Cassegrain mirror support will be somewhat less than the .5 db indicated.

These computations show a slightly better performance than that specified. This performance cannot be guaranteed since a more precise and exhaustive study of the factors degrading performance is necessary.

B. PRELIMINARY SIDELOBE CONSIDERATIONS

The design of any antenna system involves in the final analysis the compromise of a multitude of interrelated parameters. A number of factors influence basic antenna properties of gain and sidelobe levels. A multitude of cause-effect relationships act as contributing elements to the general sidelobe levels and cannot generally be treated independently. Although more detailed work will follow, thus far the major factors considered include aperture illumination of the antenna, aperture blocking by the Cassegrain reflector, spillover of the primary feed, and main reflector tolerances.

For purposes of the initial design it has been assumed that the antenna radiation pattern can be obtained by considering the illumination

in the aperture of the antenna. The radiating aperture, with the coordinate system used, is as shown in the following figure:

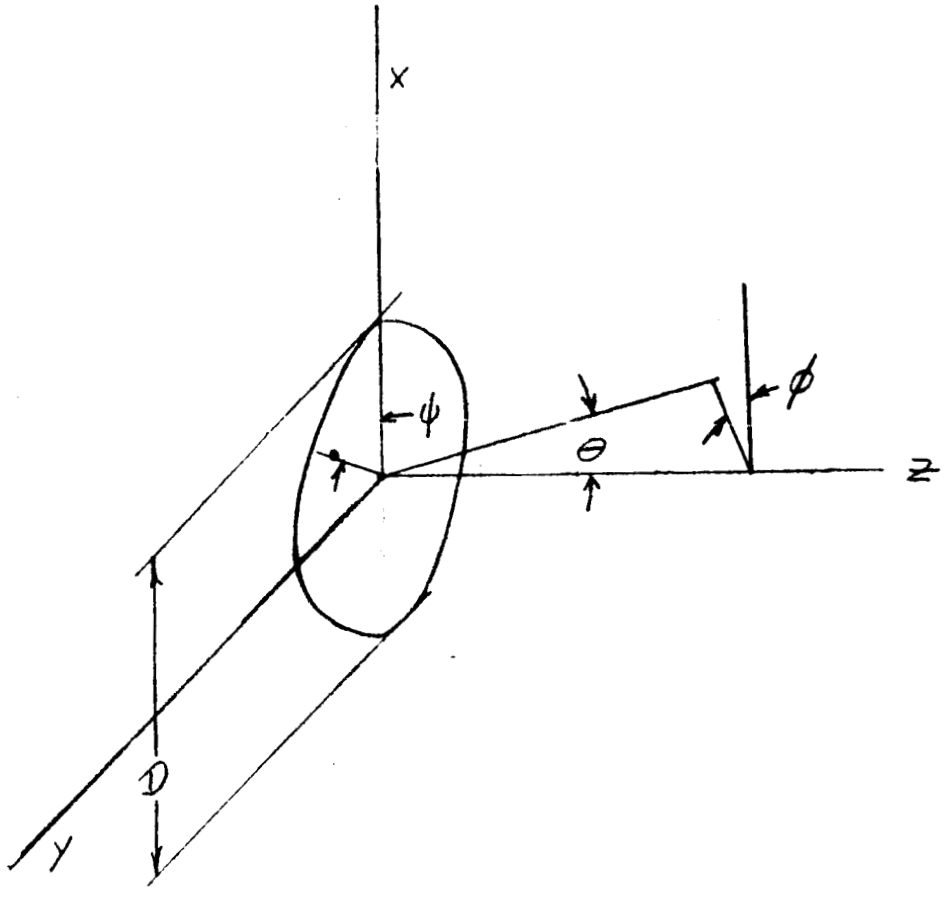

Although an exact expression for the illumination of the antenna aperture would result in a more accurate prediction of the sidelobes, it is not required at this stage of the analysis. It is possible to obtain a reasonable estimate of the primary feed size, location and subreflector configuration required for this application by considering a fairly simple distribution. It has, therefore, been assumed that the illumination can be represented by :

$$f(r) = 1 - (1-k)r^2$$

where

$$r = \rho / D$$

k = edge illumination with respect to that at the center.

This distribution does not take advantage of the possibilities of controlling the slope of the illumination at the edge of the main reflector by reducing the angle subtended by the submirror with respect to the main reflector. It will, however, give a reasonable estimate of the sidelobe level until it is possible to perform more exact calculations using measured primary illumination patterns and numerical integrations. This distribution also assumes that the illumination is in-phase over the aperture and independent of the angle ψ. Phase errors and asymmetries, in ψ, are then treated separately.

Using this type of distribution it is possible to express the antenna pattern with the approximate expression,

$$g(u) = 2\pi a^2 \int_0^1 f(r)\, J_0(ur)\, r\, dr$$

where

$$u = \frac{\pi D}{\lambda} \sin\theta$$

$J_0(ur)$ = Bessel function of first kind of order zero.

Substituting for $f(r)$, integrating the resulting expression and making use of the relation

$$\frac{J_\rho(u)}{u} = \frac{\Lambda_\rho(u)}{2^\rho \rho!}$$

yields

$$g(u) = 2\pi a^2 \left[K \Lambda_1(u) + \frac{1-K}{2} \Lambda_2(u) \right]$$

At this point it is convenient to normalize the pattern to unity at $\psi = 0$ and obtain the power pattern. This gives

$$G(u) = \left[\frac{g(u)}{g(0)} \right]^2 = \left[\frac{2K\Lambda_1(u) + (1-K)\Lambda_2(u)}{1+K} \right]^2$$

a good approximation for the values of $\Lambda_\rho(u)$, for arguments greater than 10, is

$$\Lambda_\rho(u) = \frac{\rho!}{\sqrt{\pi}} \left(\frac{2}{u} \right)^{\rho+0.5} \cos\left[u - (\rho+.5)\pi/2 \right]$$

Substitution of this expression in the normalized power pattern gives

$$G(u) = \frac{4}{\pi} \left(\frac{2}{u} \right)^3 \left[\frac{K \cos\left(u - \frac{3\pi}{4}\right) + \frac{2}{u}(1-K) \sin\left(u - \frac{3\pi}{4}\right)}{1+K} \right]^2$$

At this point the value of individual sidelobes is not of particular interest. What is desired is that the envelope of the sidelobes should remain below a specified value beyond two degrees. The envelope of this pattern is given by

$$G(u)_e = \frac{1}{\pi}\left(\frac{2}{u}\right)^3\left(\frac{2k}{1+k}\right)^2 + \frac{1}{\pi}\left(\frac{2}{u}\right)^5\left(\frac{2(1-k)}{1+k}\right)^2$$

The design being considered at this time is the 240 ft. reflector so that the minimum value of u becomes,

$$u = 61.4 \qquad D = 240'$$
$$\theta = 2^\circ$$

For this case the sidelobe value becomes

$$SL = 1.1\times10^{-5}\left(\frac{2k}{1+k}\right)^2 + 1.16\times10^{-8}\left(\frac{2(1-k)}{1+k}\right)^2$$

This expression represents the sidelobe energy due to the main reflector illumination at two degrees. The envelope of the sidelobes continues to drop at greater angles. Values of the sidelobes for various illuminations are as follows:

k	Edge Illumination in db	in db
1	0	49.6
.316	10	54.2
.1	20	64.4
.0316	30	70.9

To consider the contribution of the blocking caused by the Cassegrain reflector:

$$GAIN = a^2\int_0^{2\pi}\int_0^{1} f(r,\phi')\, e^{jur\cos(\phi-\phi')}\, r\,dr\,d\phi'$$

$$f_{MAX} = 1 \quad \text{and } f'(r,\phi') = 0, \text{ then}$$

$$GAIN = \left[2\pi a^2\int_0^{1} r f(r) J_0(ur)\,dr\right]^2.$$

This is a relative gain.
When the blocking is included,

$$GAIN = \left[2\pi a^2 \left\{ \int_0^{\cdot} r(1-(1-K)r^2) J_0(ur)\,dr - \int_0^{\infty} r J_0(ur)\,dr \right\} \right]^2$$

When $v=0$

$$G_0 = \left[\pi a^2 \left\{ 1 - \frac{1}{2}(1-K) - \alpha^2 \right\} \right]^2$$

$$= \left[\pi a^2 \left\{ \frac{1+K}{2} - \alpha^2 \right\} \right]^2$$

$$\frac{Gain}{G_0} = \left[\frac{2K\,\Lambda_1(U) + (1-K)\,\Lambda_2(U) - 2\alpha^2 \Lambda_1(u\alpha)}{1+K-2\alpha^2} \right]^2$$

Assume that the first two terms of the numerator are negligible, then:

$$GAIN \approx \left(\frac{2\alpha^2 \Lambda_1(U\alpha)}{1+K-2\alpha^2} \right)^2$$

Since we chose a 29' CASSEGRAIN REFLECTOR:

$$\alpha = .1 \qquad \frac{GAIN}{G_0} \approx \left(\frac{.02\,(-.0804)}{.98+K} \right)^2$$

k	Gain/G_o^{-1} in db
1	61.8
.316	58.1
.1	56.6
.0316	55.9
0	55.7

Summing the sidelobe levels which result as a consequence of aperture illumination and the blocking of the aperture by a 24' sub-reflector gives the following relationship to edge illumination of the aperture:

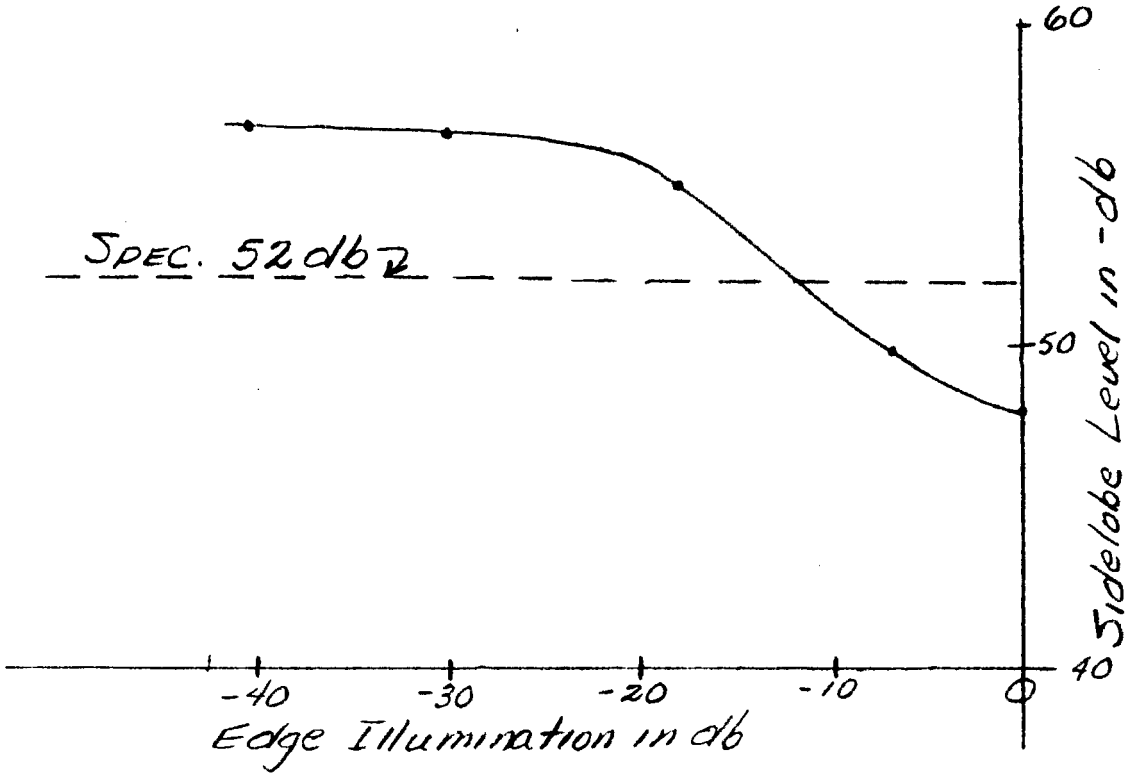

The spillover sidelobe levels for a given feed location and Cassegrain mirror size depend upon the design of the feed. The following computations will show that a square horn with a 5λ aperture and 20° flare angle will produce adequate sidelobe levels when placed 15 feet from the vertex of the main reflector and used with a 24 foot Cassegrain mirror.

The gain, G_A, of the antenna with parabolic illumination is given by the following formula:

$$G_A = .75 \frac{4\pi}{\lambda^2} \left(\frac{\pi D}{4} \right)^2$$

where .75 is the efficiency of parabolic illumination. The gain, G_H, of a horn with the aperture, A, is given by the following formula:

$$G_H = .81\left(\frac{4\pi}{\lambda^2}\right) A^2$$

where 0.81 is the efficiency of a horn in the TE_{10} or TE_{01} modes. Representing the edge illumination by the symbol, G_E, the sidelobe level, SL, is given by the following formula:

$$SL = G_E\left(\frac{G_A}{G_H}\right) = G_E\left(\frac{\eta_A}{\eta_H}\right)\left(\frac{\pi D^2}{4A^2}\right)$$

The angle subtended by the Cassegrain mirror is 30°. From figure 10.10 b, Page 359 of "Microwave Antenna Theory and Design" by S. Silver it is estimated that the edge illumination will be 14 db. Figure 10.12 b on Page 361 shows that the illumination in the other plane will be 15 db. These experimental patterns are for sectoral horns; however, it is felt that for a preliminary design these values represent the results which could be obtained for circularly polarized horns. As a result, the formula for SL shows that the sidelobe level is 53.6 db which meets the 52 db specification for sidelobe levels beyond 2° with a little to spare for neglected factors. It is expected that a more sophisticated feed design will easily surpass this performance while providing the optimum illumination for the main reflector.

The illumination of the aperture which results from this feed design has not been determined.

III. CASSEGRAIN REFLECTOR POSITION TOLERANCE

The effects of the position errors of the subreflector on the performance of the antenna have been determined by the application of the aperture field method of computing antenna patterns. This technique uses ray tracing to determine the amplitude and phase of the electromagnetic field on a plane surface in front of the antenna. An integration of the field over this surface determines the gain pattern of the antenna. The scalar approximation of this integral is sufficiently accurate to determine the effects of the position errors of the subreflector.

Appendix I shows the derivation of the formula for the change in path length resulting when the subreflector is displaced perpendicular to the axis of the main reflector. The derivations are not included for displacement parallel to the axis of the main reflector and for rotation about an axis through the vertex of the subreflector perpendicular to the axis of the main reflector since they are very similar to the derivation in Appendix I.

The following symbols will be used in the formulas for the change in path length of the rays from the feed to the aperture:

S_R = displacement of the subreflector perpendicular to the axis of the main reflector

S_x = displacement of the subreflector parallel to the axis of the main reflector

θ = rotation in radians of the subreflector about an axis through its vertex and perpendicular to the axis of the main reflector.

S = the change in the path length due to the rotation and both displacements

d = diameter of the subreflector

D = diameter of the main reflector

f = half the focal length of the subreflector

F = focal length of the main reflector

The formula for the shape of the main reflector is:

$$X = F - \frac{R^2}{4F}$$

and the formula for the shape of the subreflector is

$$\left(\frac{X + f}{a}\right)^2 - \frac{2}{ad} R^2 = 1$$

where:

X = the distance along the axis of the main reflector from the focus

R = the distance from the axis of the main reflector

R_1 = the R at which a ray intercepts the subreflector

a = a constant given by the formula

$$f^2 = a^2 + ad/2$$

The formula for the error in path length is :

$$S = -\frac{a^2 d R_1 [S_R - (f-a)\theta] \cos\phi}{f^2 R_1^2 + (ad/2)^2} +$$

$$\frac{2af R_1 \theta \sin(\phi + \phi_1)}{a^2 + f\sqrt{a^2 + (2a/d) R_1^2}} -$$

$$2\frac{f^2 - a^2}{f^2(f - X_1)^2 - a^4} a (f - X_1) S_X$$

where:

ϕ is the angle about the main reflector axis measured from the direction of the displacement S_R and ϕ_1 is the axis of rotation of the subreflector.

The shape of the illumination on the reflector is unknown and may change during the life of the antenna; however, any tapered illumination will emphasize the central region of the error curve and thus will act as if the whole reflector had the error extrapolated from the center. As a result the formula for the error in path length simplifies to:

$$S = -\frac{4R_1\cos\phi[S_R - (f-a)\theta]}{a} + \frac{2fR_1\sin(\phi+\phi_1)}{f+a}\theta - \frac{2(f-X_1)}{a}S_X$$

Comparison of the two formulas has shown that a uniform illumination will have less boresight error and less defocusing than is given by the approximate formula, so the approximate formula gives a reasonable upper bound to the effects of the errors.

Examination of the path length error formula shows that the pointing error is produced by S_R and θ, while the defocusing error is produced by S_X.

Denote the pointing error by ψ. The formula for the pointing error is:

$$\psi = .200|\theta| + .0167|S_R|$$

where:

$|S|_{MAX}$ = the maximum value of S and it is assumed that the position where a ray intercepts the aperture is directly proportion to the radius where the ray intercepts the subreflector.

The value $|S|_{MAX}$ of S occurs when R = d/2, $\phi = 0, \phi_1 = \pi/2$, and S_R and θ have the proper relationship of signs. As a result of substituting for $|S|_{MAX}$,

$$\psi = \frac{2d}{D}\left[\left(\frac{f}{f+d} + \frac{2(f-d)}{d}\right)|\theta| + \frac{2}{d}|S_R|\right]$$

With the chosen parameters, d = 24 feet and 2f = 45 feet,

$$\psi = .200|\theta| + .0167|S_R|$$

where S_R is measured in feet.

The subreflector has been allowed 1/4 of the total pointing error of $\pm .02^\circ$, namely $\pm .005^\circ$. With θ and ψ expressed in degrees the allowed displacement and rotation is given by :

$$\psi = .200|\theta| + .955|S_R| \leq .005$$

If S_R is expressed in inches,

$$|S_R| + 2.52|\theta| \leq .063$$

The mechanical designers can use this equation to balance the position tolerances.

The gain loss of an antenna due to a circularly symmetric path length error, $S(R)$, is given by the formula

$$\frac{G}{G_0} = \left| \frac{\int_A f(R) \exp. jk\, s(R)\, dA}{\int_A f(R)\, dA} \right|^2$$

where:

G = distorted gain, G_0 = undistorted gain, $f(R)$ = illumination,

A = area of reflector, and k = propagation constant.

From the formula for S it is found that :

$$S(R) = -\frac{2(f-X_1)S_x}{a} = -\frac{2\left(f-a-d\left(\frac{R}{D}\right)^2\right)}{a}$$

The constant part of $S(R)$ drops out in the loss formula leaving the expression :

$$\frac{G}{G_0} = \left| \frac{\int_A f(R)\, \exp.j\left(2\frac{d}{a}\left(\frac{R}{D}\right)^2 k S_x\right) dA}{\int_A f(R)\, dA} \right|^2$$

This formula was evaluated for $f(R)=1$ with the result :

$$\frac{G}{G_0} = 1 - \frac{1}{48}\left(\frac{k\,d\,S_x}{d}\right)^2$$

The formula was also evaluated for $f(R) = 1-\left(\frac{2R}{D}\right)^2$

with the result

$$\frac{G}{G_0} = 1 - \frac{1}{72}\left(\frac{k\,d\,S_x}{d}\right)^2$$

The result for the uniform aperture illumination $f(R)=1$ will be used since it shows the greatest loss in gain. It is realized that this result will be somewhat pessimistic since the illumination is high in a region where the approximate path length formula over estimates the path length change.

A loss of .2 db from this factor appears to be reasonable from the work done by RCA. Consequently, the allowed displacement along the axis of the main reflector is .44 inches.

The introduction of more realistic patterns and numerical integration should relax this tolerance.

IV. CASSEGRAIN REFLECTOR SUPPORT STRUCTURE

A. Gain and Sidelobes

Considerable attention has been given to the reduction in gain and the creation of sidelobes resulting from the blocking of the r.f. field by the Cassegrain mirror support structure. The initial consideration of this problem was based on the use of geometrical optics to determine the aperture blocking and the aperture field method for computing the secondary pattern. Due to the complexity of determining the actual diffraction pattern of a truss type structure it was assumed that the full circumferential width of a support leg provided geometrical optics blocking of the r.f. field.

A quadripod mirror support was evaluated to determine the blocking effects. The following figure illustrates the shadow produced by the mirror support upon the aperture.

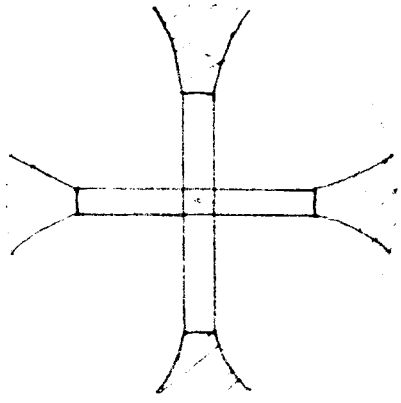

The rectangular areas represent the shadow on the aperture by rays intercepted between the main reflector and aperture. The shade areas represent the shadow cast on the aperture by rays intercepted between the Cassegrain mirror and the main reflector. The smallest possible

shadow consists of two strips the width of a support leg extending all the way across the aperture. Any quadripod support whose legs do not end on the rim of the reflector will cast a larger shadow. This demonstrates that for a given width leg, the base and the point at which the leg penetrates the aperture must be as far from the axis of the antenna as possible to minimize the area of the shadow cast upon the aperture.

The following sketch illustrates the symbols used in determing the area of the shadow cast on the aperture by a leg of the quadripod mirror support:

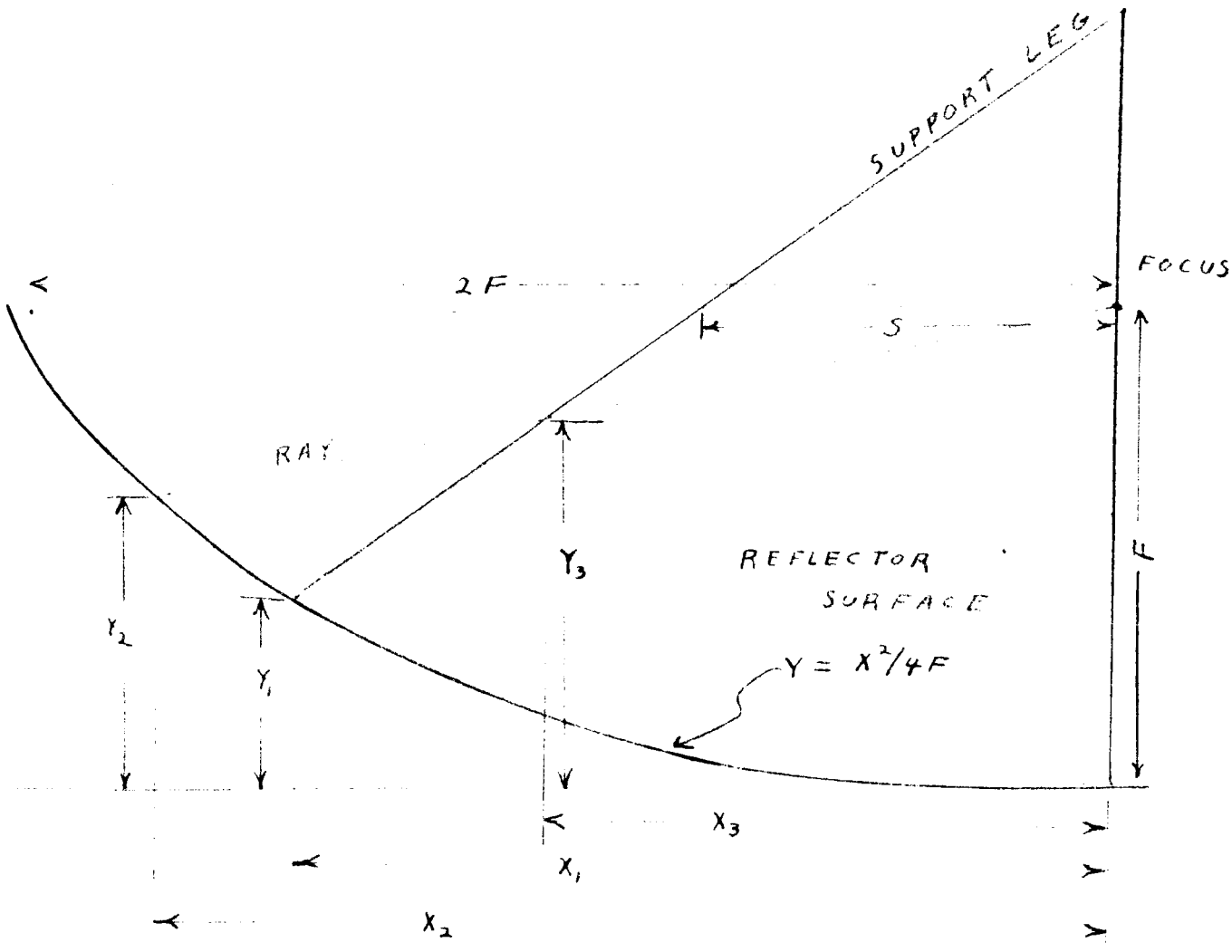

The width of the shadow projected upon the aperture, W_p, is given by the following formula:

$$W_p = W\left[\frac{X_2}{S} - \left(\frac{X_1 - S}{S}\right)\left(\frac{F - Y_2}{F - Y_1}\right)\right]$$

where W = circumferential width of the support leg.

The area, A, of the shadow cast by the support leg upon the aperture is given by the following integral:

$$A = \int_{X_1}^{2F} W_p \, dX_2 + W X_1$$

This integration can be performed to give the following result:

$$A = WF\left[\left(\frac{F}{S}\right)\left(2 - \frac{1}{2}\left(\frac{X_1}{F}\right)^2\right) + \left(\frac{X_1 - F}{S}\right)\left(\frac{F}{F - Y_1}\right)\left(\frac{X_1}{F} - 4/3 - \frac{1}{12}\left(\frac{X_1}{F}\right)^3\right) + \frac{X_1}{F}\right].$$

This result is useful for uniform illumination but gives a pessimistic result when a tapered illumination is used. The effective area, A_E, of the shadow weights the shadow area at each point by the illumination as shown in the following integration:

$$A_E = \int_0^{2F} W_p\left[f\left(\frac{X_2}{2F}\right)\right] dX_2$$

where $f\left(\frac{X_2}{2F}\right)$ = the illumination of the aperture and it is assumed that $W_p = W$ when $X_2 < X_1$. To establish a familiarity with this effect it will be assumed that the aperture illumination is partially parabolic, that is:

$$f\left(\frac{X_2}{2F}\right) = 1 - (1 - k)\left(\frac{X_2}{2F}\right)^2$$

where k^2 is the edge illumination (power).

The use of this illumination in the integral for A_E gives the following result:

$$A_E = WF\left[\left(\frac{F}{5}\right)\left(2 - \tfrac{1}{2}\left(\frac{X_1}{F}\right)^2\right) + \left(\frac{X_1 - 5}{5}\right)\left(\frac{F}{F - Y_1}\right)\left(\frac{X_1}{F} - \tfrac{4}{3} - \tfrac{1}{12}\left(\frac{X_1}{F}\right)^3\right) + \frac{X_1}{F}\right] + (k-1)WF\left[\frac{F}{5}\left(\frac{X_1^4}{16F^4} - 1\right) + \frac{X_1 - 5}{5}\left(\frac{F}{F - Y_1}\right)\left(\frac{4}{15} - \tfrac{1}{12}\left(\frac{X_1}{F}\right)^3 + \frac{X_1^5}{80F^5}\right) - \frac{X_1^3}{12F^3}\right]$$

The use of these formulas requires some information concerning the width of the Cassegrain mirror support legs. The width of the support leg will depend upon its length. Some simple mechanical considerations of simple loadings of the support structure shows that the following function for the width should be useful:

$$W = \alpha L^{2n} = \alpha\left[X_1^2 + \left(\frac{5}{X_1 - 5}\right)^2 (F - Y_1)^2\right]^n$$

where α and n are constants and L is the length of the leg. The constant n has the value 1 if the leg is limited by vibration, $\frac{3}{4}$ if the leg is limited by transverse vibration, and $\frac{1}{4}$ if the leg is limited by buckling. Some mechanical analysis performed by the microwave section indicates that the leg would be limited by vibration in the circumferential direction.

The effective area was evaluated for complete parabolic illumination (k = 1) and for uniform illumination (k = 0) for a leg whose width was limited by vibration. The figure on the follow on the following page shows the effective area as a function of the position, X_1, of the base of the leg and the position, S, at which the leg penetrates the aperture.

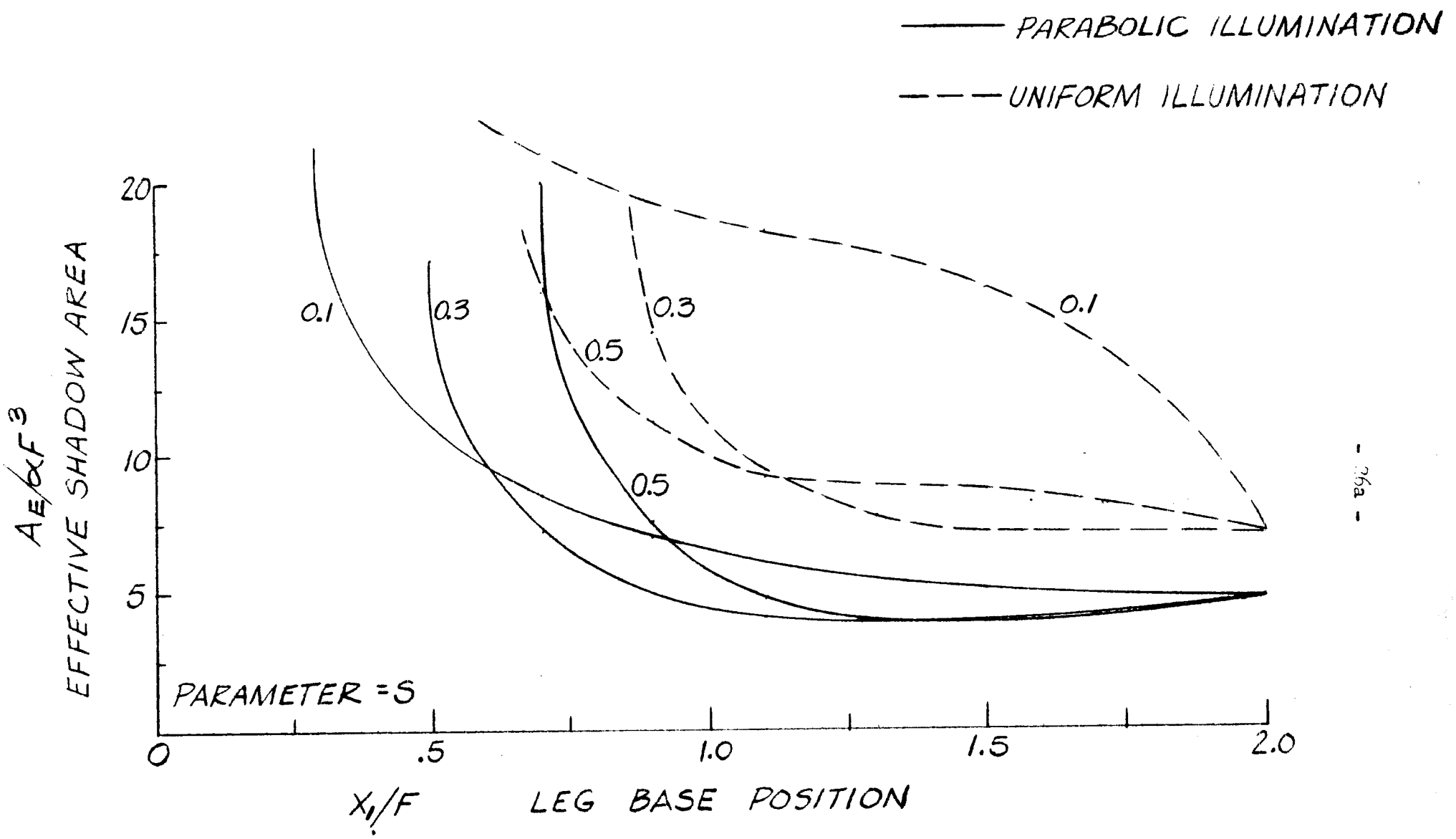
PARABOLIC ILLUMINATION
UNIFORM ILLUMINATION
$A_E/\alpha F^3$
EFFECTIVE SHADOW AREA
20
15
10
5
0
.5
1.0
1.5
2.0
0.1
0.3
0.5
0.3
0.1
0.5
PARAMETER = S
X_1/F LEG BASE POSITION

The figure indicates that with parabolic illumination the base of the support leg should be located from 1.2F to 1.6F from the axis of the main reflector while the aperture intercept point should be .3F to .5F from the axis. These distances translate to a range of 72 feet to 96 feet and one of 18 feet to 30 feet for an antenna with a diameter of 240 feet and an F/D ratio of .25. The effective shadow area will be 70% to 100% of the minimum shadow area for a leg with the given width. It should be noted that for uniform illumination, or other types of limitation on the width of the support legs, the legs should be located even further from the axis of the main reflector.

The next consideration is to determine the loss in gain and the sidelobe levels produced by a given shadow. The gain, G , of the antenna is given by the following formula:

$$G = \frac{4\pi}{\lambda^2} \frac{\left| \int_{A_A} F_3(r, \phi') \exp\{ j u r \cos(\phi - \phi') \} dA \right|^2}{\int_{A_A} |F_3(r, \phi')|^2 dA}$$

where

λ = wavelength

$u = \frac{\pi D}{\lambda} \sin\theta$

D = diameter of reflector

ϕ' = angular position of the element of area

r = normalized radius of the element

$F_3(r, \phi')$ = the shadowed illumination of the aperture, θ and ϕ are the normal spherical polar coordinates when the Z axis points along the axis of the antenna beam.

A_A designates the area of the aperture.

This formula can be rewritten in the following form which makes the shadow effects explicit:

$$G = \frac{4\pi}{\lambda^2} \frac{\left| \int_{AA} F(r,\phi') \exp\left[j\frac{2\pi}{\lambda} r \cos(\phi - \phi') \right] dA - \int_{AS} F(r,\phi') \exp\left[j\frac{2\pi}{\lambda} r \cos(\phi - \phi') \right] dA \right|^2}{\int_{AA} |F(r,\phi)|^2 dA - \int_{AS} |F(r,\phi)|^2 dA}$$

where $F(r,\phi')$ = the unshadowed pattern and AS designates the area of the shadow.

First consider the gain, G_M, of the beam on the axis which is given by the following formula:

$$G_M = \frac{4\pi}{\lambda^2} \frac{\left| \int_{AA} F(r,\phi') dA - \int_{AS} F(r,\phi') dA \right|^2}{\int_{AA} |F(r,\phi)|^2 dA - \int_{AS} |F(r,\phi)|^2 dA}$$

For uniform illumination the equation reduces to the following:

$$G_M = \frac{4\pi A_A}{\lambda^2} \left(1 - \frac{A_S}{A_A} \right).$$

This is the usual simple formula for the gain of a blocked aperture. For the generalized parabolic illumination the formula for the gain is as follows:

$$G_M = \frac{4\pi}{\lambda^2} \frac{\left| \left(\frac{1+h}{2} \right) A_A - 4 A_E \right|^2}{A_A \left[\pi + \tfrac{1}{3}(1-h)^2 \right] - 4 A_{E1}}$$

where A_E is the effective area of the shadow of a leg and $A_{E'}$ is a similar effective area defined by the formula:

$$A_{E'} = \int_{A_S} |F(r,\phi')|^2 \, dA$$

This effective area has not been computed or evaluated, but it is obvious that $A_{E'} \leq A_E \leq A_S$. A good pessimistic approximation to G_M for complete parabolic illumination (k = 1) is the following:

$$G_M = 3/4 \left(\frac{4\pi A_A}{\lambda^2}\right) \frac{\left(1 - 8\frac{A_E}{A_A}\right)^2}{\left(1 - 12\frac{EW}{A_A}\right)}$$

If a 240 foot diameter antenna has parabolic illumination then a leg which results in .2 db loss in gain can be only 2.2 feet wide. For uniform illumination the leg must be even narrower.

The relative sidelobe level will be represented by g and is given by the following formula:

$$g = \left| \frac{\int_{A_A} F(r,\phi') \exp j u r \cos(\phi - \phi') \, dA - \int_{A_S} F(r,\phi') \exp j u r \cos(\phi - \phi') \, dA}{\int_{A_A} F(r,\phi') \, dA \; - \; \int_{A_S} F(r,\phi') \, dA} \right|^2$$

The blocking sidelobes will be much larger than the far out sidelobes of the unblocked aperture, so g can be rewritten as follows for the generalized parabolic illumination:

$$g = \left| \frac{\int_{A_S} F(r,\phi') \exp j u r \cos(\phi - \phi') \, dA}{\frac{1+k}{2} A_A - A_E} \right|^2$$

The sidelobe will have the shape of a plus. The length of the arms of the plus will be many times the width of the main beam and their width will be approximately that of the main beam. Their magnitude is found from the formula for g by separating the shadow into two pieces, each of which forms a bar of the plus. Essentially each is formed by half the shadow area so that in the sidelobe g is given by the following:

$$g = \left| \frac{2 A_E}{\frac{1+K}{2} A_A - A_E} \right|^2$$

This is approximately the following:

$$g \approx \frac{16}{(1+K)^2} \left(\frac{A_E}{A_A} \right)^2$$

Though the complete parabolic illumination gives a smaller effective area for a given support leg, the better efficiency of the uniform illumination causes the sidelobe levels due to the support structure to be essentially independent of the shape of the illumination when the support is near the optimum position. Since $A_E = FW$ for parabolic illumination, the sidelobe level due to legs 2.2 feet wide are 38 db. The three db width of the lobes (major width) is 10^0. The following sketch is a contour plot of the main beam and support blocking side lobes (not be scale):

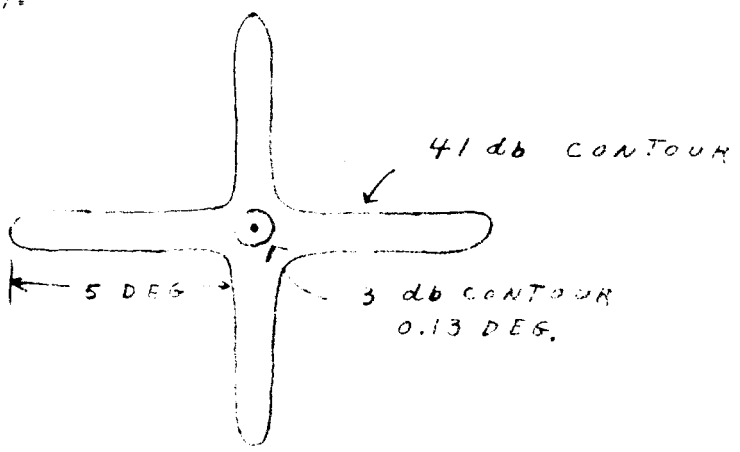

The sidelobe levels determined above will not meet the specification for the DSIF antenna that the sidelobes beyond 2^{o} be down 52 db from the main beam. In fact, to just meet the 52 db specification while ignoring all other sidelobe contributions the support leg can only be 5.6" wide. Since the lobe must be at least 6 db below 52 db to allow for other major sidelobe sources the support leg should actually be only 2.8" wide.

A Cassegrain mirror support structure with legs only three inches wide is obviously not possible. This geometrical optics approach demonstrates that the sidelobes produced by the support structure will not meet the sidelobe specification for the DSIF antenna.

Perhaps the gross approximations of the geometrical optics method produce a false conclusion. To study this possibility the diffraction of energy from the support legs was considered more closely from the point of view of diffraction theory. The general theoretical results for diffraction from a cylinder show that the members of a truss structure which is several wave lengths deep will not significantly shadow each other. Neglecting resonance and multiple scattering effects, the effective scattering width of a wide and deep truss should be the sum of the widths of the members in a cross section. Consider the following sketch of the cross section of a truss:

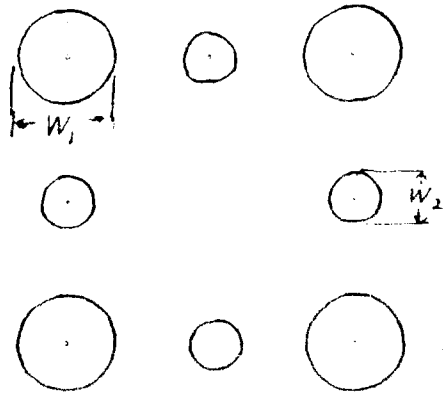

The effective blocking width, W, of this truss would be $4(w_1 + w_2)$. Evaluating this width with the above geometrical optics formulas shows that the combined width of a large member and a small member of the truss can only be .7". We do not believe that a truss with members this size would satisfy the mechanical requirements of the Cassegrain mirror support structure.

To make the case even stronger, the blocking width of such smaller members is considerably greater than their physical width.

Obviously, this simplified treatment of the diffraction of the r.f. field from the Cassegrain mirror support structure is not adequate to completely dispose of the problem.

Until more rigourous evidence is available which shows the opposite result, we believe that the sidelobes produced by the Cassegrain mirror support structure will not meet the 52 db sidelobes beyond 2° specification for the DSIF antenna. The best that can be hoped for is to design a support structure which will produce the minimum possible sidelobes. This will require extensive r.f. analysis and experiment and ingenious mechanical design. As an alternate, a more realistic specification should be set for sidelobes generated by the support structure.

A subsidiary result of the diffraction theory application to this problem shows that these sidelobes depend on the polarization of the r.f. field and will rise and fall as the polarization changes.

Some of the diffraction effects that need closer investigation are resonances between members and at junctions, the effect of finite member lengths, illumination that is not normal to the members, illumination by spherical or near spherical waves, and multiple reflections. Exact computations for a complex structure do not seem to be feasible, but reasonable estimates of the diffraction effects should be possible.

B. Orientation

The effect of the Cassegrain reflector support structure on the antenna performance is an important consideration. Section IV-A considers the sidelobe levels and gain loss produced by the support structure both of which contribute to reducing the effective figure of merit. However, only the sidelobe positions are significantly influenced by the orientation of the feed structure.

The sidelobes due to aperture blocking by a tripod will be asymmetric, and their magnitude will vary with the polarization of the received signal. As a result, the tripod should cause a greater boresight error than a quadripod and a boresight error that varies with polarization. In compensation, a tripod might produce less aperture blocking because it has three legs instead of four and the sidelobes of the legs are not superimposed.

In the absence of a computation of the boresight error due to a tripod and since the comparative mechanical data available for a tripod and quadripod indicates a preference for the quadripod, the quadripod seems to be the best choice.

Two orientations of the quadripod support are considered. The first looks like an X when the antenna is pointed horizontally, and the other looks like a plus sign.

It is desirable to be able to listen close to the sun and other interfering sources in the ecliptic. The sidelobes due to the support structure should be oriented so that they do not pick up the interfering sources in the ecliptic. The figure on the following page is a plot of the angle between a vertical plane passing through the antenna and the ecliptic as a function of the hour angle for various angles of the elliptic above the horizon.

Since the earth rotates at a constant rate, constant time periods are spent traversing equal hour angles. The result of differentiating the functional relationship between these angles combined with the fact that the sidelobes due to the X position of the support structure intercept the ecliptic twice (if at all) shows that the X position will produce more than twice the period of interference than the plus position will. As a result, we prefer the plus position for the support structure.

As a compensation to the use of the X position it should be noted that there will be no interference during the winter months; however, there will be excessive periods of interference in the spring and fall months.

As a by product it should be observed that the X position is preferable for a polar mounted antenna since the sidelobes created by the support structure would never intercept the ecliptic and pick up the interfering sources.

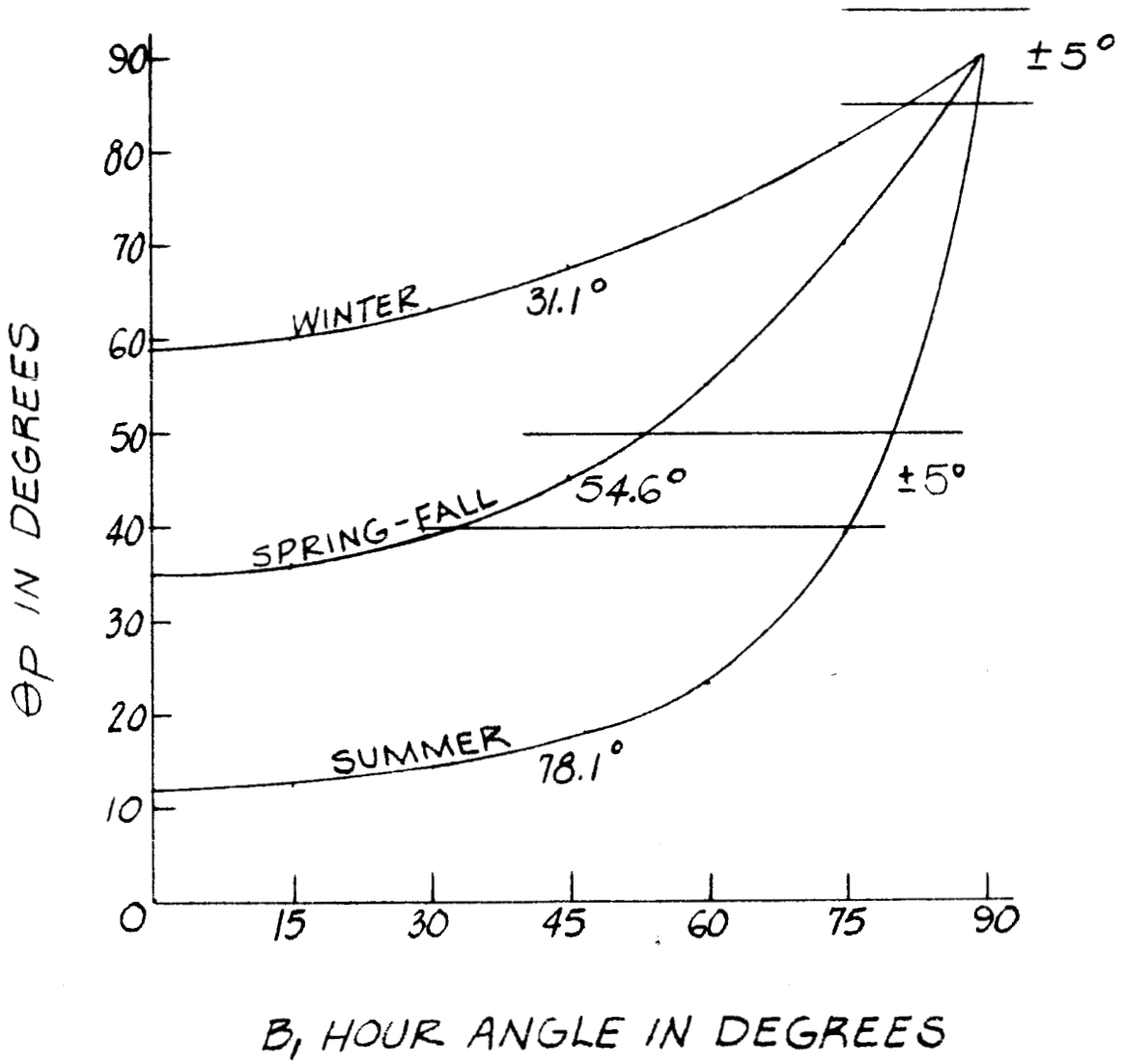
90
80
70
60
50
40
30
20
10
0
15
30
45
60
75
90
θp IN DEGREES
B, HOUR ANGLE IN DEGREES
WINTER
31.1°
±5°
SPRING-FALL
54.6°
±5°
SUMMER
78.1°

V. STEEL AS THE MAIN REFLECTOR SURFACE

Westinghouse has proposed the use of a steel surface for the sub-reflector of the DSIF antenna. Since steel has more resistive loss than the common conductors such as aluminum and copper, the power loss in the steel should be determined.

Since we have been unable to locate any data concerning the reflection of electromagnetic energy from steel a value of loss must be computed. Application of reflection theory shows that the ratio of the reflected power to the power incident on a surface is given by the formula;

$$\frac{P_{REFLECTED}}{P_{INCIDENT}} = 1 - 2\sqrt{2}\sqrt{\frac{\epsilon_0 \omega}{\sigma}\left(\frac{\mu_m}{\mu_0}\right)}$$

where

P = power,

ϵ_0 = dielectric constant of free space,

μ_0 = permeability of free space,

μ_m = permeability of reflecting material,

ω = frequency in radians per second, and

σ = conductivity of reflecting material.

The conductivity of a common steel, SAE 1045, is $4.5 \cdot 10^6$ miles per meter. The other constants are as follows:

$\epsilon_0 = 3.85 \cdot 10^{-12}$ farads per meter and

$f = \frac{\omega}{2\pi} = 2295$ mc.

As a result,

$$\frac{P_{REFLECTED}}{P_{INCIDENT}} = 1 - 0.00047 = -0.00216 \text{ db}$$

where it has been assumed that $\mu_m = \mu_0$

Since steel may not be completely nonmagnetic at 2295 mc perhaps a larger μ_m should be used. The best available magnetic materials would have $\mu_m < 10\mu_0$ at 2295 mc. As a result,

$$\frac{P_{REFLECTED}}{P_{INCIDENT}} = 1 - 0.0015 = -\ 0.0065\ db.$$

The effective noise temperature, T_R, of the steel reflector is given by the following formula,

$$T_R = 400\left(1 - \frac{P_{REFLECTED}}{P_{INCIDENT}}\right) = 0.19^\circ K$$

where the antenna temperature is assumed to be 400° K. Even if $\mu_m \neq 0$, the noise temperature of the reflector must be less than .6° K.

Since this noise temperature is not prohibitive, steel would be usable as a reflecting surface. It should be noted, however, that a coating will be required on the steel for protection from corrosion. In addition this coating should provide for reflection and scattering of incident thermal energy to reduce heat absorption in the structure and thermal concentration at the feed point. An evaluation of possible coatings is being made. The final coating chosen may increase the skin loss and become the major determining factor in this contribution to the noise temperature.

It should be noted that a solid copper antenna would have a noise temperature of .055° K and a solid aluminum antenna would have a noise temperature of .07° K. A perfectly conducting mesh with a 99% reflection factor would have a noise temperature of 4° K.

VI. PROGRAM FOR NEXT PERIOD

During the next period the total effort in the general area of the "Microwave Optics System" will divide into three general categories:

a. Substantiated determinations of factors influencing basic mechanical problems (i.e. particularly factors influencing pointing accuracy):

1. Tolerances on Cassegrain mirror location (essentially complete)
2. Tolerance "split" between main and Cassegrain reflector (essentially complete)
3. Feed location tolerances (partially complete)
4. Cassegrain reflector support recommendations (partially complete)
5. Degradation tolerances due to increased wind velocity
6. Consideration of effects of drain holes and cracks.

b. Continued specific studies influencing evaluation of postulated designs:

1. Evaluation of factors influencing noise temperature (partially complete)
2. Continued study of factors influencing sidelobe levels (partially complete)
3. Figure of Merit and Transmit Gain Calculations.

c. Design Considerations of Source System

The design details of the Source System influence to a very limited extent the "basic" mechanical designs. For this reason the source feed

system and the microwave plumbing arrangement required to satisfy the specification requirements have been retained for study during the latter part of the program. During the next period we will develop in detail the Source System.

APPENDIX I - CONSIDERATION OF CASSEGRAIN REFLECTOR DISPLACEMENT ON POINT ANGLE, PARTICULAR CASE

Derivation of the path length change due to a displacement of the subreflector perpendicular to the axis of the main reflector.

The following sketch shows a ray between the feed at A and the aperture, with the original hyperbola drawn dashed. Only a section of the hyperbola is shown.

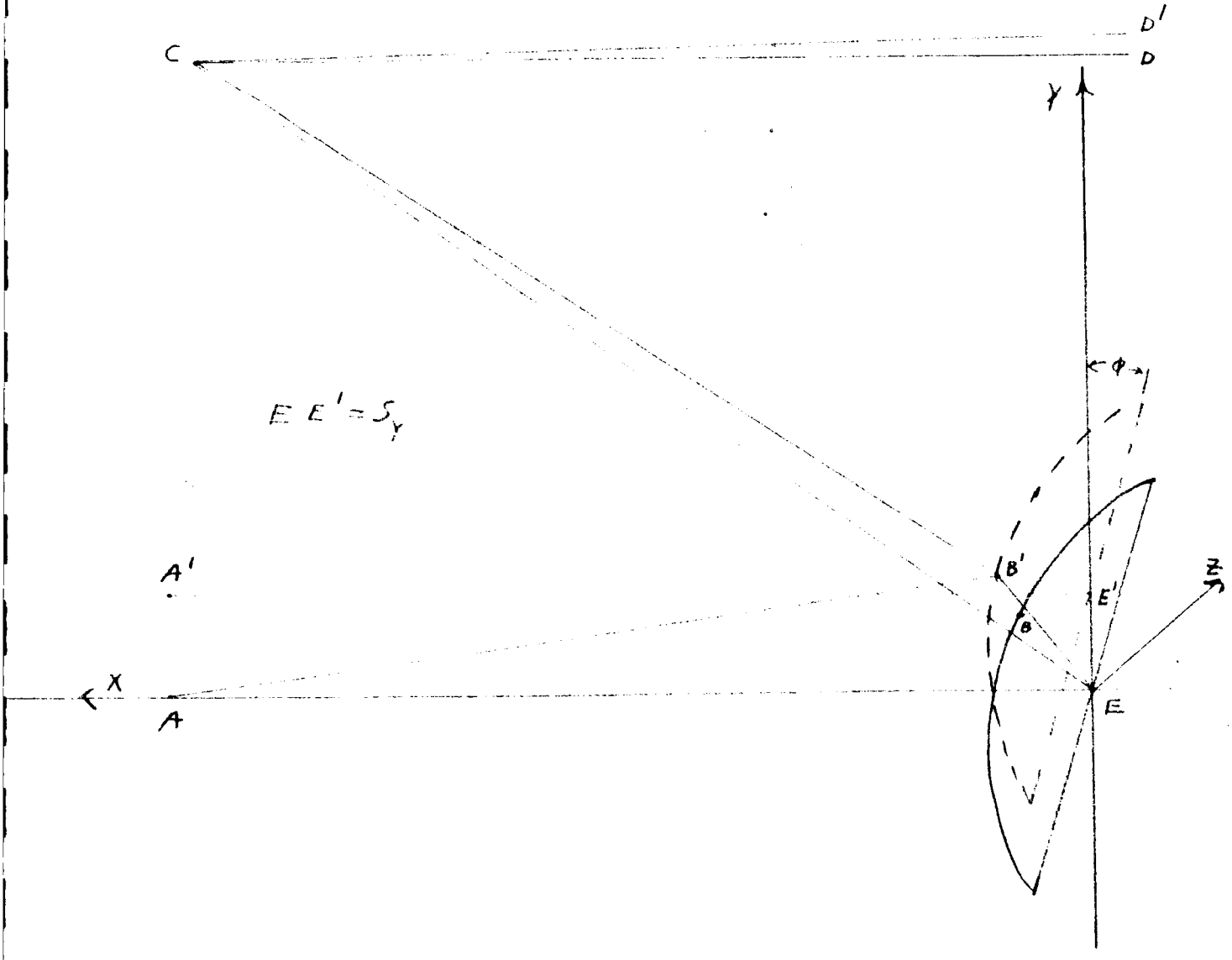

A' and E' are the displaced foci of the hyperbola. B' is the point where the ray $AB'CD'$ intercepts the hyperbola, C is the point where it intercepts the parabola, and D' is the point where it intercepts the aperture. B is the original position of B'. E is the focus of the parabola. D is the point where the ray ECD intercepts the aperture. The length of ECD is given by $EC+CD=2F$ where F is the focal length of the parabola. Since the angles $B'CE$, $B'EC$, and DCD' are very small (less than $.2^{\circ}$), $CD'=CD$, and $CB'+B'E=CE$. The lengths of AB' and EB' are given by $AB'=\sqrt{(2f-x_1)+(Y_1+S_Y)^2+Z_1^2}$ and $EB'=\sqrt{X_1^2+(Y_1+S_Y)^2+Z_1^2}$ where X_1, Y_1, Z_1 are the coordinates of B, and Y_1+S_Y is the Y coordinate of B'.

The equation of the hyperbola is

$$\left(\frac{X_1}{a}\right)^2-\frac{2}{ad}\left(Y_1^2+Z_1^2\right)=1$$

Let $R_1^2=Y_1^2+Z_1^2$

It can be shown that

$$\sqrt{X_1^2+Y_1^2+Z_1^2}=\frac{f^2-a^2}{a}-\frac{f}{a}X_1$$

and that

$$\sqrt{(2f-X_1)^2+Y_1^2+Z_1^2}=\frac{f^2+a^2}{a}-\frac{f}{a}X_1$$

It is also approximately true that

$$\sqrt{X_1^2+(Y_1+S_Y)^2+Z_1^2}=\sqrt{X_1^2+Y_1^2+Z_1^2}+\frac{Y_1S_Y}{\sqrt{X_1^2+Y_1^2+Z_1^2}}$$

and

$$\sqrt{(2f - x_1)^2 + (y_1 + s_1)^2 + z_1^2} = \sqrt{(2f - x_1)^2 + y_1^2 + z_1^2} + \frac{y_1 s_y}{\sqrt{(2f - x_1)^2 + y_1^2 + z_1^2}}$$

The length of the ray $AB'CD'$ is given by

$$AB'CD' = AB' + B'C + CD'$$

$$= AB' + CE - B'E + CD$$

$$= 2F + AB' - B'E .$$

Now

$$AB' - B'E = \sqrt{(2f - x_1)^2 + (y_1 + s_1)^2 + z_1^2} - \sqrt{x_1^2 + (y_1 + s_y)^2 + z_1^2}$$

$$= 2a - \frac{2a\, y_1 s_y}{\frac{f^2}{a^2}(f - x_1)^2 - a^2}$$

and then,

$$AB'cD' = 2F + 2a - \frac{2a\,Y_1\,S_Y}{\frac{f^2}{a^2}(f-x_1)^2 - a^2}$$

Since $Y_1 = R_1 \cos\phi$, we get

$$AB'cD' = 2F + 2D - \frac{2a\,R_1\,S_Y\cos\phi}{\frac{f^2}{a^2}(f-x_1)^2 - a^2}$$

This completes the derivation of the length of $AB'cD'$. Since the length of the undisturbed rays from the feed to the aperture is $2F + 2a$, the change in the path length, S, is the following:

$$S = -\frac{2a\,R_1\,S_Y\cos\phi}{\left(\frac{f}{a}\right)^2(f-x_1)^2 - a^2}$$

The approximations used in this derivation are very good and cannot significantly affect the results.

C. ANTENNA SYSTEM

POSITION SENSING

Because of the large physical size of the antenna structure, the severe environment conditions of wind and temperature and the need for extreme accuracy in pointing and position indication, the synchros normally coupled to the moving shafts are suitable only as "coarse" systems. Such a system will be included but a "fine" system is also required. The "fine" system is to be very accurate. One of the requirements for it is a stable "ground" reference from which the antenna rotation about its two axis are to be measured. Such a reference will be made available by extending a vertical tower above the pintle bearing around which the antenna structure rotates in azimuth. Surrounding the tower will be a windshield protecting it from external disturbances so that it remains fixed relative to the earth. On top of the tower will be located two miniature units. One of these will be an equatorial mount while the other unit will be an AZ-EL mount. These two units will be located at the intersection of the two axis of rotation of the antenna. A model of the dual unit is shown on Photo No. 1. A simplified arrangement of the functional parts is shown in Fig. 1. It is to be noted from the photo and from the figure that axis of the miniature AZ-EL unit may be made to coincide with the AZ-EL axis of the antenna. Furthermore, the Hour Angle (HA) and Declination (DEC) axis of the equatorial unit coincide with the AZ-EL axis of the miniature unit. With suitable servo systems the dual miniature units will be made to follow the AZ-EL motions of the

antenna. Therefore, with encoders or position indicating transudcers, the shaft motions of the miniature units may be indicated at a remote location.

Successful operation of the position indicating systems depends on a stable reference on the antenna. Such a reference will be available behind the vertex of the antenna and will consist of a mount which will be supported from the main structure so as to be free from its distortions. On this will be located the bore sight telescope to which the main dish will be aligned. Also, on this structure will be mounted an autocollimator and an optical mirror. These will be aligned with other optical mirrors and autocollimators on the AZ-EL mount and on the equatorial mount of the monitor unit respectively. The arrangement is shown in Fig. 2.

The function of the autocollimator is to provide a parallel beam of light and direct it toward the mirror, which reflects it back toward the autocollimator. If the return beam lies precisely along the axis of the forward beam the voltage output (signal) from the autocollimator is zero (nulled condition). However, if the beams are not in line - which is the case when the mirror is not at right angles to the beam of light - an error signal is produced which is proportional to the misalignment. Furthermore, this signal is phase-sensitive so that it may be applied to control servo motor which in turn rotate the mirror or the autocollimator until the beams are precisely in line. The autocollimators to be used are of the "twin" type having two orthogonal light beams so that two servo systems are available

for correcting the position of the mirror in two directions at right angles to each other.

With a twin autocollimator mounted behind the antenna and with a mirror on the miniature AZ-EL unit, the two orthogonal light beams (within limitations) will produce error signals which are applied to the proper servo motors controling the axis of the AZ-EL units. (Refer to Fig. 3.) The servo motors rotate the mirror until the reflected beams are precisely in line with the forward beams. Under this condition the error voltage becomes zero and the servo motors stop. If now the antenna is moved an amount within the sensitivity of the autocollimator, the error detection system will automatically reposition the mirror. The position indicating transducers will automatically transmit a corrected AZ-EL position indication to the readout and to the servo system.

A similar arrangement exists for the miniature equatorial unit except in this case the mirror is mounted behind the antenna while the twin autocollimator is mounted on the miniature equatorial unit. With this arrangement, the equatorial axis are provided with the proper error signals in order to re-orient the autocollimator and its beam toward the mirror. If now the antenna is moved any amount within the sensitivity of the autocollimator, an error is produced. This error, however, is in equatorial coordinates and is entirely suitable for applying to the servo motors which control motions in the same coordinates. Therefore, by using a miniature equatorial unit on top of the tower, the AZ-EL motion of the

antenna is automatically converted into equatorial motion and the coordinates are transmitted to remote indicators by means of transducers on the shafts of the equatorial unit.

The accuracy of the position indicating systems depend entirely on the accuracies of the components. Autocollimators are now available with a basic accuracy of $\pm$ 1 second of arc. Some position indicating transmitters have a basic accuracy approaching $\pm$ 0.001 degrees. These, however, are not completely adequate. Further study is needed that speed of response of the mount drive can be made fast enough to permit following the antenna at maximum velocity without excessive error. Range of the most sensitive autocollimator is $\pm$ 10 minutes. For initial alignment and in case the mirrors and autocollimators become out-of-phase a "coarse" synchro system will be used. Operation of such a system will be described later.

Since the coordinates are 'readout' from the axis of the miniature units, deflections or displacements of the antenna support structure do not affect pointing accuracy. The flat mirrors used with the autocollimators permit parallel displacements between the axis of the antenna and the axis of the miniature units without any misalignment of the optical beams. Such displacements do not affect accuracy of pointing. However, any angular displacements are measured as errors for which corrections are made by the servo systems.

High precision angle encoder connected to Azimuth and Elevation shafts of the instrument mount is proposed to give

a digital indication of antenna position. Such an encoder is available from Norden Div., United Aircraft Company, which has a resolution of 0.001° and with auxiliary equipment can provide a six decade binary coded decimal signal of shaft position, at speeds up to 100 degrees per second.

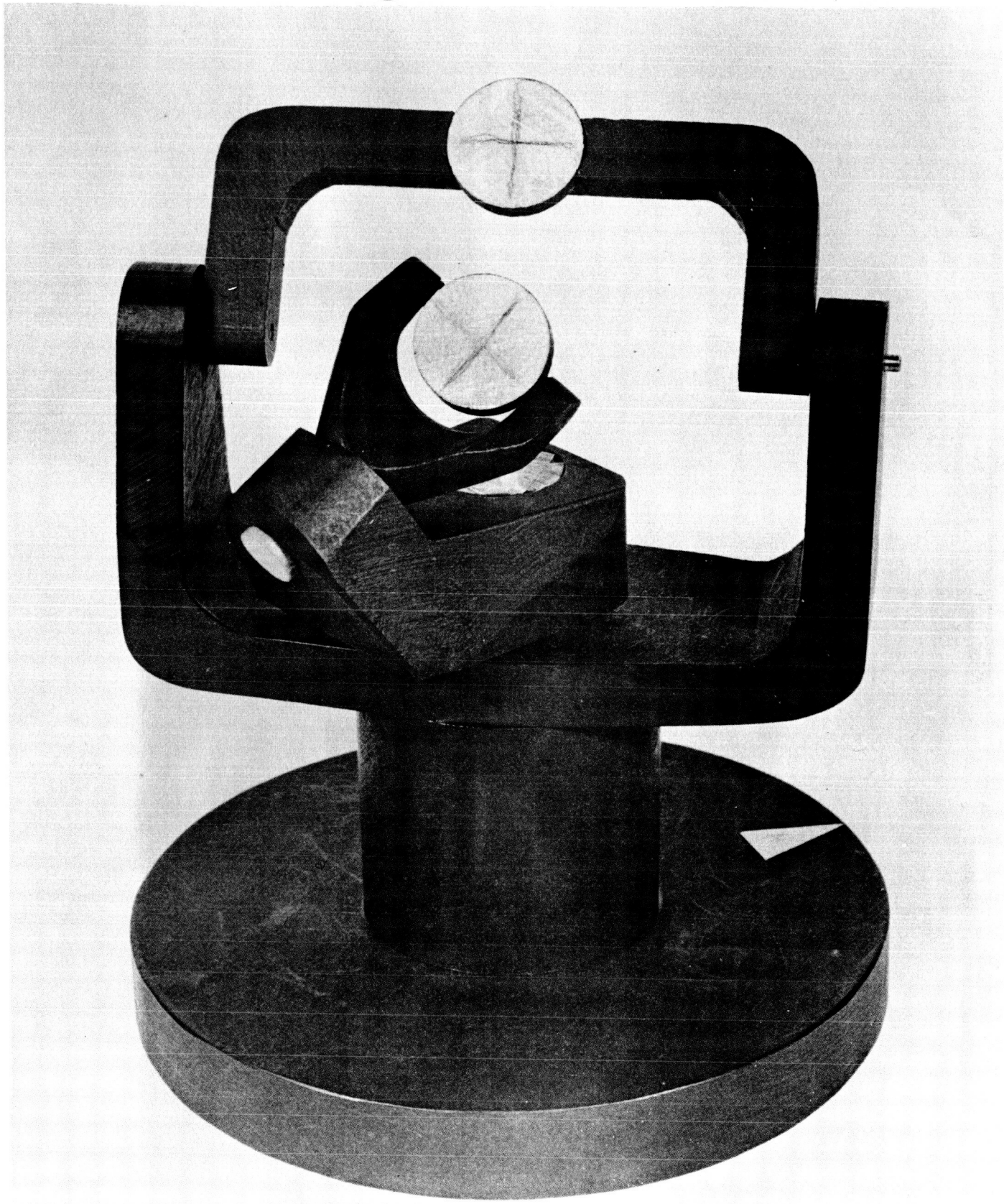

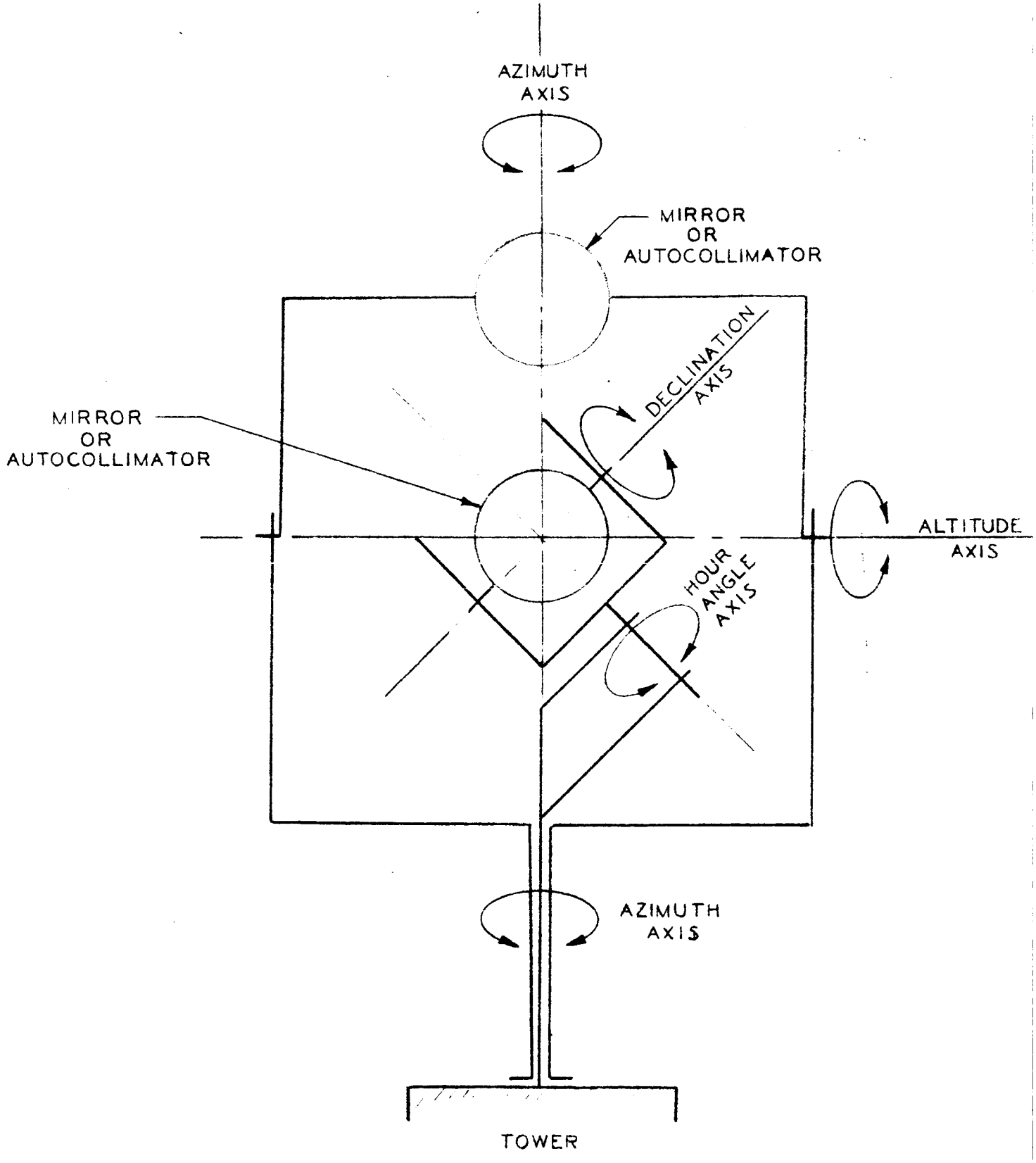

FIGURE NO. 1

MINIATURE EQUITORIAL AND ALT-AZ UNIT

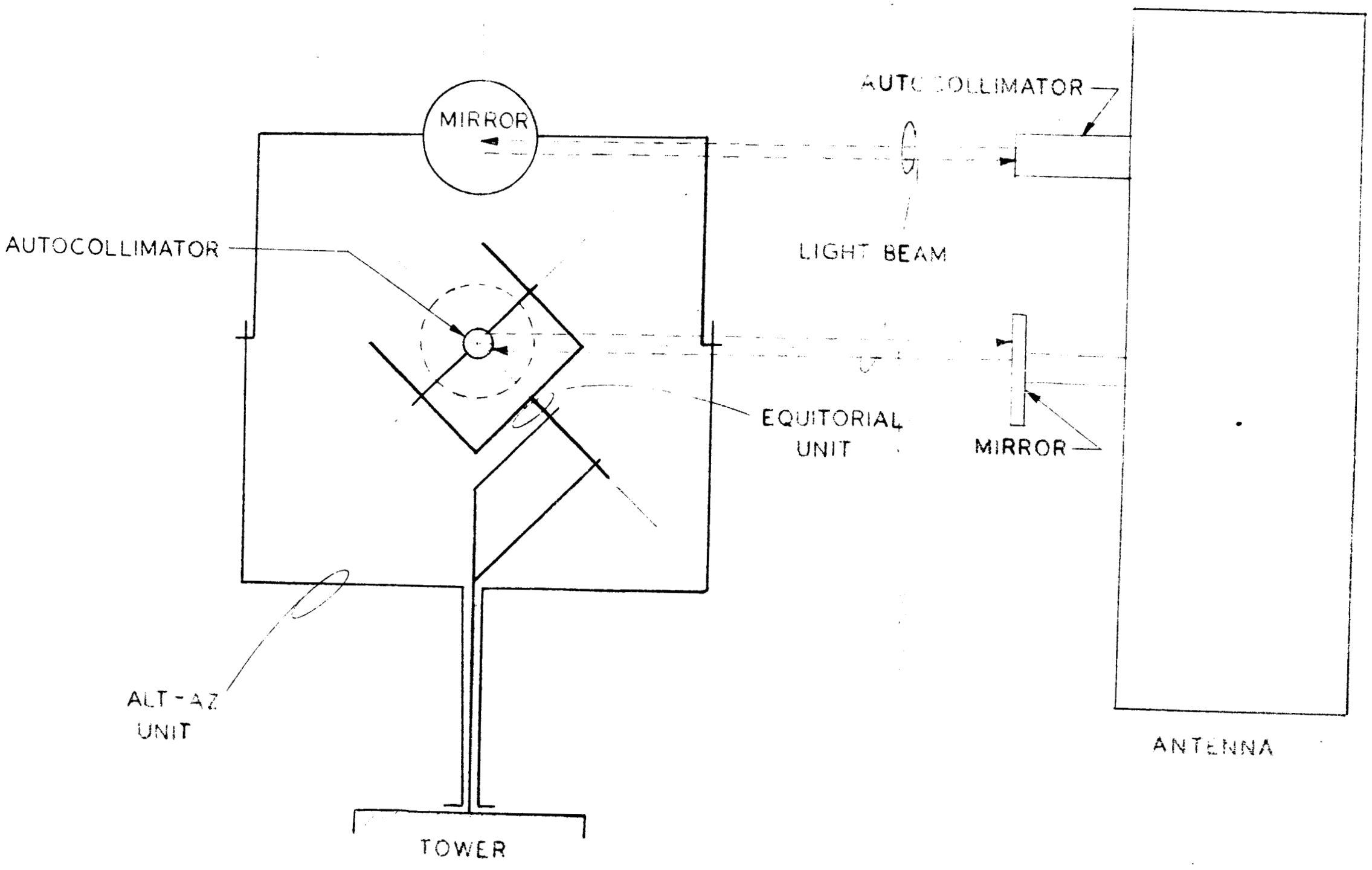
MIRROR
AUTOCOLLIMATOR
AUTOCOLLIMATOR
LIGHT BEAM
EQUITORIAL UNIT
MIRROR
ALT-AZ UNIT
TOWER
ANTENNA

FIGURE NO. 2

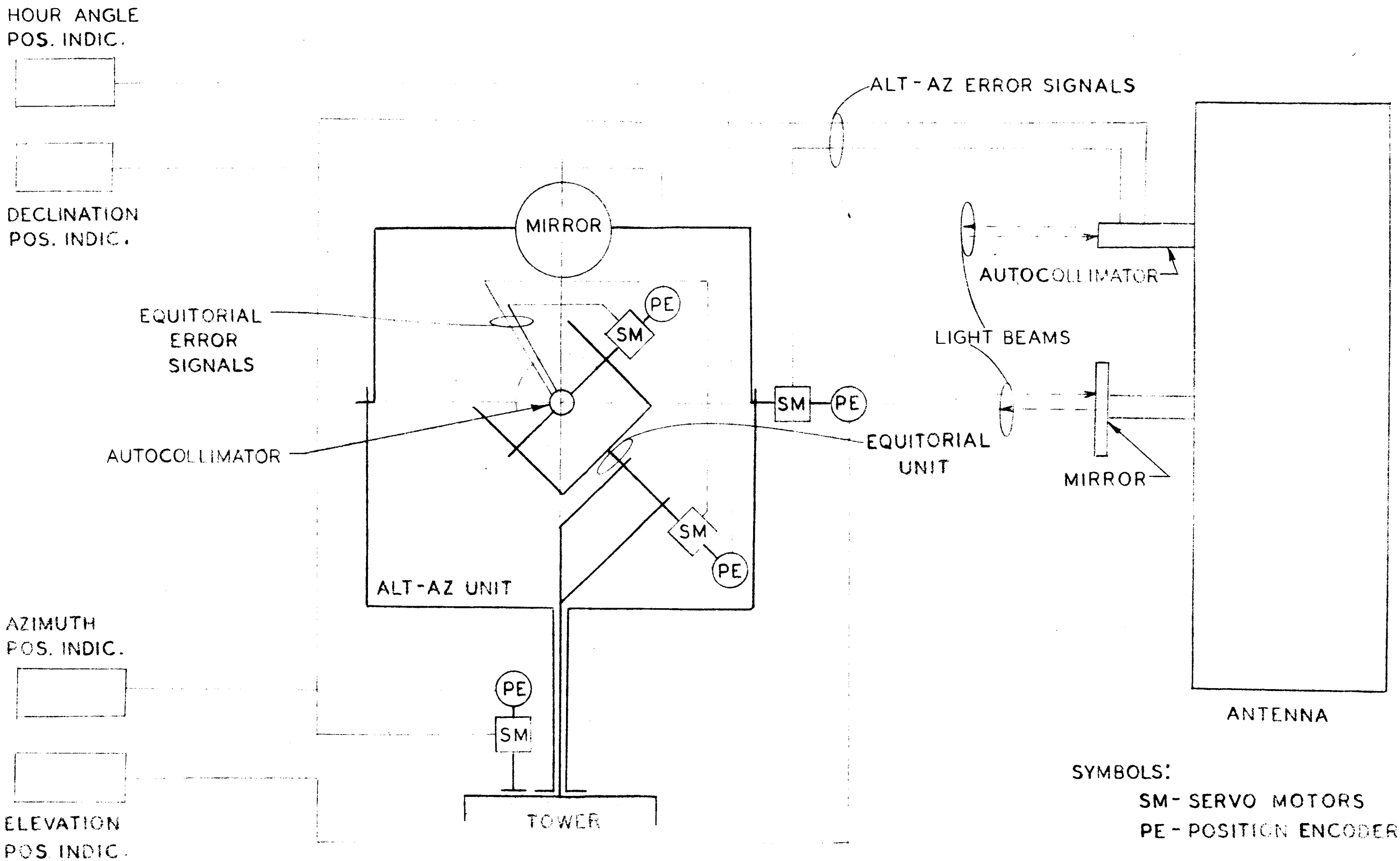
HOUR ANGLE
POS. INDIC.
DECLINATION
POS. INDIC.
ALT-AZ ERROR SIGNALS
MIRROR
EQUITORIAL
ERROR
SIGNALS
PE
SM
AUTOCOLLIMATOR
LIGHT BEAMS
AUTOCOLLIMATOR
EQUITORIAL
UNIT
MIRROR
ALT-AZ UNIT
AZIMUTH
POS. INDIC.
ELEVATION
POS. INDIC.
TOWER
ANTENNA
SYMBOLS:
SM- SERVO MOTORS
PE- POSITION ENCODERS

FIGURE II-C.3

B. ALIGNMENT AND SHAPE MEASUREMENT

INTRODUCTION

A highly directional antenna for optimum performance depends upon careful adjustment of the phase path. This is to a degree dependent upon the maintenance of a correct parabolic reflector surface and accurate knowledge of its mechanical directional axis.

To do this there must be an alignment system to establish and verify basic aligning references. This overall system includes equipments and procedures to provide:

1. Geodetic system coordinate check-out, bench marks, theodolite piers, etc.
2. System orthogonality checkout.
3. Boresight telescope alignment and checkout.
4. AZ-EL axes tower checkout.
5. Collimation tower alignment and checkout.
6. A system to monitor Cassegrain Position.
7. A system to monitor the paraboloidal surface.

The context of this report presents methods considered as feasible to provide certain of the above stated systems.

ALIGNMENT AND OPTICAL TECHNIQUES

A. SCOPE

The techniques, equipment and procedures for verifying the paraboloid of the 240 foot dish are given. The technique of establishing the boresight axis, the Cassegrain axis and for referencing these to each other is developed in the context of this report. The overall DSIF alignment system is given in outline form. This report does not include the method of establishing ground references for the original erection plan of the supporting structures or the collimation towers.

B. REQUIREMENT

The center of the feed horn aperture the feed horn directional centerline, the focus of the paraboloidal dish, the center of curvature of the Cassegrain are colinear and on the mechanical axis. These are to be positioned and monitored with respect to the mechanical pointing axis and to each other. To do this the following must be done or established.

1. The parabolic surface must be monitored to indicate conformance with this requirement and to indicate deviation in surface configuration greater than an rms deviation as stated elsewhere. A fixed envelope concept of discrete points representing the dish configuration are referenced to each other and with respect to the mechanical axis of the dish.

2. A boresight telescope axis parallel to the machanical axis.

3. The positioning and centering of the center of curvature of the hyperboloid Cassegrain mirror with respect to the mechanical axis.

C. SYSTEM TO INITIALLY ALIGN AND REFERENCE TO THE MECHANICAL AXIS, THE SHAPE OF THE PARABOLOIDAL DISH

This is shown in Fig. (1).

1. It will consist of an array of collimated light sources and ACC units. The instrument will be mounted on a specially constructed platform which will be aligned with its axis colinear to that of the AZ-EL axes of the tower reference. This will be done by autocollimation to the antenna reference mirror and the AZ-EL axis. See Figs. (1) (7).

   The unit will index to selected levels and to angles within the limits established by Fig. 3 and Fig. (2).

   The fixed envelope of the dish will be similar to the configuration of Fig. (4). The initial parabolic shape will be established in accordance with the mathematical model of the antenna design. Numbers of light sources and automatic autocollimation units will be placed in accordance with the configuration of the supporting structure members. Distribution will be by statistical analysis. The rms 0.25 inches has been stated elsewhere as the standard σ deviation.

Reading of the indexing machine will be by ACC (Automatic-Autocollimation) provide a proportional signal to be compared with a 'go' or 'no go' indication. Any area of the dish requiring configuration correction can then be re-read manually to provide adjustment direction.

The AAC system is shown in Fig. (5).

It is emphasized that an equivalent number of light sources and automatic autocollimators will be in the dish and in the indexing light source machine.

The second reading to determine the location of the reference point with respect to the mechanical axis will come from the light sources mounted at the surface to the indexing-autocollimator unit.

In both cases, physical readout of the objective target on the AAC can read to 0.001 inch.

The set-up from this unit will in turn provide the reference installation for the next step of the requirements.

2. A boresight telescope axis.

The boresight telescope will be an astronomical telescope. It will be mounted on an adjustable base controlled from the reference mirror of the mechanical axis of the dish.

This reference setting to the mechanical axis will initially be made by autocollimation. See Fig. (6). It will be automatically adjusted and capable of being manually locked in set position.

A television camera mounted onto the double view telescope will provide remote viewing as needed. Viewing of the telescope can be done manually from the telescope cage.

3. The initial positioning and centering of the center of curvature of the hyperbolic reflector.

A small light source on an adjustable mount will be placed onto the boresight platform. This will project collimated light into an AAC mounted permanently on a bracket on the Cassegrain. The light source orientation will be monitored by the Mechanical axis reference sensing unit (Fig. (6)) which will also orient the boresight axis.

This will insure parallelism of these axes. The AAC mounted on the Cassegrain will provide a proportional signal to a recorder to indicate extent of misalignment present which in turn will send a display signal to be compared for correctional use as needed. See Fig. (7),

Initial information indicates that accurate initial placement of the hyperbola can be defined to provide minimum adjustment. Limits of permissible error are defined in the section Discussion of systems and notes.'

The system defined in Fig. (7) will provide parallelism of axes of the Cassegrain to the mechanical axis. Laterial adjustment will be defined by a telescope to which the collimated light source for the Cassegrain is integrally mounted. This same system will be permanently installed for monitoring.

4. The monitoring of the parabolic surface

The method of monitoring the parabolic surface is feasible with the equipments presently available or readily developed.

For systems considered see 'Disucssion of Considered Systems'. It can be 'on surface mounted' or attached to the non-reflecting side of the dish. Both systems are explained.

In Fig. (8) the system for 'on surface' monitoring is shown.

This system consists of a special array of light sources (collimated light) directed at AAC units mounted just at the surface. The light projects into the AAC's which are at precise positions selected and set at the time of establishing the original parabolic shape. See Figs. (1), (2), (3) and (4).

Upon actuation of control units the light source projects a collimated beam into the collimator which impinges upon a central prism. The split beam is then directed upon sensitive light cells. Any difference in current intensities are compared in an amplifier and transmitted to an indicator for display. Comparison of the readings given are overlayed on the basic parabolic dish shape premarked on a display panel. Limits are designated and data read for correctional use.

The ancillary scopes mounted to the boresight telescope platform are oriented to the boresight axis in the same manner as the Cassegrain light source. See Fig. (6). These units fixed to this axis reference look

through discretaly mounted pentaprisms onto a displacement target mounted and preset at the time of the AAC alignment. Any radial displacement from the reference mechanical axis and boresight axis is read, manually, directly.

These two readings, (1) the signal (angular error) translated to a displacement parallel to the mechanical axis and boresight axes, (2) and the radial displacement from this mechanical axis, will then be tabulated (See Fig. 9) eliminating estimating non-linear error.

It is intended to provide a triangular mounting sub-surface to the reflector to provide maximum area average coverage of deviations. The triped mounting locations to be derived from the geometry of the supporting structure for maximum efficient area representation.

5. 'Off surface' monitoring system.

Thesystem for 'off surface' monitoring is as shown in Fig. (10).

This system will provide essentially the same data as the 'on surface system'. Difficulties are present in that final structure calculation must provide movement limits to determine sizes of optic objective lenses needed. Equipments will be the same in either 'on surface' or 'off surface' mountings.

The advantages here are in removing the problems of beam deviation due to air density or temperature variations. However, beam deviation over 100 ft. based upon a refraction number of $1 \pm 8 \times 10^{-6}$ indicates an error of only 2 arc seconds over the maximum monitoring distances.

6. Summary.

The methods described are based upon existing equipments. No major difficulties in providing the coordinated checks described are expected, with equipments now available. Errors expected are tabulated below.

Autocollimators	3 sec. arc.
Pentaprisms	2 sec. arc.
Target readings	1 sec. arc.
Collimator angular readings	15 sec. arc.
	21 sec. arc.
The ability to establish and maintain coordinated axes alignment with the mechanical axis	20 sec. arc.
Maximum error in data amplification to controls. 5% of total ranges of 250 sec. arc.	13 sec. arc.
Non-linear distance variations	25 sec. arc.
	38 sec. arc.

The rms error

$$\sqrt{\frac{21^2}{3} + \frac{20^2}{3} + \frac{38^2}{3}} = 27.3 \text{ sec. arc.}$$

DISCUSSION OF CONSIDERED SYSTEMS

DISCUSSION OF PARABOLOID MONITORING SYSTEM REQUIREMENTS

In conformance with prior evaluations in Westinghouse study proposal, the objectives of the study effort were stated to be:

1. Reduction of excessive antenna noise.
2. Increased antenna gain.
3. Increased pointing accuracy.
4. Maximum system reliability.

Each of the above four items contain sigma σ in the formula. This is a standard deviation of the surface from the true paraboloid. In addition σ may be usually considered some constant fraction of the diameter of the dish or d/σ

By maintaining a true surface with 1/16 wave length at 2290 Mc a limit is established. This limit can be used to point the direction of effort for a surface sensing system.

SYSTEM LIMITS

To sense a paraboloidal surface with 1/16 λ at a frequency of 2290 Mc:

$$\frac{\lambda}{16} = \frac{300 \text{ meters}}{16(2290)} \times \frac{39.37 \text{ inches}}{1 \text{ metre}} = .378"$$ Surface deviation from true paraboloidal shape.

For preliminary discussion and system determination the figure of rms .250" has been arbitrarily selected.

A paraboloid diameter of D = 240ft is defined by the dimensions as shown in Figs. (1) and (2).

Consideration was given to reading of surface angular positions from the theoretical center of the Cassegrain intersected by the principal axis of the dish and from the vertex.

Selection of a point at 60 ft. from the Cassegrain show the movement radially from such a line of sight of 1/4 inch would be approximately 1 minute of arc. To read this angle the system between the Cassegrain and the surface point would need to be read to an accuracy of $\pm$ 6 sec. of arc.

To read a second reference which wouldderive displacement from the theoretical paraboloid, the following indicates the instrument range and accuracy required.

Suppose that an optical instrument were placed on the vertex of the paraboloid, and sighted from there to various points on the paraboloid surface. A displacement of one of these points on the surface by 1/4 inch parallel to the axis, requires the instrument to be tilted by a small angle, which is a function of the radial distance from the axis to that point. This is given in the following table.

Radius to Point on Surface Inches	Angle of Tilt, Min. of Arc.
240	3.6
480	1.8
720	1.17
1200	0.69

Furthermore, the range of tilt required is shown in the following table. See Fig. (2) and (3).

Radius to Point on Surface Inches	Direction From Vertex to Point on Surface
288	5° 40'
576	11° 20'
720	14°
1296	24° 10'

This would indicate that single source, see Fig1 (3), sighting along a single path must operate through the range of 0° to 25° and be able to read to an accuracy better than 30 sec. of arc.

SYSTEMS CONSIDERED

In consideration of various type systems, the following two systems have been considered, only in principal.

1. An energy system suggested by Dr. Swarup of Stanford, "IRE Transactions Jan. 61 Phase Adjustment of Large Antennas." This consists of placing modulated gas discharge tubes, acting as scatterers, at various points on the paraboloidal surface and to monitor the phase path from a signal generator through the feed at the focus to each discharge tube in turn and back. By means of a second probe, possibly a dipole situated at the vertex of the paraboloid it is possible to triangulate on deflections. The phase of the modulated reflected wave produced by the discharge tube is determined by adding it to a reference C-W wave of large amplitude and applying the resultant to a receiver sensitive to the modulating frequency. A null is obtained when the two waves are in quadrature. The coherent detection system allows measurement of the phase of the modulated reflection even when its amplitude is below -130 dbm. The system has been

demonstrated using a 10 mw S band signal generator, and no difficulty was found in detecting the reflection from a small discharge tube placed 100 ft. away from a 3 x 4 inch horn. This indicates use as a surface configuration sensor for large paraboloids. Westinghouse, Baltimore Plant, is now investigating applicability of this system, which is considered not fully developed.

2. Dual Frenquency Beam

A system has been suggested by Davidson Manufacturing Co. This system suggests use of a dual frecuency beam with the interface of the dual frequency beam seen as a line between the two phases of light as viewed through the eyepiece.

This requires a dual parallel beam to be directed into a collimator with the incidence or lack of incidence of the interface indicating exact axial coindidence. Angular deviation is indicated by one or the other of the two out of phase frequencies being sensed instead of the null interface. The field of view of this system has not yet been defined. Exact knowledge of the requirement for a parallel source or the width of angular divergence to which the nulls may be aligned is not yet defined. Accuracy to which this may be read has been stated as to be as low as 0.1" of arc. This sensitivity needs be checked against system vibration amplitude and may be too great but if the unit can perform reliably it will be further pursued as possibly one leg of a two angle checking system to locate movement within the standard or maximum variation from the true parabola.

3. A system of using a modulated light beam

Monitoring the paraboloidal fixed envelope by modulated light beam. This plan considers the feasibility of distance measurement from a position near the focus to a mirror located in the reflector surface. This employes a light beam that is pulsed or modulated at a frequency that can be handled with routine electronic techniques. The distance or differential measurement involves the equivalent of a phase shift deformation. Equipments of these types are commercially available - know as Geodometers. However, while these are succesfully used for mapping from long range, the accuracy obtainable for the dimensions involved in measurement of the parabola of the antenna of standard equipments is not within the required limit of $\pm$ 0.25".

4. Equipments

Items mentioned are AAC - Automatic Auto-Collimators. These are presently available and sizes of aperture (objective lenses) can be as needed to assure that the light source will be able to pick up - regardless of windload, deformation, temperature expansion, gravity, etc.

In the items mentioned as telescopes for aligning the principle axes of the systems - in some cases theodolite adaptations will provide the stability and accuracy desired. Optically, the use of auto-reflection or auto-collimation, is not considered since the present state of the art rules out usages past 40-60 feet. However, assurance is expressed that using a separate aligned light source direct into the

collimator no distance problems are involved for this installation.

5. Hyperboloid Positional Tolerances - These data can be established to provide a table of limits of positional monitoring tolerances.

A. Effect of Tilt

It will be assumed throughout that the hyperboloid is small enough so that one need consider only the reflections near the mirror vertex, V. A geometrical optics approach is used.

The hyperbolic arc in the correct position (continuous line), and tilted by an angle α (broken line), is shown in Fig. 1. The reflector is shown tilted about its vertex V.

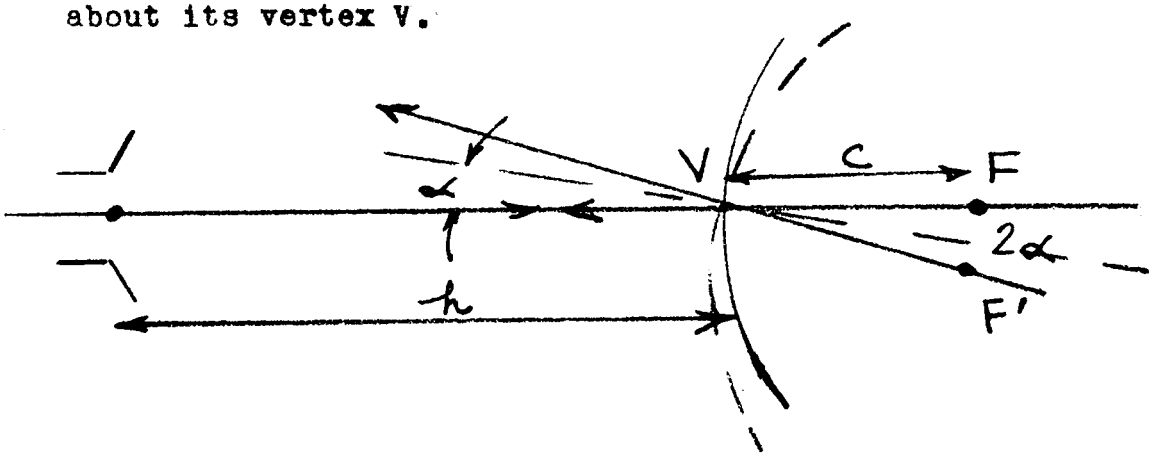

Fig. 1 Effect of Tilt

The feed horn aperture is located at H, and a virtual image is formed at F, the focus of the paraboloid. F and H are conjugate foci of the hyperboloid. When the mirror is tilted, the image of H in the mirror moves

from F to f'. The small displacement FF' is given by

$$FF' = 2c\alpha$$

Note that a clockwise rotation has displaced F downwards. Example: If the tolerance on beam direction is 0.02 degrees, and if one quarter of this is allowed for tilt error, 0.005 degrees, then with a focal length of 60 feet, F can be displaced 0.063 inch and the maximum permissible tilt α is then 0.063 in/2c. If c is 3 feet, for instance, this is 0.05 degrees; if c is 6 feet, it is 0.025 degrees.

b. <u>Effect of displacement perpendicular to axis.</u>

This is shown in Fig. 2

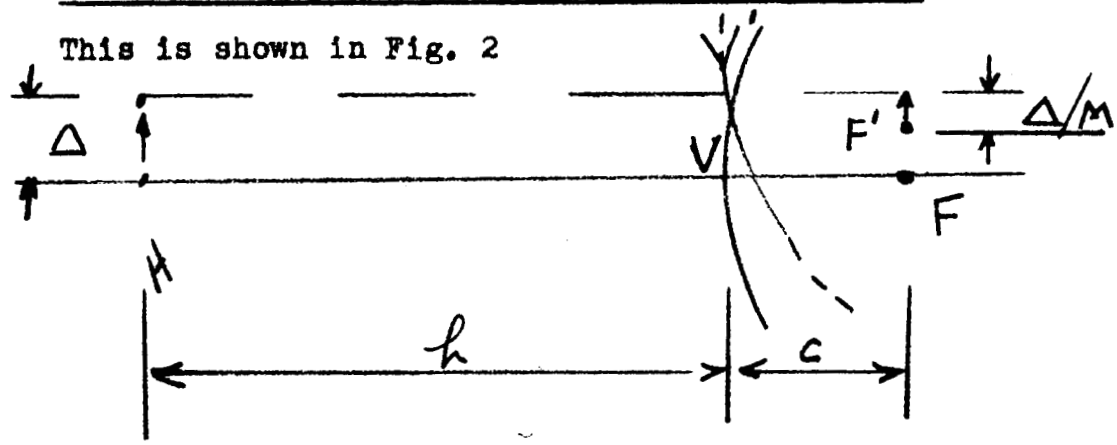

Fig. 2. Effect of displacement perpendicular to axis.

Let M = magnification

$= h/c$

It can be seen from Fig. 2, that for a mirror displacement Δ, the image moves from F to F', where

$$FF' = \Delta\left(1 - \frac{1}{M}\right) \approx \Delta\left(1 - \frac{c}{h}\right)$$

$$= \frac{2\Delta}{e+1}$$

Where $e = (M+1) / (M - 1)$ is the eccentricity.

Note that the virtual image moves in the same direction as the mirror.

Example: If the tolerance on beam direction is 0.02 degrees, and if we allow one quarter for the tilt error, viz. 0.005 degrees, then with a focal length of 60 feet, F can be displaced by 0.063 inch, and the hyperboloid by slightly more than this, depanding on the magnification M. If, for instance, $M = 9$, then the mirror may be displaced by 0.071 inch to produce a beam pointing error of 0.005 degrees.

c. Self-compensation

If we can arrange the hyperboloid support in such a way that (in terms of Figs. 1 and 2) an upward displacement always goes with a clockwise rotation, then the two displacements of F are in opposite directions and oppose each other. Is it then possible to cancel them completely, leaving F undisturbed (to the first order)? That this is indeed possible can be shown as follows. We require:

$$\Delta \left(1 - \frac{1}{M}\right) = 2c\alpha$$

Referring now to Fig. 3, it is seen that if the center of rotation is at C,

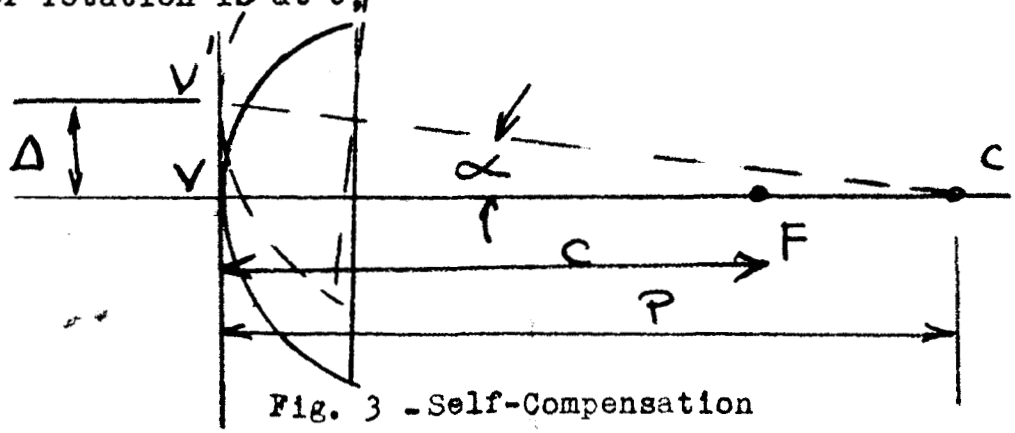

Fig. 3 - Self-Compensation

a distance p behind V, then $\Delta = p\alpha$

$$\therefore p = \frac{\Delta}{\alpha} = \frac{2c}{1-\frac{1}{M}}$$

if the virtual image at F is to stay there undisturbed

$$\therefore p = \frac{2Mc}{M-1} = \frac{2h}{M-1}$$

$$= \frac{2hc}{h-c}$$

It can be shown that this is also the radius of curvature of the hyperboloid at the vertex, V. Thus the center of rotation of the mechanical supporting structure should be placed at the center of curvature of the hyperboloid taken at the vertex.

When $h \gg c$,

then $p \approx 2c$

Examples If the focal length of the paraboloid is 60 feet, then referring to cases 1, 2, 3, on JPL sketch sheet 2-10-4004, dated 1-13-61 and referring to the Westinghouse proposal as Case 4, we obtain:

Table I.

Case	1	2	3	4
A (feet)	24.4	32.6	35.6	45
d (feet)	9.9	13.3	17.2	24
c (feet)	2.25	3.0	3.8	5.2
h (feet)	22.15	29.6	31.8	39.8
p (feet)	5.0	6.7	8.6	12.0
M	9.8	9.9	8.4	7.7
e	1.23	1.23	1.27	1.30

It is seen that p is always alightly more than twice c, being about 2-1/4 times c. Thus if case 2

were selected, the hyperboloid supports should be arranged to 'hinge' about a fixed point on the focal axis, at a distance $p \simeq 6.7$ feet behind the hyperboloid vertex. Small rotations about this point should result in only second-order beam pointing errors.

System to establish parabolic contours 3/1/61 Vaughan

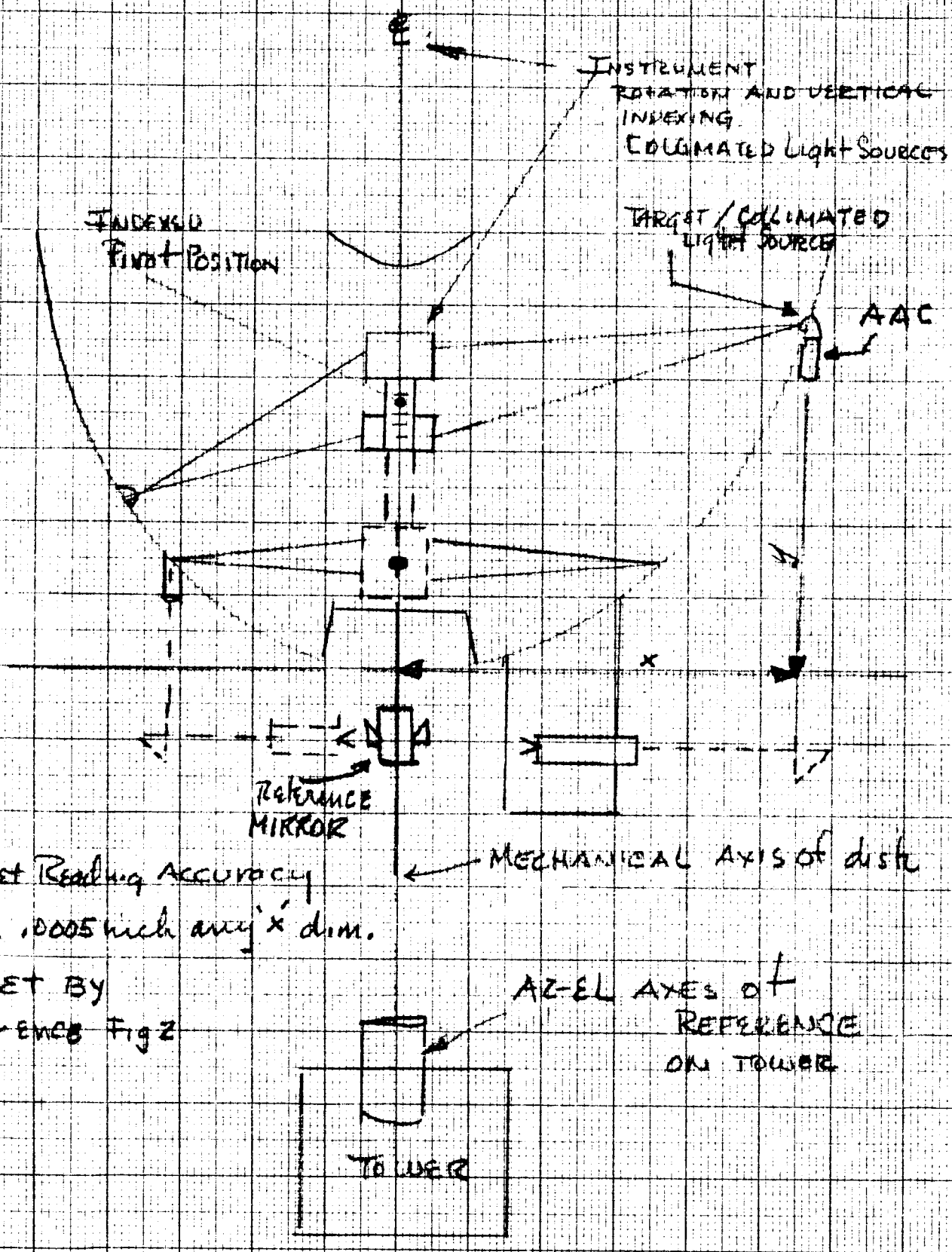

Target Reading Accuracy to ± .0005 inch any 'x' dim.

℄'s SET BY reference Fig 2

WESTINGHOUSE ELECTRIC CORPORATION

C-I-29 CURVE NO. Fig 2 sht 1

3/1/61 J Gumpert

Parabolic 'Dish' at USIP - UPL

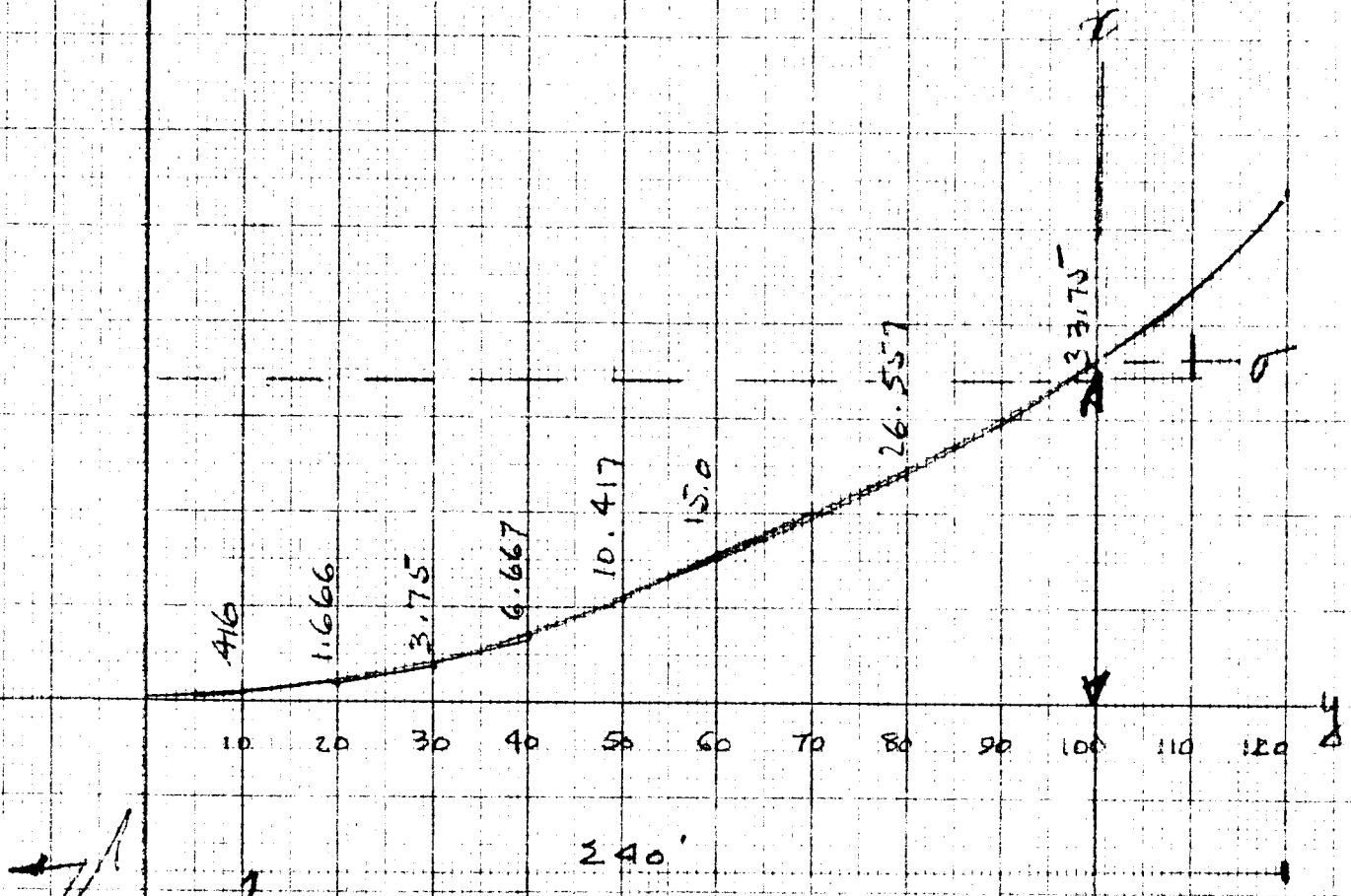

240'

90°

MAJOR AXIS

$x = \frac{y^2}{240}$

{ These points and 0 must always be read in x, y co-ordinates

FORM 1769

SIGNATURE DAT CURVE NO.

WESTINGHOUSE ELECTRIC CORPORATION

C-I-30 CURVE NO. Fig 3 } Elevation

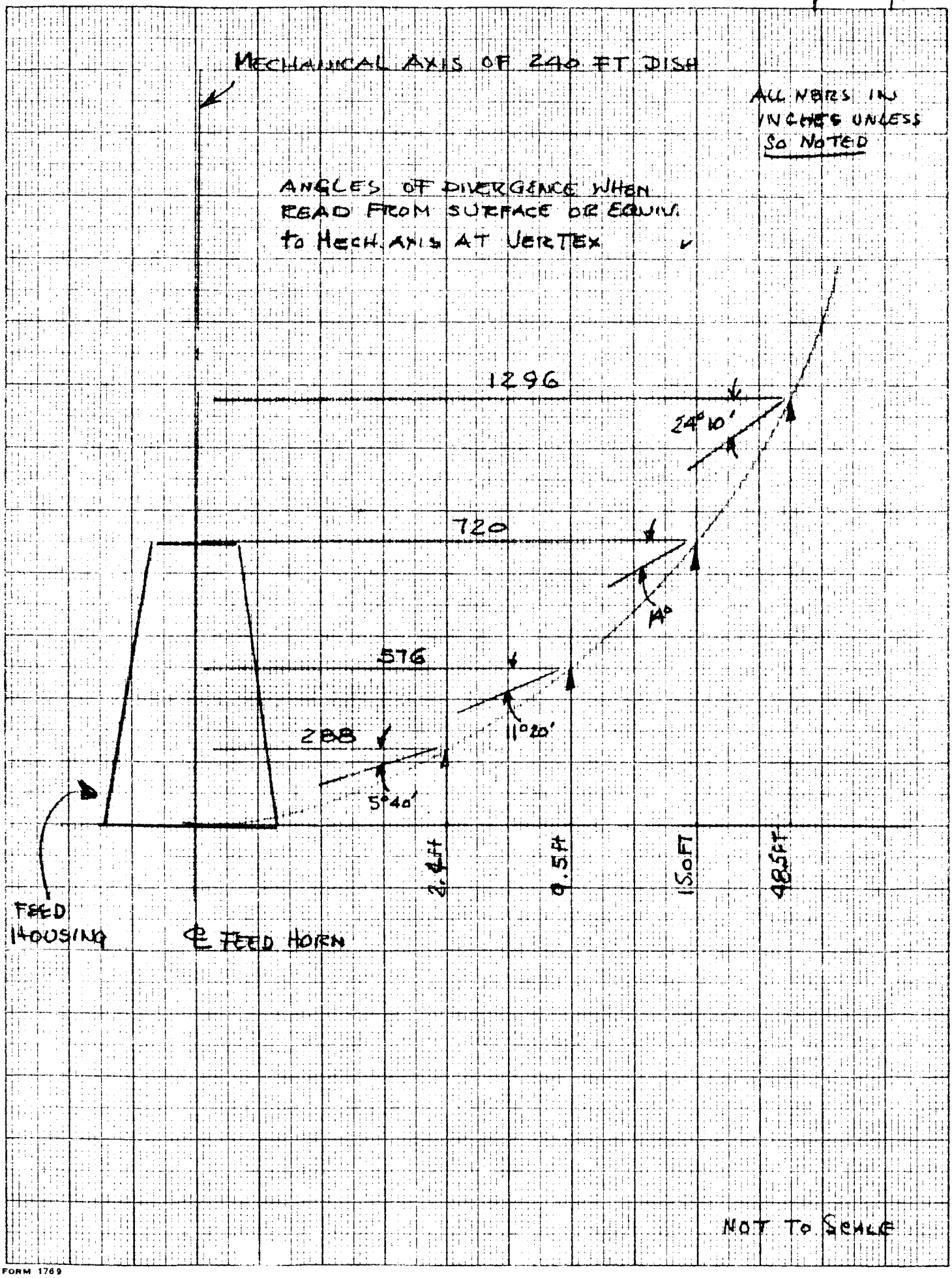

FORM 1769

SIGNATURE DATE CURVE NO.

PLAN VIEW of PARABOLIC DISH

⊕ AAC

× Light Sources (Collimated) or Monachromatic

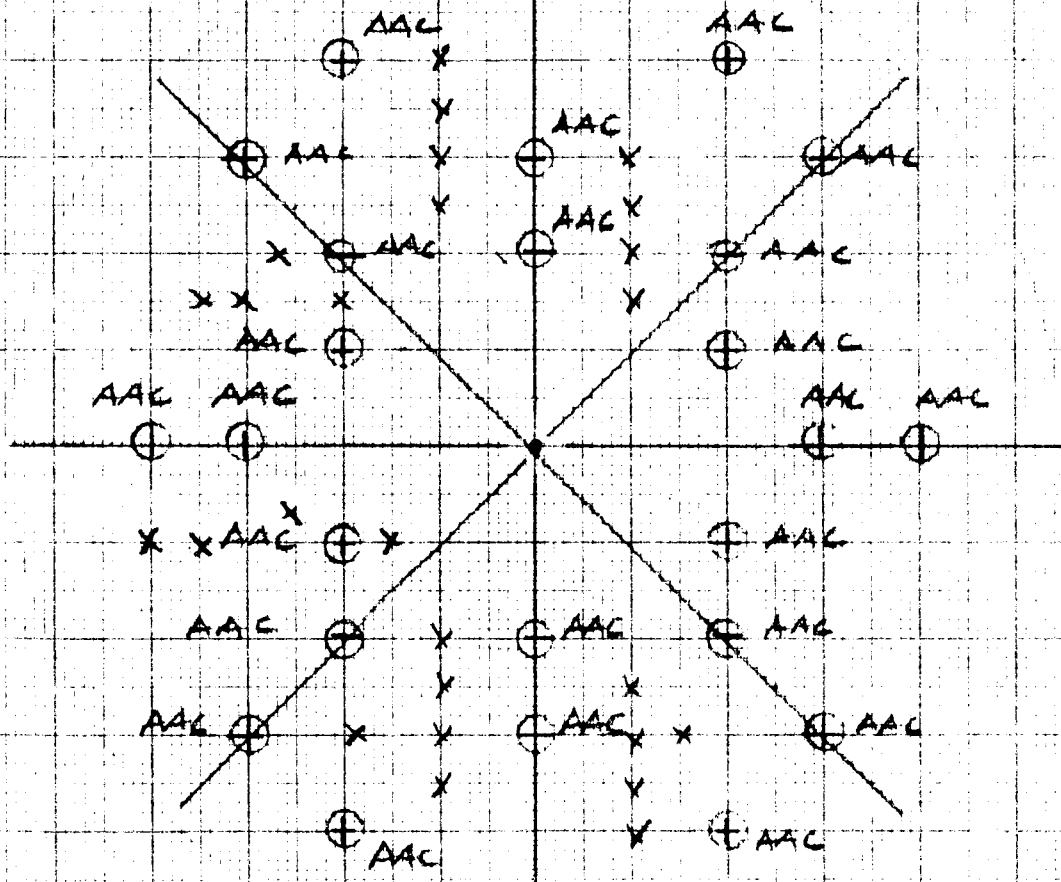

PROBABLE ARRANGEMENT OF AAC FOR CONTINUOUS SURFACE MONITORING.

COLLIMATED BEAM SYSTEM

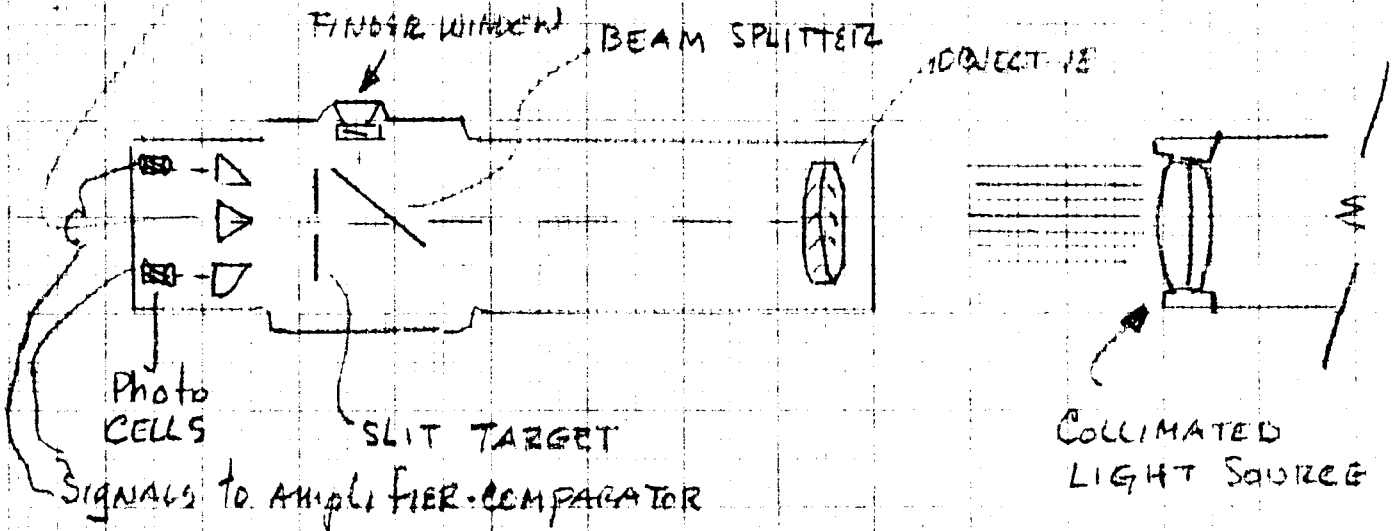

Signals generated by the photo-cells are compared in an amplifier and the difference is transmitted to an indicator for display. The amplifier output can be readout on a moving coil instrument calibrated in seconds of arc.

Schematic of axis sensing & alignment

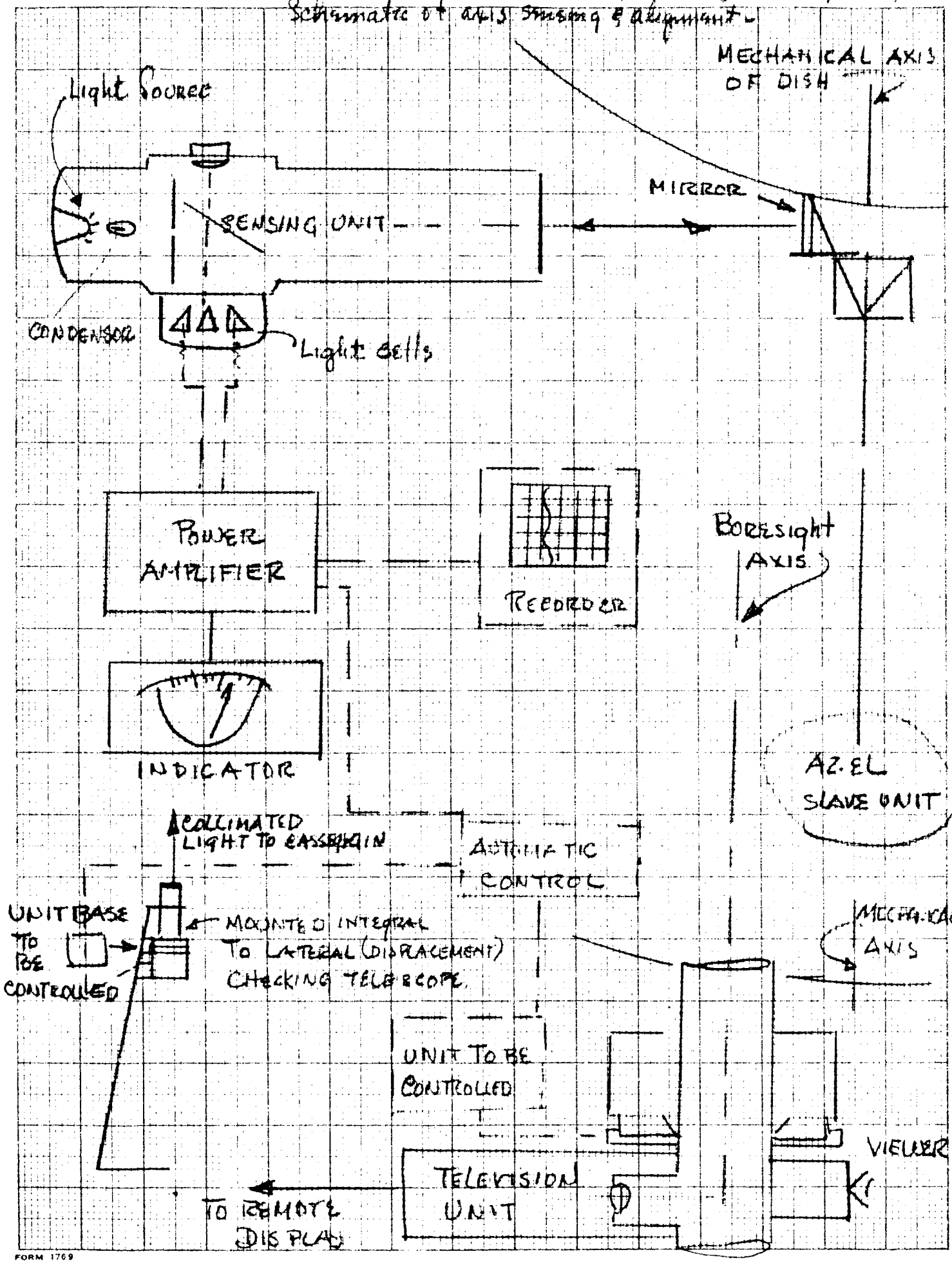

PARALLELISM of CASSEGRAIN AXIS to MECHANICAL AND BORESIGHT AXES

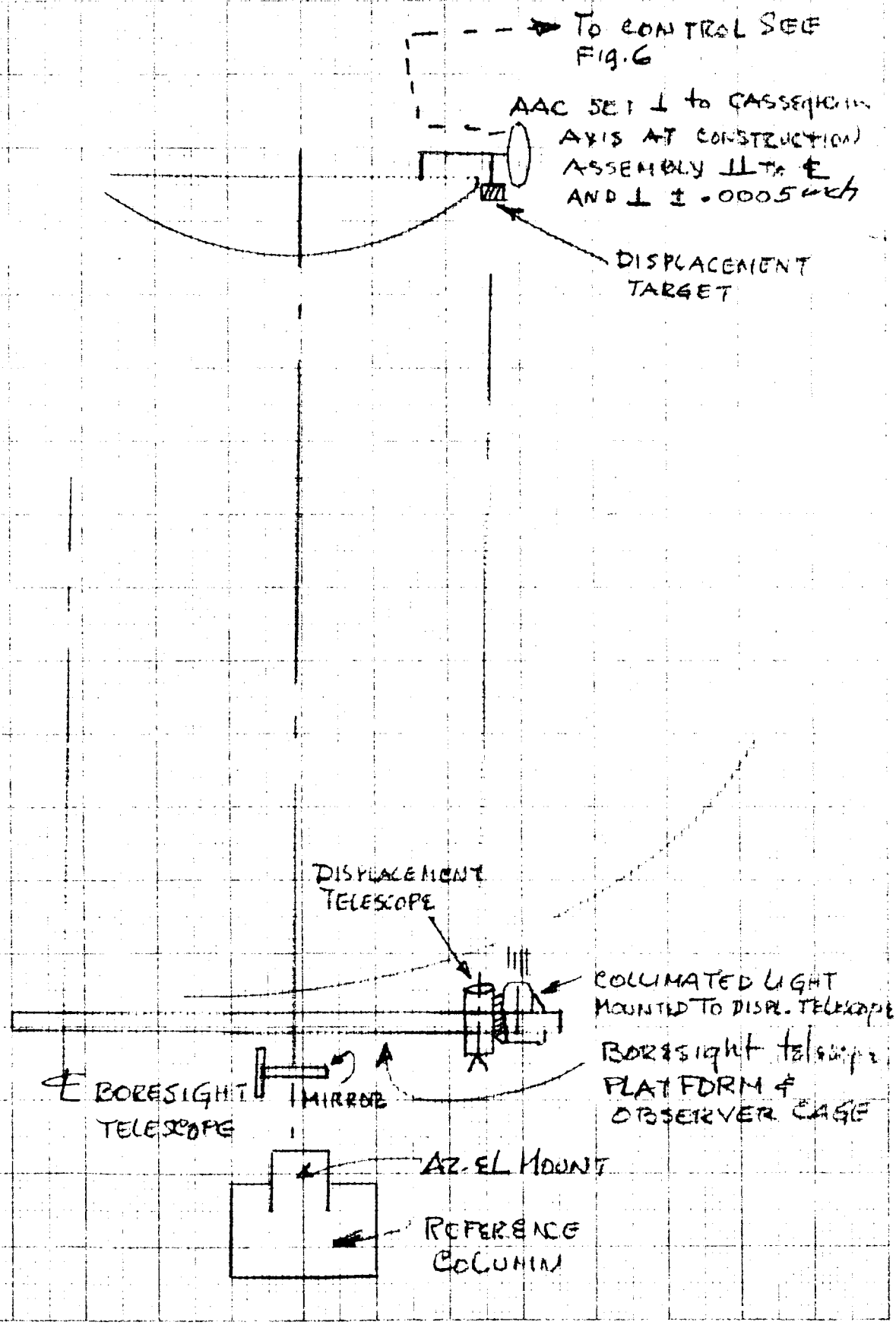

Monitoring System on Surface

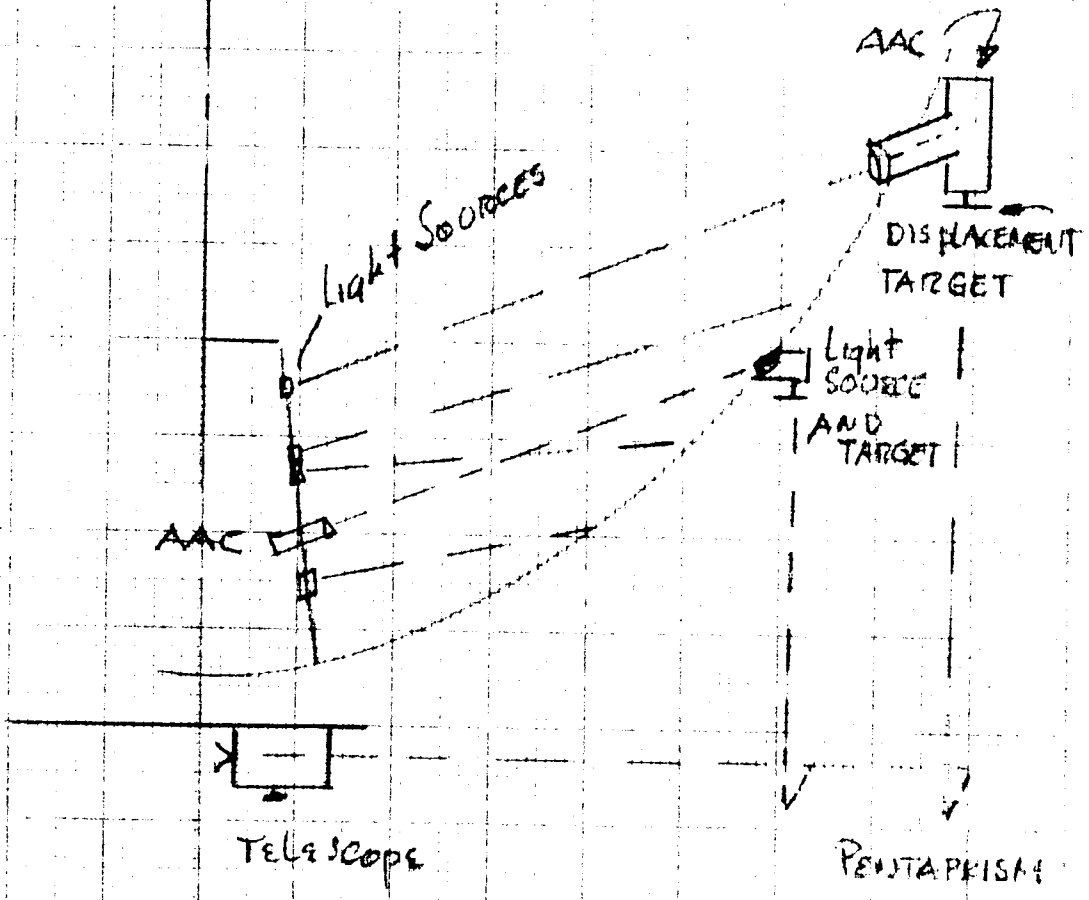

Mech Axis / Boresight Axis

1. Light Sources to be collimated on MONOCHROMATIC AND ALIGNED
2. AAC UNITS
3. PENTAPRISMS External ON SUPPORT STRUCTURES

ALL Items typical for DISCRETE PLACEMENT

SEE Fig 1-2-3-4 for positioning of UNITS

WESTINGHOUSE ELECTRIC CORPORATION

C-I-36

CURVE NO. Fig 9

Sigma

Coordinate Scale for σ readings –

k = constant of Parabola Axis FOR LIMIT CORRECTION

CORRECTION AMOUNT	Sta	X (FT)	Y (mils)	Δ X	Δ Y	k
0	1	10	+.128	0	0	

FORM 1759

SIGNATURE DATE CURVE NO.

The System for off SURFACE Monitoring -

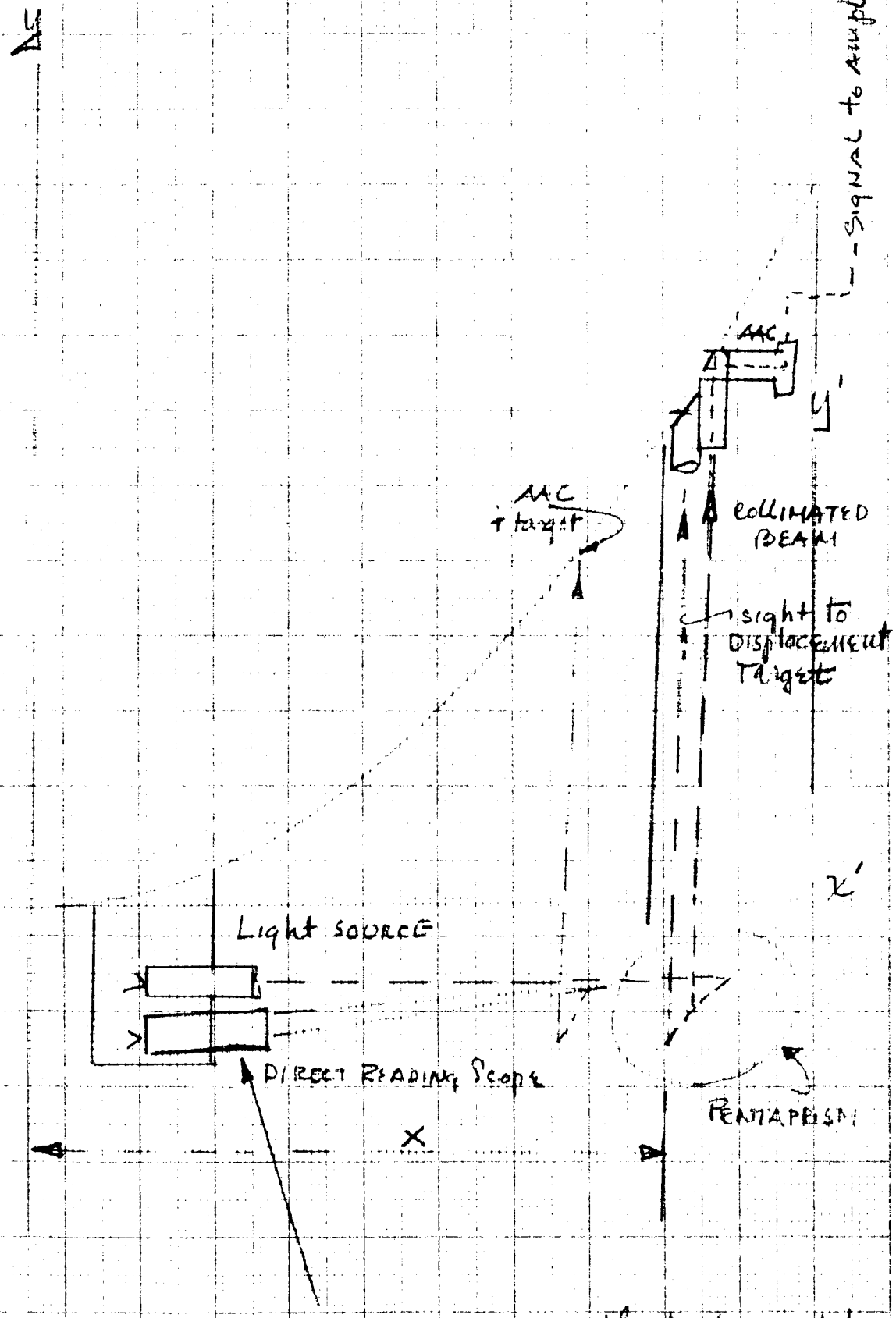

CALIBRATED - DIRECT READING SURFACE with displacement target to be read by telescope to ± 0.001 inch for position checking and/or

II. REFLECTOR DESIGN

The general arrangement of the elevating structure is shown on arrangement Dwg. L-4794 and in the photographs of the model in Section III. Details of the structural members are now shown, only the envelopes of the structural parts are depicted.

A. REQUIREMENTS

The deflection requirements of the antenna surface are such that the deviation of the surface from the paraboloid at any angle of elevation shall not be more than .25 inches rms. It is also desirable to have the least deviation in the middle portions of the surface since the illumination is greater in this area.

The torsional stiffness requirements (rotation of one trunnion girder relative to the other) is 1.0×10^{10} lb/ft./RAD. This requirement is based on the second mode of torsional vibration about the trunnion axis with the elevation gear locked. Statically determinate analysis indicates the structure is 50% above this.

A third requirement of the elevating structure is ease of erection. A minimum amount of false work should be required to support the structure during erection.

A fourth and most important requirement is that weight be kept to a minimum. Due to the large

focal length to diameter ratio the penalty of excess structure weight is two-fold since increased counter weighting is required to balance structure weight.

B. ELEVATION STRUCTURE

Initial design studies of the elevating structure indicated that a ring-radial girder type design would be advantageous. With the advent of the Ground reference tower, the available depth of the ring and the radial girders was decreased; this reduction in depth then required a structural weight which was greater than the box structure.

An early design concept of the box structure utilized a double primary girder design - here again due to space limitations the depth of the two trunnion girders on each side was unequal. This unequal depth of girders introduced variable deflections on the antenna surface with respect to elevation angle. The single girder split tower was conceived which eliminated this problem and reduced the weight of the elevating structure.

The present design has a square primary girder system and a series of secondary girders which carry the load to the primary system. The trunnion shaft is located at the midspan of the trunnion girders. This shaft is supported by two hydrostatic pad bearings. The thrust loads are carried from the chords of the secondary structure to the trunnion shaft by compression and tension members.

The design criteria of these members must be based on the combined spring constant of the azimuth structure and the elevating structure. The present analysis of reflector surface deflections is confined to two angles of elevation - 0^{o} and 90^{o} and is further limited to dead weight loads only. Preliminary analysis assuming statically determinate systems indicate the maximum deflection of the primary girders to be .270 inch. On the basis of the statically determinate analysis the primary and secondary girders were sized and a matrix analysis of half of the antenna structure is in progress. The matrix analysis presently being used is a 25 x 25 matrix of the secondary system and is based on beam theory rather than structural theory. The deflections obtained from beam theory are assumed to be 2/3 the deflections which would be obtained using truss theory. This analysis is being made with the antenna at the 90^{o} position with only dead loads applied. The present matrix analysis is considered to yield only qualitative results with respect to the deflection and load distribution of the secondary and primary system. It is expected that the results of this analysis will lead to a final truss design.

The final matrix analysis will consist of a 36 x 36 matrix which will consider both the primary and secondary structure. The completion of this

analysis should give realistic values of the deflections of the elevating structure.

Preliminary work done with the antenna at the 0^{o} position indicates that the deflections will be much less than at the 90^{o} position. This analysis will not be fully considered until the 25 x 25 matrix solution is completed.

C. CASSEGRAIN SUPPORT

The design of the Cassegrain support is dictated primarily, by the allowable deflections of the sub reflector, R-F considerations of the support and resonant frequency requirements of the Cassegrain supports. Optical analysis of the sub-reflector show that the error in pointing can be held to a minimum if the error due to angular rotation is counter-acted by the error due to lateral displacement. Thus the support system should be designed so that there is an equivalent fixed point of rotation for the sub-reflector. Optical analysis shows this point to be behind the sub-reflector at a distance of approximately 2-1/4 times the depth of the sub reflector.

Present design studies are based on two configurations a quadruped with straight legs and a crossed parabolic arch.

At this time no definite conclusions have been reached as to which configuration would be most satisfactory. Major problem in this area,

presently, is the lateral resonant frequency of the supports.

D. ANTENNA SURFACE

The design concept of the antenna surface must consider weight, wind, thermal deflections, minimum weight and ease of fabrication. Two basic concepts are being investigated. The first is to restrain each panel at its boundaries and allow thermal expansion to take place as buckling within the panels. The second concept is to allow free thermal expansion of the panels and utilize expansion joints at the boundaries. In either concept both mild steel and aluminum is being considered. An assigned weight of 15 lb/ft.^{2} has been allowed for the surface but it presently appears that the second concept of allowing free expansion with expansion joints at the boundaries will be well below this figure.

A heat reflective, protective paint will be necessary to limit temperature differentials and to provide corrosion protection. Two paint systems have been selected and evaluation studies are presently being made.

The paint systems have the same preparation, i.e., a sandblast, wash primer and zinc chromate in alkyd vehicle primer.

The finish coat differs in that one system uses a titanium dioxide latex water base. The

second system would use a titanium dioxide alkyd paint. Evaluation studies are presently being made on the two systems, preliminary work indicates that the water base paint is preferable since it is flatter, would not become as brittle with time and will not discolor as much with time.

III. SUPPORT STRUCTURE

Pointing accuracy requirements of the antenna dictate a support structure designed primarily for stiffness and smooth rotation about its axes. Vibratory characteristics of the structure and its components must be such that no resonances can occur which will impair the accuracy of the antenna. The criteria established is that all modes of vibration shall be 3 cps or above.

The general arrangement of the mount support structure is shown on arrangement drawing. L-4794 and in the photographs of the model. Structural members are not shown in detail, rather the space envelopes encompassing the structural steel truss framework are indicated. Initial studies show that the mount structure can readily meet all requirements for strength, stiffness and vibrational characteristics. Design requirements have been established and design studies are currently being conducted to determine best configuration of structural members.

The mount is essentially an integral structural frame carrying all of the weight and loads of the rotating parts to the foundation. Four equally spaced bearing points support the mount from the fixed azimuth bearing. A central pintle bearing positions the mount and carries any lateral loads on the antenna. The elevating parts are carried by trunnion bearings mounted on towers on the mount structure.

The azimuth bearing points are located in line with the trunnion bearings to achieve maximum stiffness of the towers. Also, an integral part of the mount structure is a windshield which completely encircles the ground reference tower, and supports the R-F equipment room. Mounted on and rotating with the mount structure are azimuth and elevation drive units and the bearing lubrication systems.

A. LOADS AND MOMENTS

The loads and moments acting on the structure result from static weights, acceleration forces, and wind pressure forces. Fig. 1 summarizes the calculated values of the weight loads, antenna inertias, and moments due to acceleration. Wind loads are given in a following section.

The magnitude and direction of the loads acting on the trunnion, pintle and azimuth bearings are given on Figs. 2, 3, and 4.

TABLE 1. WEIGHTS AND INERTIA MOMENTS

STRUCTURE	WEIGHTS LBS x 10^6	INERTIA LB FT^2 x 10^{10}	
		MIN	MAX
REFLECTOR	3.5	1.7	2.1
MOUNT	3	2×10^{10}	

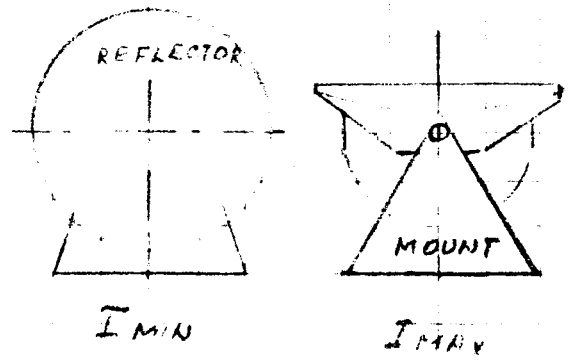

TABLE 2. DRIVE MOMENT DUE ACCELERATION

DRIVE	ACC. M LB FT x 10^6			
	.20°/SEC^2		1°/SEC^2	
	MIN.	MAX.	MIN.	MAX.
ELEVATION	1.54		9.2	
AZIMUTH	4	4.4	20	22

BEARING LOADS

TRUNNION JOURNAL BEARING

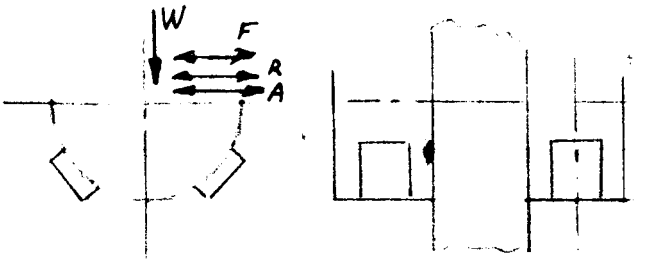

THE POSSIBLE LOADINGS ON TRUNION BEARINGS

W - REFLECTOR WEIGHT — 1

F - WIND LOAD

R - DRIVE REACTION AGAINST WIND MOMENT LOAD

A - ACCELERATION DRIVE REACTION AGAINST MASS INERTIA

TABLE 1 TRUNION JOURNAL BEARING

WEIGHT LOAD	ACCELERATION DRIVE				WIND LOADS - MAXIMUM			
	ELEVATION		AZIMUTH		WIND LOAD		WIND MOMENT	
	.2°/SEC²	1°/SEC²	.2°/SEC²	1°/SEC²	30 M/H	70 M/H	30 M/H	70 M/H
1.75×10^6 LBS	±22000 LBS	±60000 LBS	±29000 LBS	±78000 LBS	$\pm .18 \times 10^6$ LBS	$\pm .43 \times 10^6$ LBS	±90000 LBS	$\pm .21 \times 10^6$ LBS

TRUNNION THRUST BEARING

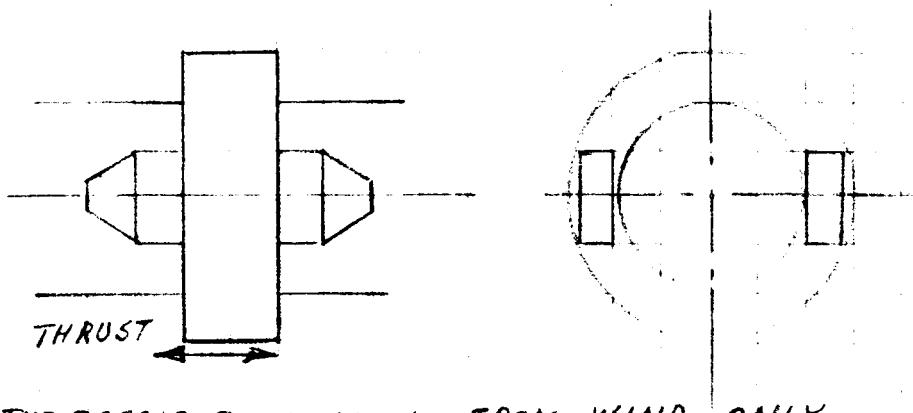

THE POSSIBLE LOADING FROM WIND ONLY

T_{MAX} = 100000 LBS

PINTLE BEARING

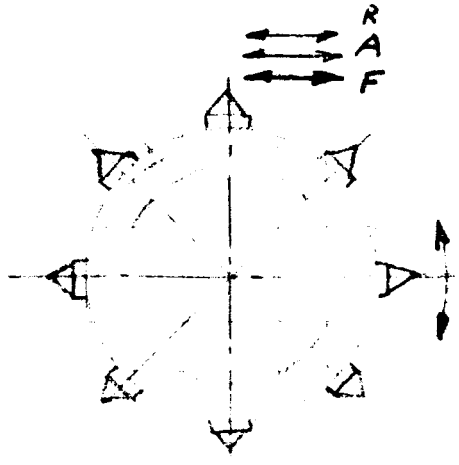

POSSIBLE LOADS:

F WIND LOAD

A ACCELERATION ON ELEVATION DRIVE

R DRIVE AGAINST WIND MOMENT ON ELEVATION DRIVE

TABLE 2 PINTLE BEARING

WIND LOADS IN LBS				Acc. LOAD IN LBS	
WIND LOAD		WIND MOM. EL. DRIVE			
30 M/H	70 M/H	30 M/H	70 M/H	.2°/sec²	1°/sec²
$.36 \times 10^6$	$.86 \times 10^6$	$.18 \times 10^6$	$.42 \times 10^6$	$.044 \times 10^6$	$.12 \times 10^6$

AZIMUTH THRUST BEARING

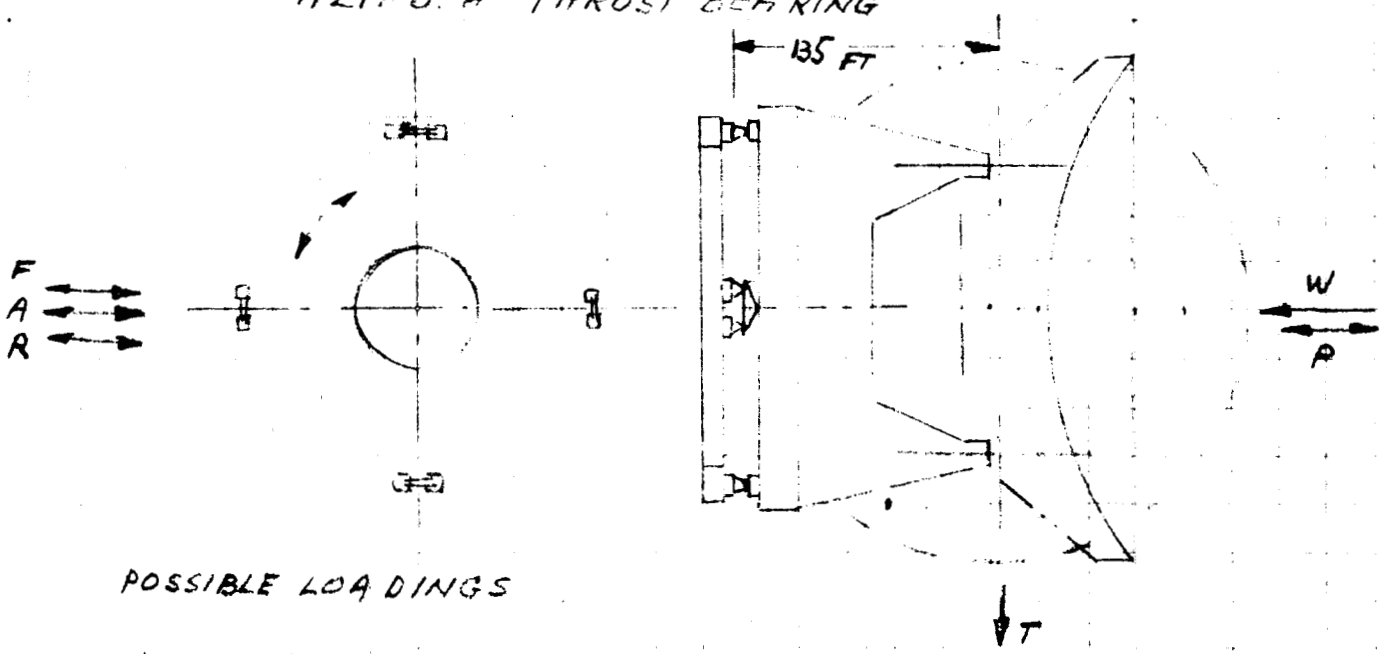

POSSIBLE LOADINGS

W – WEIGHT OF REFLECTOR AND MOUNTS

P – WIND LIFT LOAD

F – WIND LOAD OVERTURNING MOMENT

A – ELEVATION ACCELERATION OVERTURNING MOMENT

R – ELEVATION DRIVE OVERTURNIG MOMENT

T – WIND THRUST BEARING LOAD – OVERTURNING MOMENT

TABLE 3 AZIMUTH THRUST BEARING

WEIGHT LBS	OVERTURN. MOMENT LB FT	ACCEL. MOM ELEV. DRIVE LB FT		WIND LIFT LBS	WIND LOADINGS LB FT				REMARKS
					WIND LOAD MOM.		ELEV. DRIVE WIND MOMENTS		
		.2°/SEC²	1°/SEC²		30 M/H	70 M/H	30 M/H	70 M/H	
6.5×10^6	450×10^6	6×10^6	16×10^6	$+.65 \times 10^6$ $-.18 \times 10^6$	49×10^6	116×10^6	24×10^6	56×10^6	THRUST WIND LOAD NEGLECT.

Wind Forces

The wind forces acting on the antenna have been calculated considering the geometry of the structure and assumed air flow characteristics. In addition, data from wind tunnel tests of a model of a similar antenna conducted by Massachusetts Institute of Technology (MIT Wind Tunnel Report 993) was converted to forces and moments acting on the 240 foot antenna under consideration. The wind tunnel data is used as an order of magnitude check on the calculated values as well as giving a more complete qualitative picture of the variation of forces and moments over the complete range of azimuth and elevation angles. The wind tunnel data cannot be used directly because the model tested had a different F/d ratio and different supporting structure. It is felt that the maximum air forces from the wind tunnel tests should not differ greatly from those acting on this antenna. The moments, however, may differ considerably due to differences in location of the azimuth and elevation axes with respect to the dish and structure.

The following table gives the calculated values of maximum wind forces and moments acting on the antenna. The calculations are based on a velocity gradient varying approximately with the 1/7 power of height from the specified velocity at 50 feet elevation, and on a velocity pressure from the ASCE formula, $p = .0033V^2$.

Maximum Wind Loads

Wind Vel. MPH	(1) $P_{50'}$ #/Ft^2	(2) Wind Force-#	(3) $M_{Elevat.}$ #-Ft (Pitching Moment)	(4) $M_{Azimuth}$ #-Ft. (Yawing Moment)
30	2.9	175 000	2.9×10^6	2.5×10^6
45	6.6	395 000	6.8×10^6	5.7×10^6
60	11.7	702 000	11.7×10^6	10.0×10^6
70	16.0	960 000	16.0×10^6	13.7×10^6
120	46.7			

(1) Wind pressure due to specified velocity at 50 ft. above the ground.

(2) Wind force on 240 ft. diameter dish with center 130 ft. above ground level.

(3) Moment with dish perpendicular to wind and 26° from zenith position.

(4) Moment with dish in vertical direction and wind at an angle of 64° from paraboloid axis.

The following four curves give values of drag, lift, side force, and yawing moment based on the wind tunnel data. It is seen on Curve 1 that the maximum value of drag force at 70 mph 855,000 pounds, compares well with the calculated value of 960,000 pounds given in column 2 of the previous table. The maximum yawing moment on Curve 4, 20,000,000 ft. lbs., is considered high for the 240' antenna since the model had less structure back of the azimuth axis to assist in balancing the wind moment. The calculated value of yawing moment at 70 mph is 13,700,000 ft. lbs.

WIND FORCES

DRAG

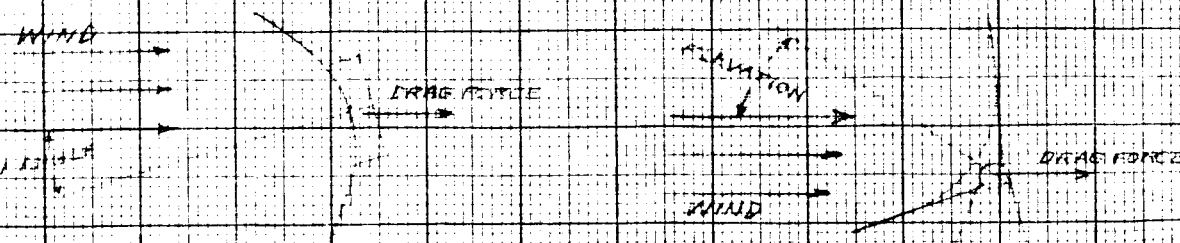

CURVES ARE FOR 70 MPH WIND.
P POINTS ARE FOR 120 MPH WIND.

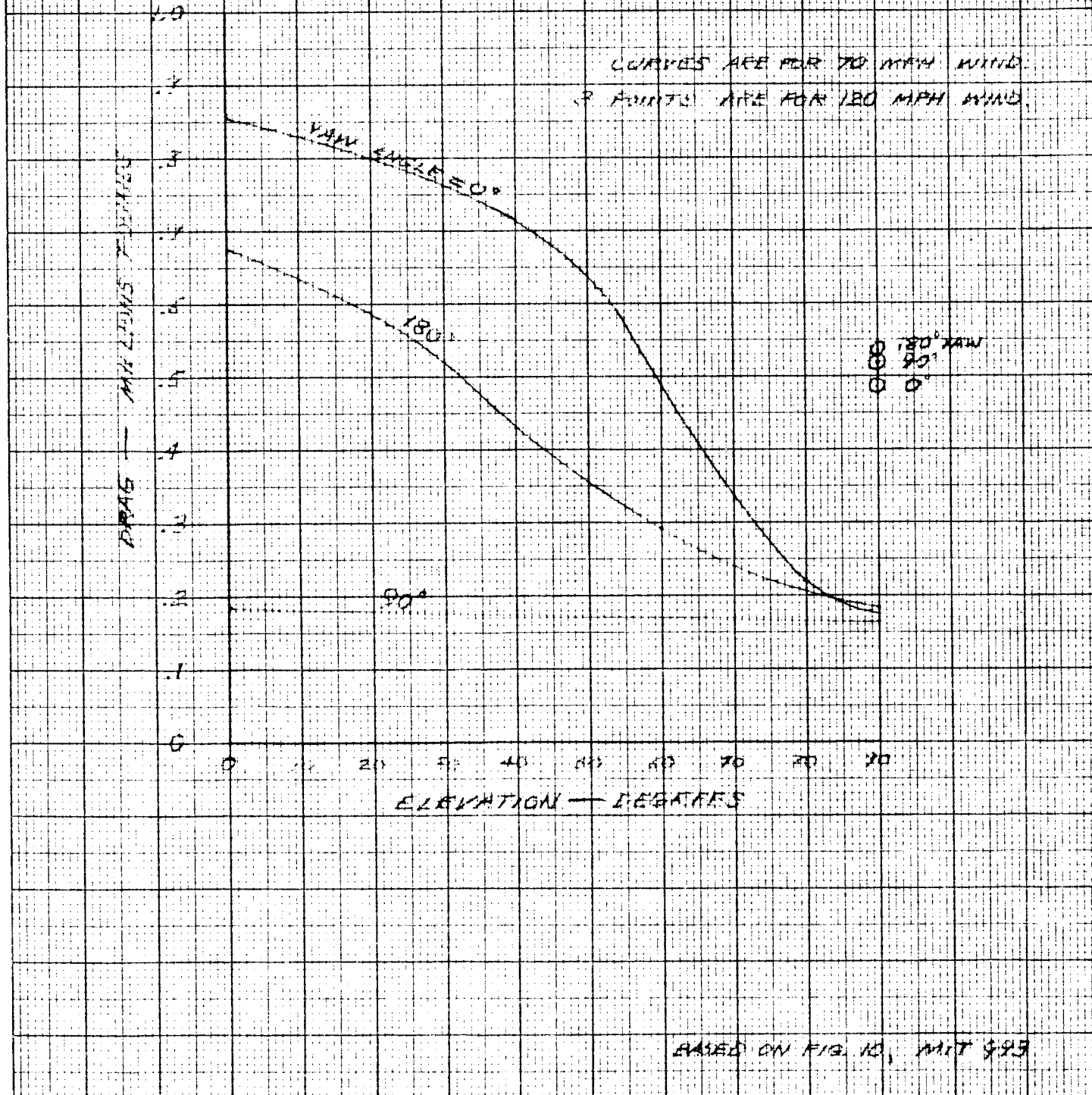

BASED ON FIG. 10, MIT $93

FORM 1/69

SIGNATURE _____ DATE 3-[illegible]-61 CURVE NO. 1

WESTINGHOUSE ELECTRIC CORPORATION

C-III-10 CURVE NO. _____

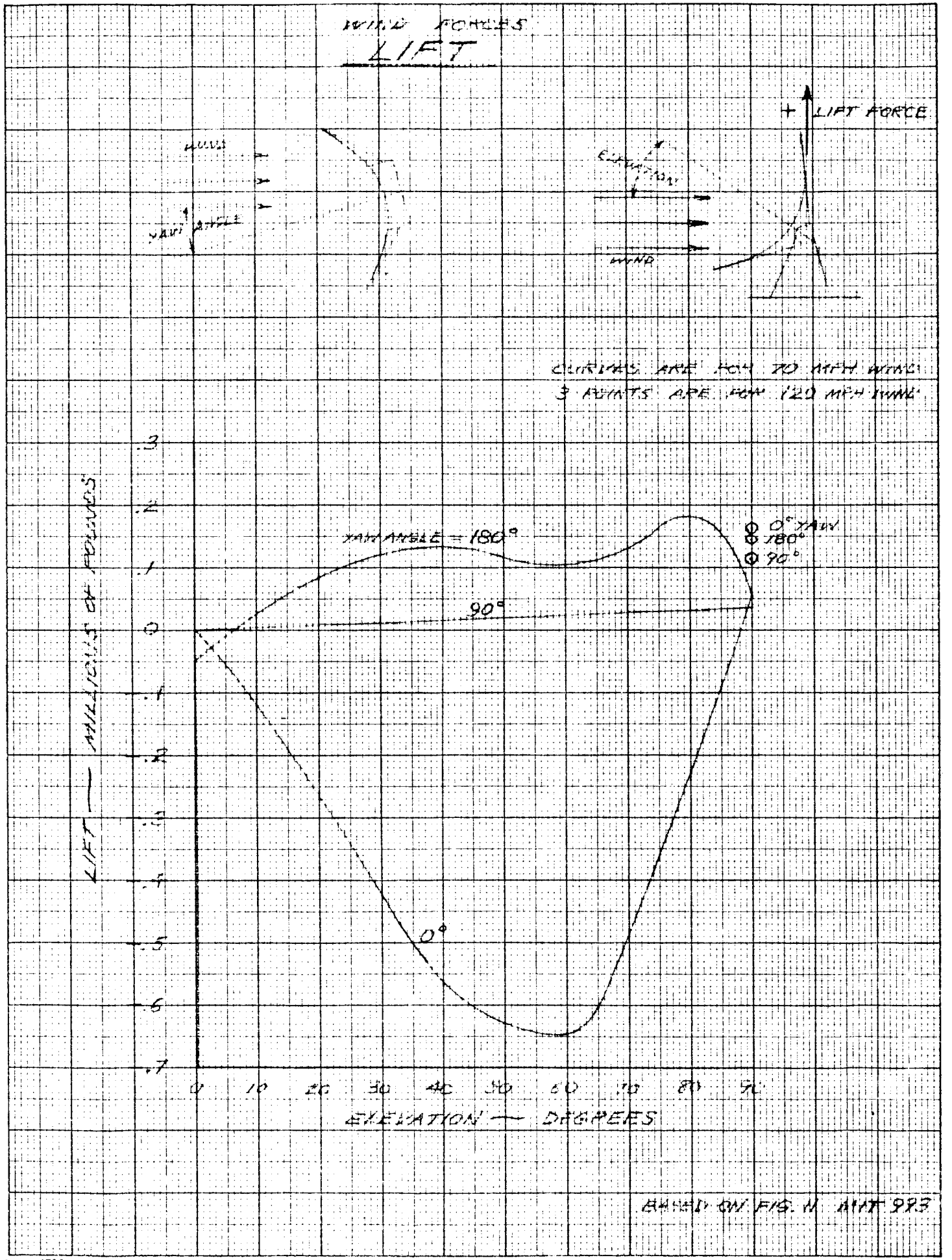

SAME AS FIG. 11 AMT 923

FORM 1769

SIGNATURE _____ DATE 3-5-41 CURVE NO. 2

WIND FORCES
SIDE FORCE

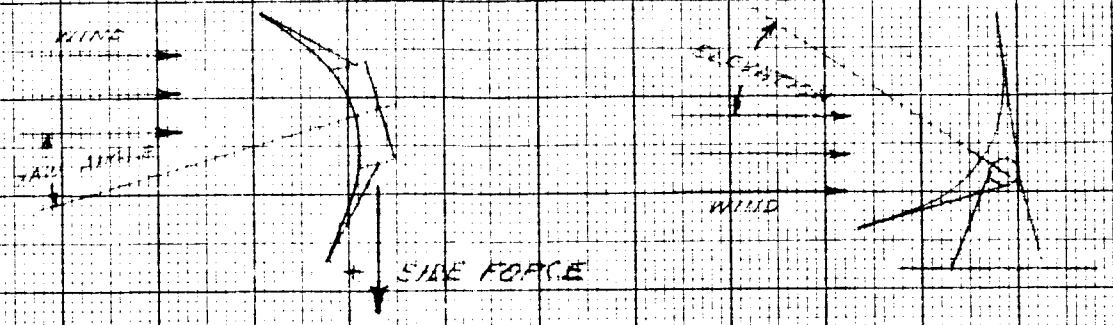

CURVES ARE FOR 70 MPH WIND

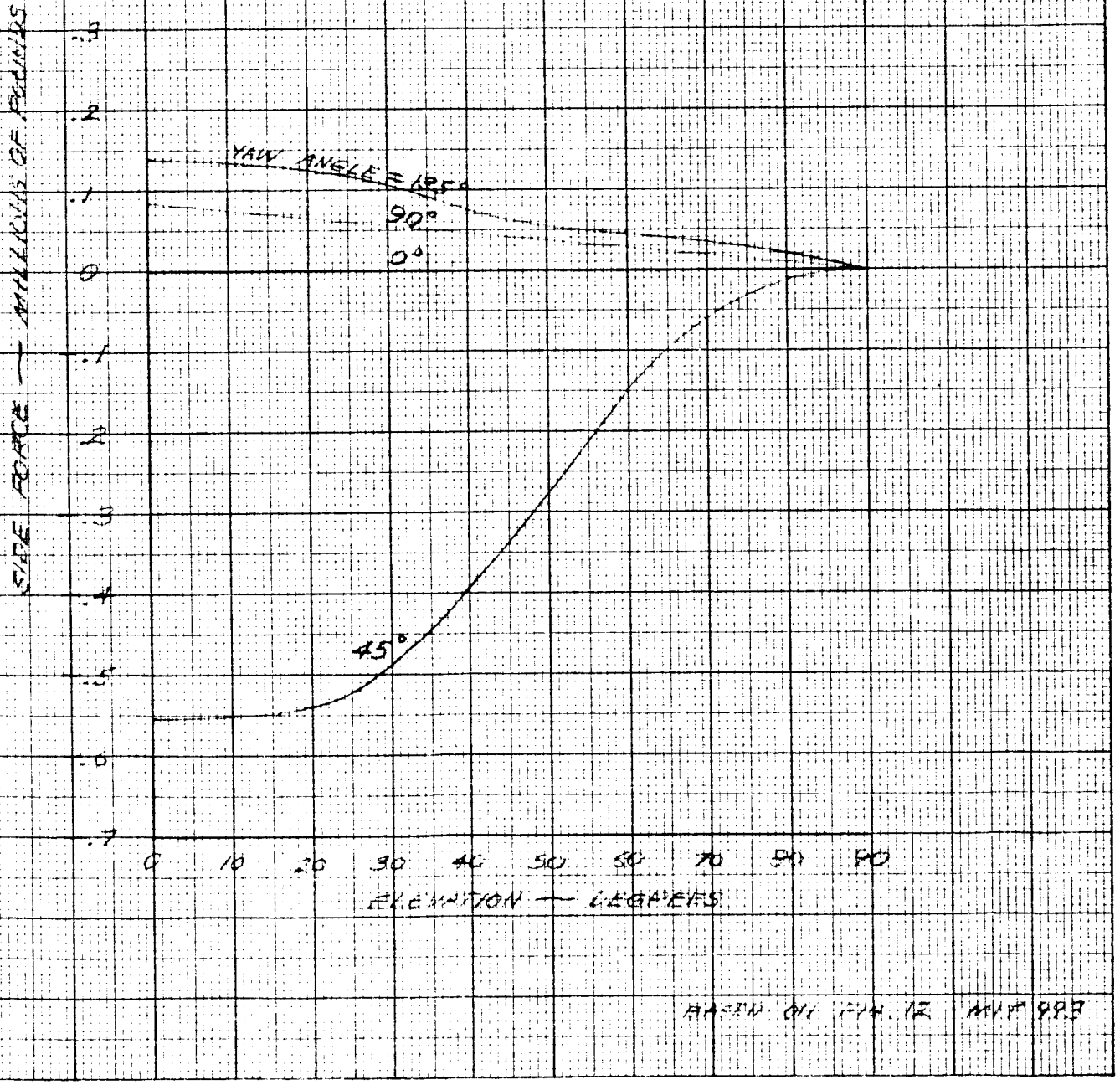

BASED ON 17H.12 MAY 1943

FORM 1769

SIGNATURE _____ DATE _____ CURVE NO. 3

WESTINGHOUSE ELECTRIC CORPORATION

C-III-12 CURVE NO. _____

WIND FORCES
YAWING MOMENT

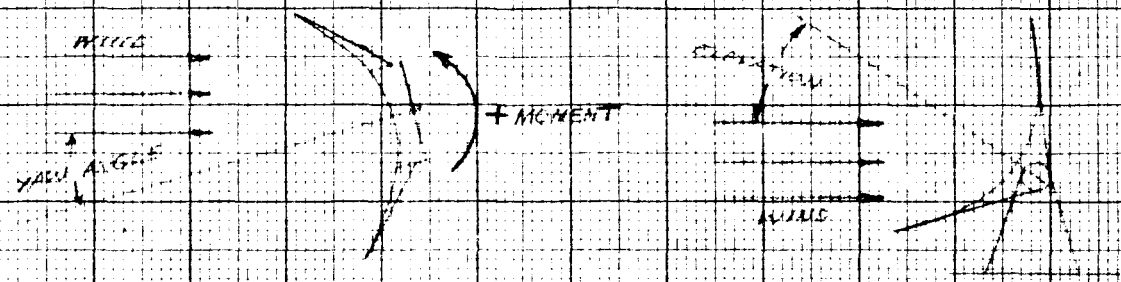

FOR 70 MPH WIND

YAWING MOMENT — FT. LBS. PER FT.

20
10
0
10

YAW ANGLE = 135°
90°
0°
50°

0 10 20 30 40 50 60 70 80 90

INCLINATION — DEGREES

BASED ON FIGURE 16, MIT 1943

FORM 1769

SIGNATURE _____ DATE _____ CURVE NO. 4

B. VIBRATORY CHARACTERISTICS OF MOUNT

The principle modes of vibration of the antenna and supporting structure are shown on Figs. 5 and 6. In all modes the resonant frequency must be above 3 cps. Table 1 on Fig. 5 gives a natural frequency in the vertical direction of 5.8 cps. In this case the mount cross sections are dictated by the torsional and bending spring constant and are more than adequate for vertical deflection. Table 2 shows that an average cross section moment of inertia of 40×10^6 in.^{4} is necessary to obtain the required bending spring constant considering the influence of the mass of the mount.

Table 3 gives a required shear cross section of 650 in.^{2} at an average radius of 70 ft. to exceed the torsional spring constant corresponding to 3 cps vibration with the base fixed.

In Table 4 the torsional frequency considering the gear drive is shown. In this case the natural frequency is 3.5 cps.

Tables 5, 6 and 7 on Figure 6 give natural frequencies for torsional vibration about the trunnion axis considering the elevating drive in three different conditions.

MODES OF NATURAL FREQUENCIES

TABLE 1. VERTICAL VIBRATION

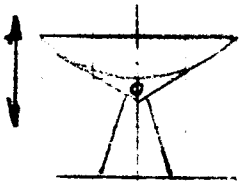

WEIGHT LBS x 10^6	3CPS SPRING CONST	DESIGN SPR. CONST	DESIGN FREQUENCY	REMARKS
3.5	3.2 x 10^6 LB/IN	12 x 10^6 LBS/IN	5.8 CPS	TORSIONAL AND BENDING SPRING CONSTANT NEED LARGER CROSSECTION

TABLE 2 BENDING VIBRATION

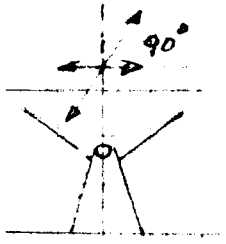

2 MODES

WEIGHT LBS x 10^6	3CPS		NEEDED SP.CO DUE INFL. OF THE MOUNT MASS	SPLIT MOUNT SPRING CONSTANT	REMARKS
	SPR. CON.	DEFL.			
3.5	3.2 x 10^6 LB/IN	1.1"	4.1 x 10^6	2.05 x 10^6	NEEDED AVER. CROSS SEC. I $I_{AV} = 40 \times 10^6$ IN^4

TABLE 3 TORSIONAL VIBRATION - AZIMUTH

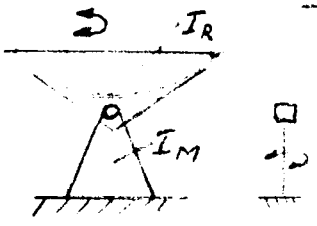

ONE MASS SYSTEM

REFL. INERTIA	MOUNT INERTIA INFLUENCE	CONC. MASS	3CPS SPR. CON	REMARKS
2.1 x 10^10 LB FT^2	.3 x 10^10 LB FT^2	2.4 x 10^9 LB FT^2	27 x 10^10 LB FT/RAD	NEEDED SHEAR CROSSECTION FOR AVERAGE 70 FT A 650 IN^2

TABLE 4 TORSIONAL VIBRATION - AZIMUTH

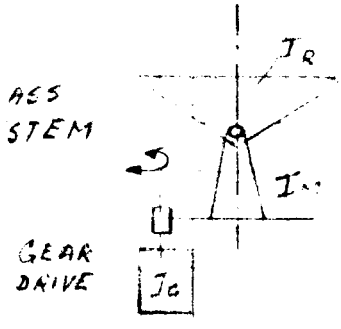

REFL. INER. + M. REFL.	GEAR MASS CONC			CONSTR. SPR. CON.	FREQ.	REMARKS
	MOUNT	GEAR	TOTAL			
2.4 x 10^10 LB FT^2	1.7 x 10^10 LB FT^2	4.2 x 10^10 LB FT^2	5.9 x 10^10 LB FT^2	26 x 10^10	3.5 CPS	TWO MASS SYSTEM

TABLE 5 TORSIONAL VIBRATION - ELEVATION DRIVE

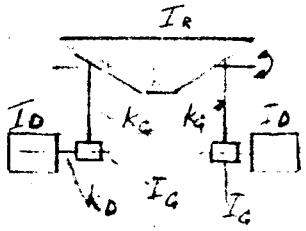

I_R REFL. INERT	GEAR SPRING CONST	GEAR INERTIA	DRIVE SPR. CONST	DRIVE INERTIA	FREQ.	REMARKS
1.7×10^{10} LbFT^2	$2k_G$ 120×10^{10} LbFT/RAD	$2I_G$ $.4 \times 10^{10}$ LbFT^2	$2k_D$ 800×10^{10} LbFT/RAD	$2I_D$ 4.2×10^{10} LbFT^2	7.7 CPS	DRIVES IN PARALLEL

TABLE 6 TORSIONAL VIBRATION - ELEVATION DRIVE

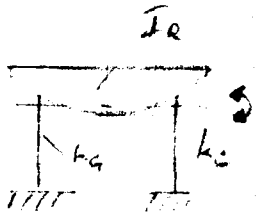

REFL. INERTIA	GEAR SPRING CON	FREQ.	REMARKS
I_R: 1.7×10^{10} LbFT^2	$2k_G$ 120×10^{10} LbFT/RAD	8.7 CPS	GEAR FIXED WITH BRAKES

THBLE 7 TORSIONAL VIBRATION - ELEVATION DRIVE

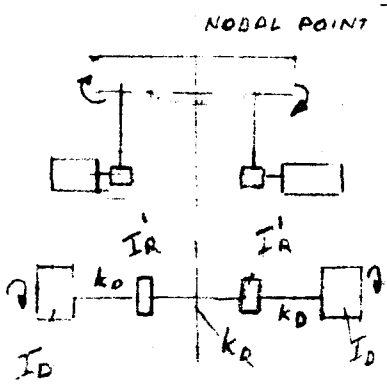

DIVIDED REFL. INERTIA	NEEDED REFLECTOR SPR.CON.	DRIVE SPRING CONST	GEAR INERTIA	FREQ	REMARKS
I'_R: $.43 \times 10^{10}$ LbFT^2	K_R = 15×10^{10} FT/RAD	KD: $400\ 10^{10}$ LbFT/RAD	I_D: 2.1×10^{10} LbFT^2	3CPS	THE DRIVES OUT IN PHASE

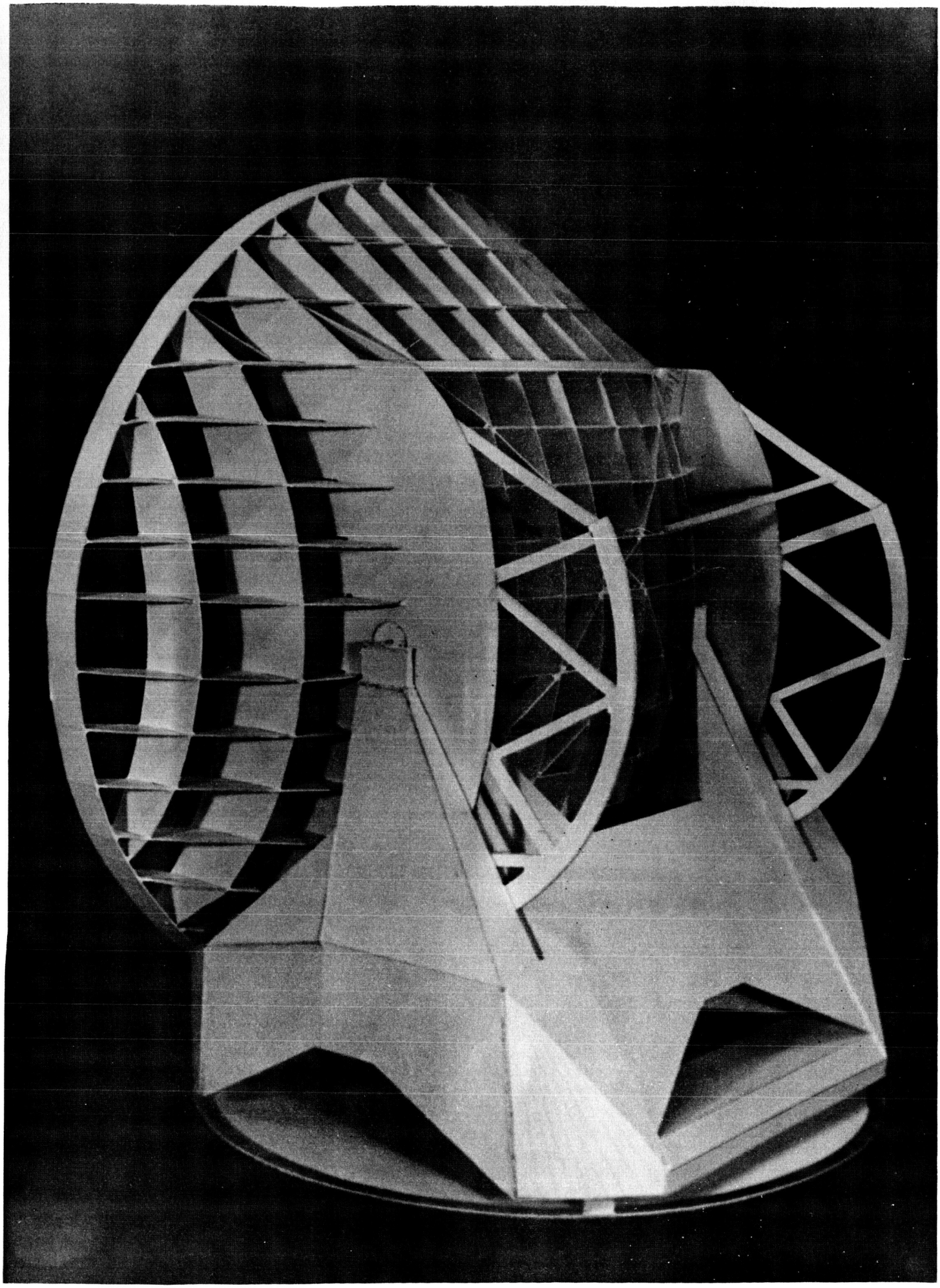

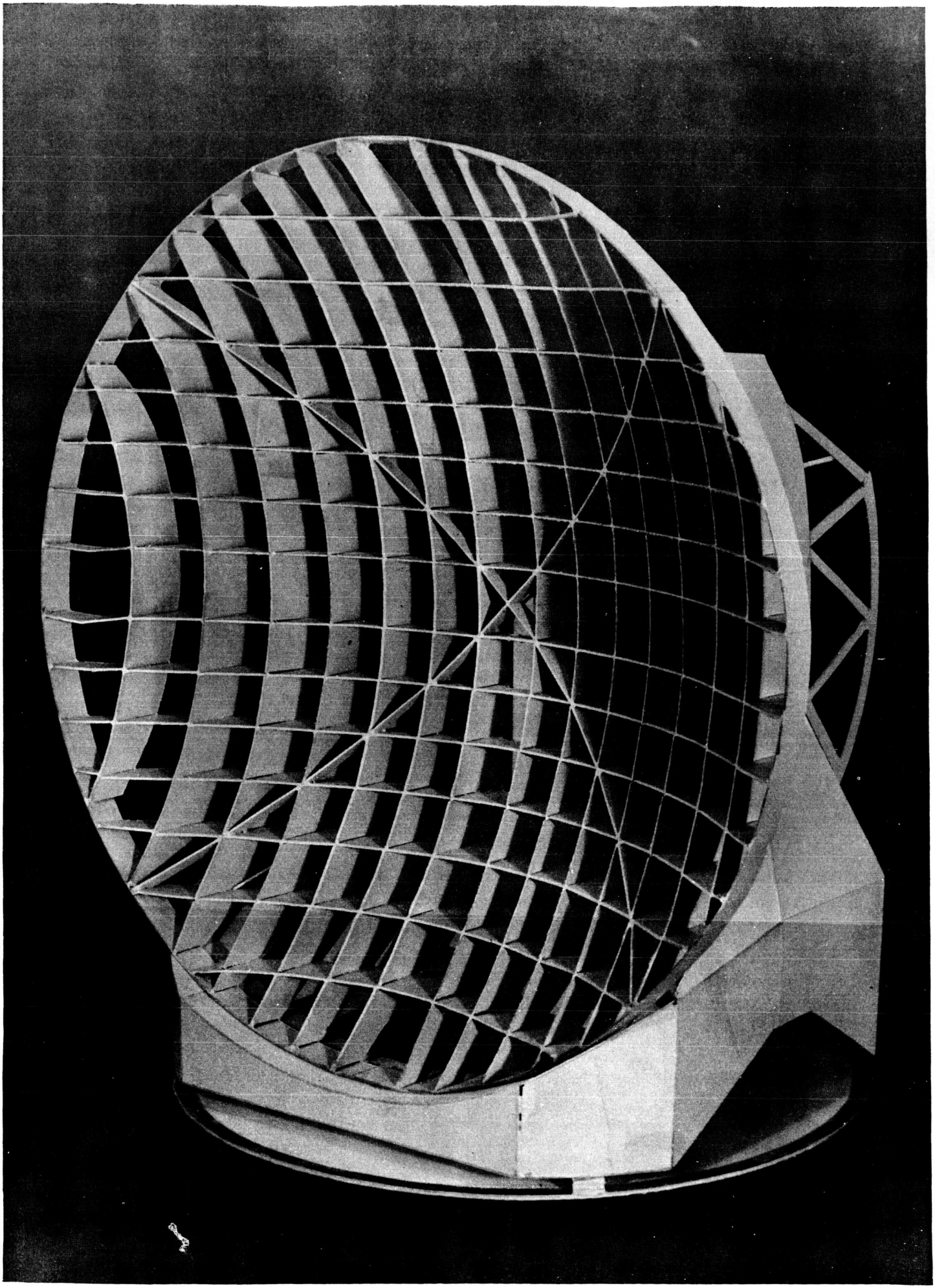

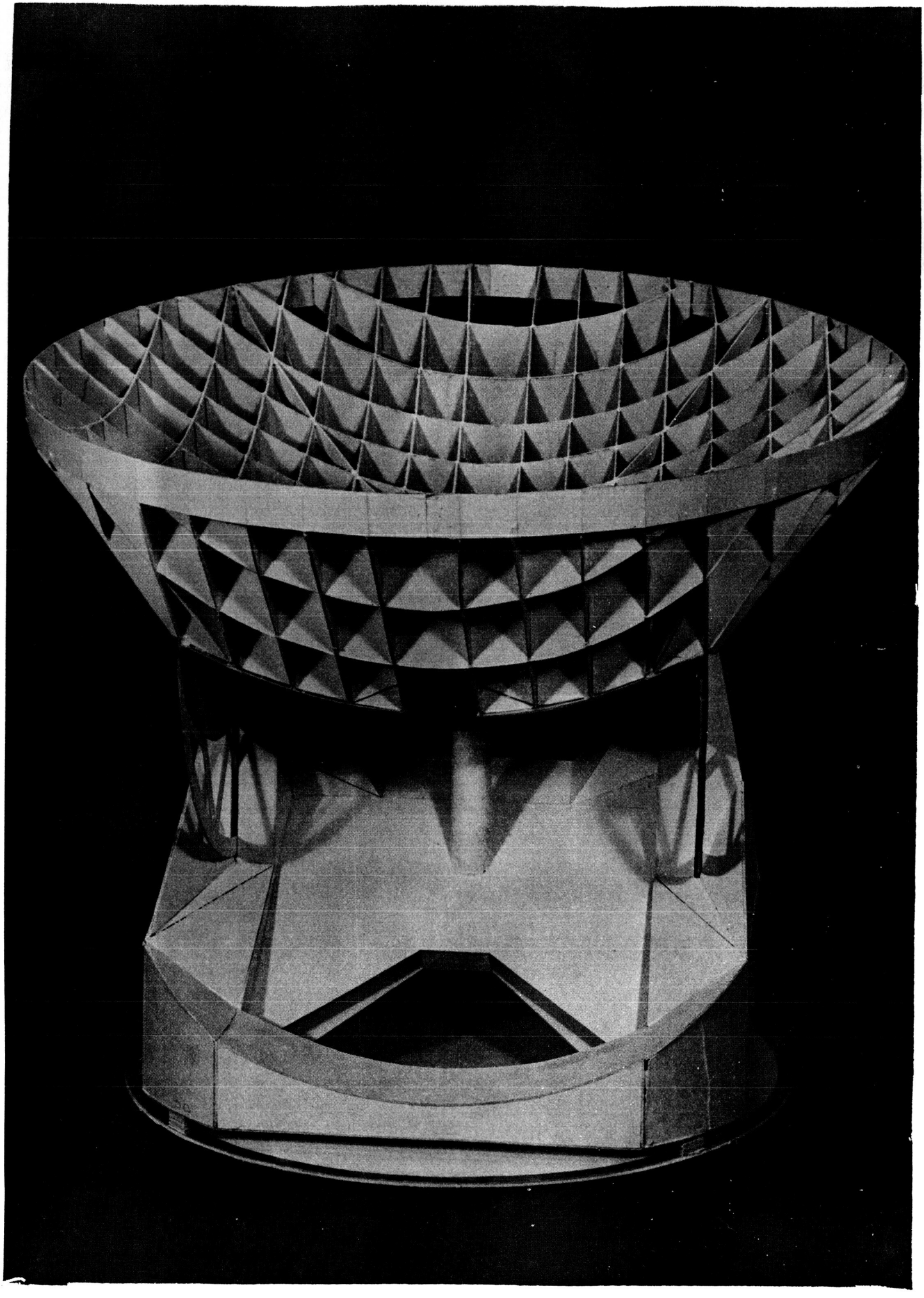

C. BEARINGS

Hydrostatic pad type bearings will be used in the following locations on the mount structure:

1. Trunnion journal bearings
2. Trunnion thrust bearings
3. Pintle guide bearings
4. Azimuth thrust bearing

In all cases the hydrostatic bearing oil films will provide structure support whether the antenna is in motion or not. The friction coefficient for this type of bearing is extremely low; therefore, there is little resistance to antenna motion, leading to smooth transition from no motion to motion and with speed changes. The hydrostatic bearing has a load adjusting characteristic in that an increase in load causes a decrease in film thickness which in turn increases the load carrying capacity of the bearing. Thus, the oil film thickness at the bearing pads will adjust to carry load variations resulting from changes in antenna position, acceleration forces, and wind forces.

Although the bearing pads will carry the loads imposed upon them, load equalization is obtained from deflection of the supporting structure. The structure is designed to have spring constants which will satisfy the requirement that the lowest natural frequency be no less than 3 cps; however, these structural spring constants are many times lower than the oil film spring constants. The structure deflection, therefore, will

tend to equalize loads on the pads.

Each of the two trunnion journal bearings is provided with four hydrostatic bearing pads mounted in pairs at 45° from the vertical as shown on Fig. 7. A double acting trunnion thrust bearing is located at each mount to carry any side loads on the trunnions. Each thrust bearing consists of four pads - two acting in each direction.

The pintle guide bearing shown on Fig. 8 consists of multiple pads equally spaced around the pintle ring. They are designed to carry the maximum possible wind loading combined with maximum acceleration forces. All pads are manually adjusted to align the antenna to the pintle journal and to obtain equal oil film thickness under static conditions.

The azimuth thrust bearing which supports the entire rotating structure consists of four pairs of pads located 90° apart on load equalizing rockers. The arrangement of the pads and load equalizing rocker is shown on Fig. 9. The load adjustment between rockers will be a built-in characteristic due to the relative flexibility of the mount. The runner ring and concrete foundation ring are designed to minimize the deflection of the runner, yet to meet the minimum load capacity of the ground, 2000 lbs/ft.^{2}. The runner ring and concrete foundation ring are designed to uniformly distribute the load over the entire concrete ring ground bearing area by making the load distribution on elastic foundation

spread from one bearing over an 180° arc. Two pads on each rocker serve to reduce load concentration and distribute the antenna loading more evenly on the foundation.

Initially, the load on the bearings will be adjusted manually for the static condition by equalizing the hydrostatic bearing pressure on all pads carrying the same load. During the dynamic condition the load distribution between bearings will depend on the vertical and bending spring constants of the mount, the vertical spring constant being 6×10^6 lbs/in. per mount, the bending spring constant being 2.05×10^6 lbs/inch per mount. The hydrostatic oil film spring constant will vary as a function of film thickness and diameter of oil supply tube or orifice. When carrying full load, the oil film thickness will be approximately .003 inch. The structure vertical deflection will be about .28 inch and the bending deflection will be about .83 inch.

From the above deflection comparison it is evident that the higher relative flexibility of the mounts will tend to distribute the load between respective bearings.

Load distribution between each pair of pads for the azimuth thrust bearing is done by the rocker which carries the thrust element. Four such thrust elements are attached to the mount structure. Their effective spring constant will be equal to the structure vertical spring constant divided by four which gives a spring constant of 3×10^6 lb/in. The static load per thrust element is 1.6×10^6 lbs. and the deflection will be

about .53 inch.

With an oil film thickness of .005 inch, it is evident that the static load distribution between pads will be equalized due to the flexibility of the pad supporting system. The 200 ft. bearing diameter was chosen to have a safety factor of 2.5 against overturning of the antenna with a 70 mph wind or with a 120 mph wind with the reflector pointing at zenith.

WESTINGHOUSE ELECTRIC CORPORATION, SUNNYVALE, CALIFORNIA

CALCULATION SHEET | **FIGURES BY:** N. ANDRES

REFER TO: | **DATE**

TRUNNION BEARING
HYDROSTATIC THRUST AND JOURNAL BRG.

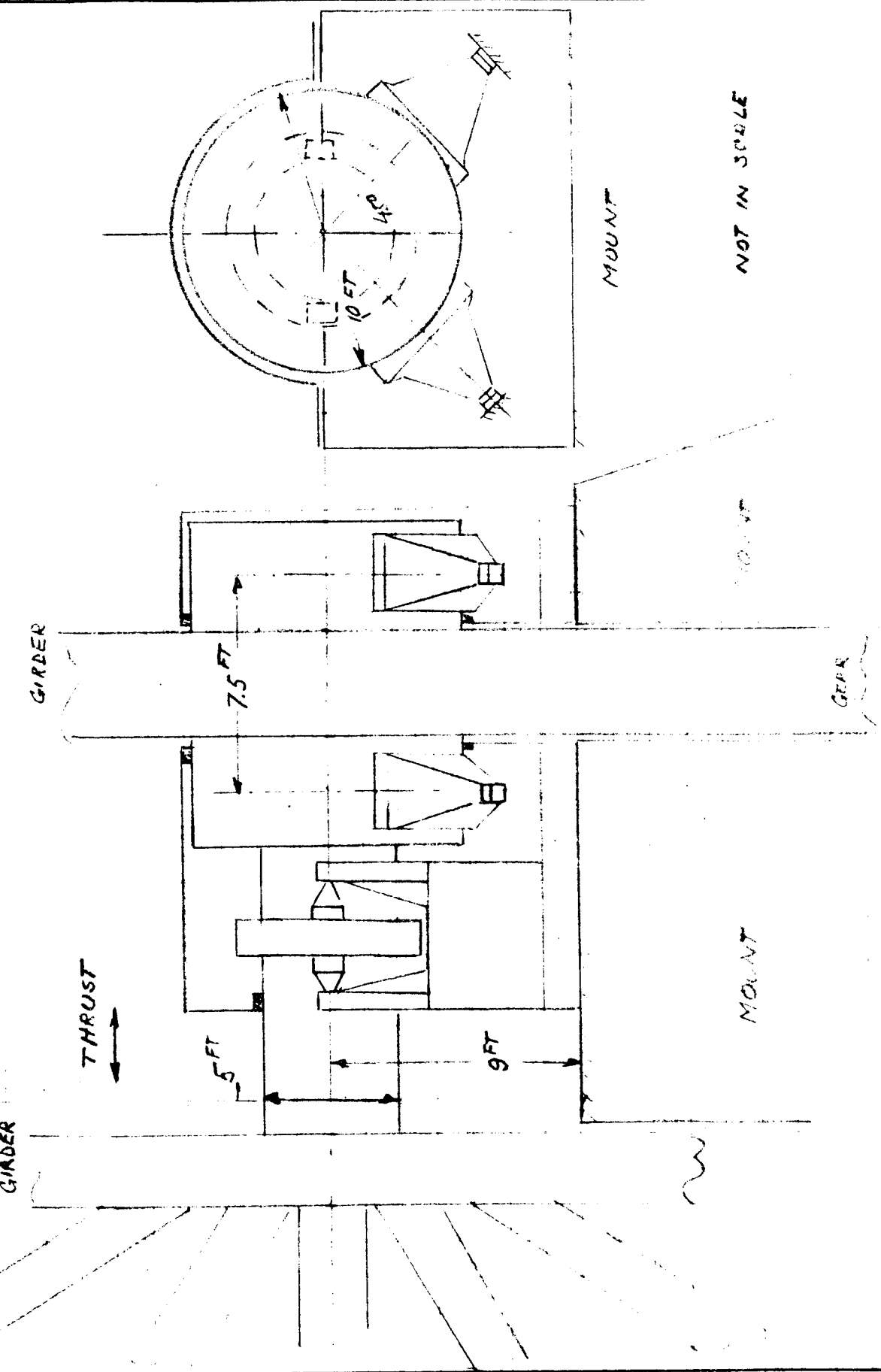

SUBJECT: | **NO. SHEETS** | **SHEET NO.** FIG. 7

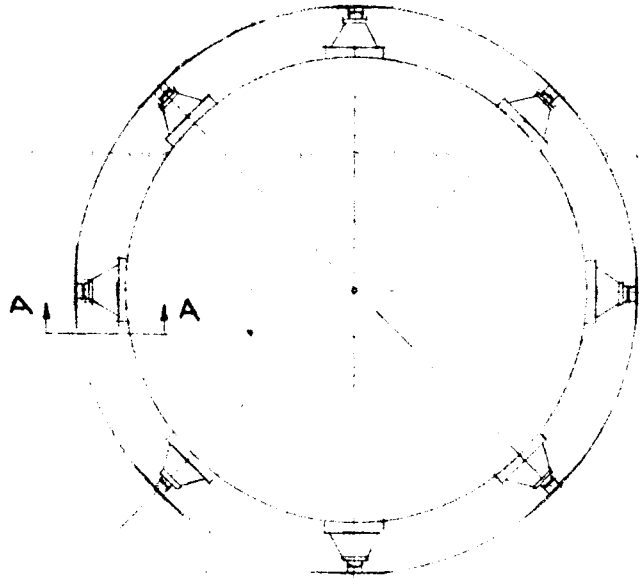

SCALE 1/10 SIZE

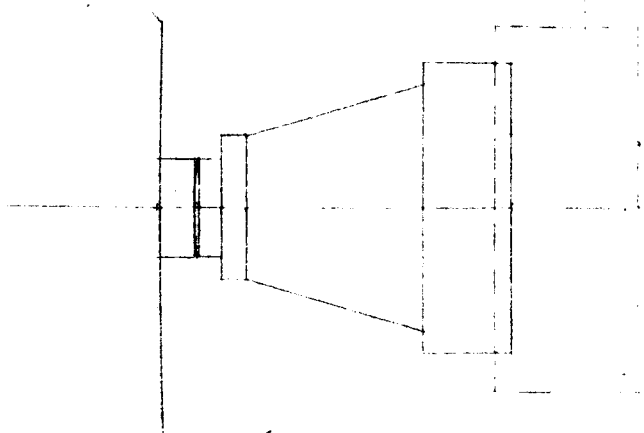

VIEW A-A
SCALE 1/16 SIZE

DSIF ANTENNA
PINTLE BRG.
FIG. 8

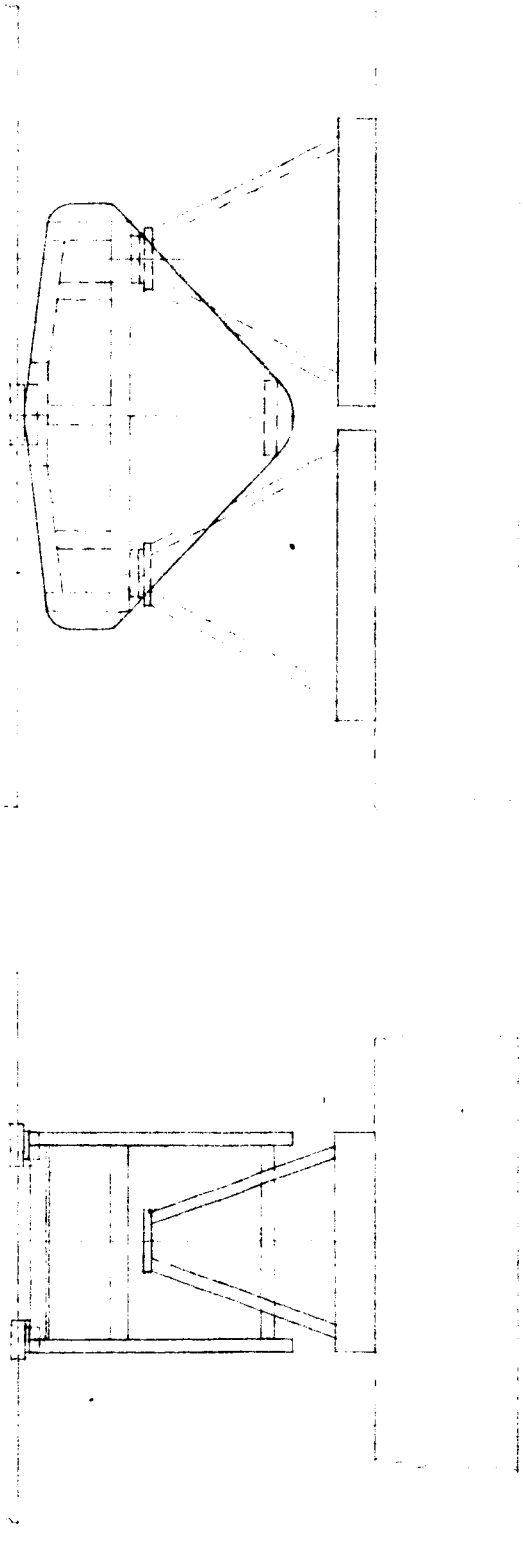

DSIF ANTENNA
200FT DIA. THRUST BRG.
SCALE 1/32 SIZE

FIG. 9

FIG. 9

D. GROUND REFERENCE TOWER

The ground reference tower is intended to provide a stable reference location free of lateral or angular deflection at the intersection of the azimuth and elevation axes of the antenna. In order to assure that the antenna supporting structure does not disturb the reference location, the tower is completely independent of the support structure. Shielding is provided around the tower to prevent distortion from wind loads and differential thermal expansion.

In preliminary design form the tower consists of a fabricated steel cone 15 ft. diameter at the base and 4 ft. diameter at the top. The wall thickness varies from 1/2 inch at the base to 1/8 inch at the top. Analysis of this design considering the instrumentation at the top to weigh 800 pounds gives a natural frequency of 4 cps. Further calculations will optimize the design. Effects of the foundation on the stability of the reference location are presently being studied.

IV DRIVE GEARING

The basic problem in the design of gears to drive the antenna in azimuth and elevation are:

A. Load capability for driving the antenna at the required acceleration; including inertia, friction and wind loads up to 70 miles per hour.

Power in the design of azimuth gearing is based on:

1. Drive to stow in 70 MPH wind
2. Maximum on drive = 13.7×10^6 lb. ft.
3. Maximum accel. at $1^o/sec^2$ = 22.6×10^6 lb. ft.
4. Maximum tracking in 60 MPH wind

Drive load	10×10^6 lb. ft.
Accel. $0.2^o/sec^2$	4.4×10^6 lb. ft.
	14.4×10^6 lb. ft.

5. Max. azimuth drive in 60 MPH wind 10×10^6 lb.ft.
   Accel. $0.5^o/sec^2$ 11×10^6 lb.ft.
   21×10^6 lb.ft.

Power in the design of elevation gearing is based on:

1. Drive to stow in 70 MPH wind
   T on drive 16×10^6 lb. ft.
2. Max. accel. at $1^o/sec^2$ 9.2×10^6 lb. ft.
3. Max. tracking in 60 MPH wind

Drive	11.8×10^6 lb. ft.
Accel. $.012^o/sec^2$	1.8×10^6 lb. ft.
	13.6×10^6 lb. ft.

4. Max. elevation drive (60 MPH wind) 11.8×10^6 lb. ft.
   Accel. ($0.5^o/sec^2$) 4.6×10^6 lb. ft.
   16.4×10^6 lb. ft.

The elevation gearing must then have 78% of the power required for the azimuth drive.

B. Forward and reverse rotation with equal drive power and control.

C. Speed control from 0^o/sec to 0.5^o/sec.

D. The rotating elements must have high torque capacity, adequate torsional stiffness for minimum deflections and a high spring rate while at the same time have low inertia to produce the required accelerations.

E. Backlash must be eliminated in the azimuth and elevation gearing in both directions of rotation.

F. Constant mesh conditions must be maintained in spite of differential expansions between the azimuth main gear support and its pinions.

G. Power distribution around the antenna base to minimize distortion.

H. Bearing mountings must be rigid to eliminate clearance contributing to motion due to lash.

Solutions to the above problems were developed in a configuration providing bias torque as shown in Fig. 1. Each of eight (8) units on the azimuth gearing contains two separate counter rotating drives providing opposite directions of torque facilitating speed control and anti-backlash. On a gear diameter of 190 feet 16 pinions are

arranged similar to bevel gears. Each gear and pinion tooth tapers approximately .0005 inches per inch of length, giving full face contact. The pinions are very nearly spur gears due to a cone radius of 1140 inches. This type of gear eliminates any variation of mesh position since radial expansion is limited to the gear tooth axis.

The arrangement for one half of a gear unit is shown in Fig. 2. All pinions and gears are supported on both ends by anti-friction bearings. The pinion teeth are covered, except directly over the rack teeth. A seal is provided between the first pinions and the second gear, providing a total enclosure for the remainind gear train.

The entire assembly consists of only three rotating masses excluding a tachometer drive running at 3000 RPM at the end of the input pinions.

The total ratio of the antenna is 7200 to 1. RPM of the coupling output is 600, reducing to .083 RPM at the antenna.

Gear data showing ratios, diameters, length of face, RPM, pressure angle and number of teeth are shown in Fig. 3.

Support for the gear case is provided by a deep web arranged tangentially in reference to the azimuth main gear. Driving forces are taken half way between the pinion bearings, almost directly in line with the pinion shaft to minimize deflection under power.

The elevation gears shown in Fig. 4 are the same general arrangement as the azimuth drives except the main pinion size is based on a segment radius of 75 feet. Six units consisting of 12 separate gear drives are located on two segments. Each gear case is rigidly mounted in a spur type arrangement since radial expansions of the segment and the support structure are the same.

Gear capacity is designed as shown in Figs. 5 through 16.

WESTINGHOUSE ELECTRIC CORPORATION

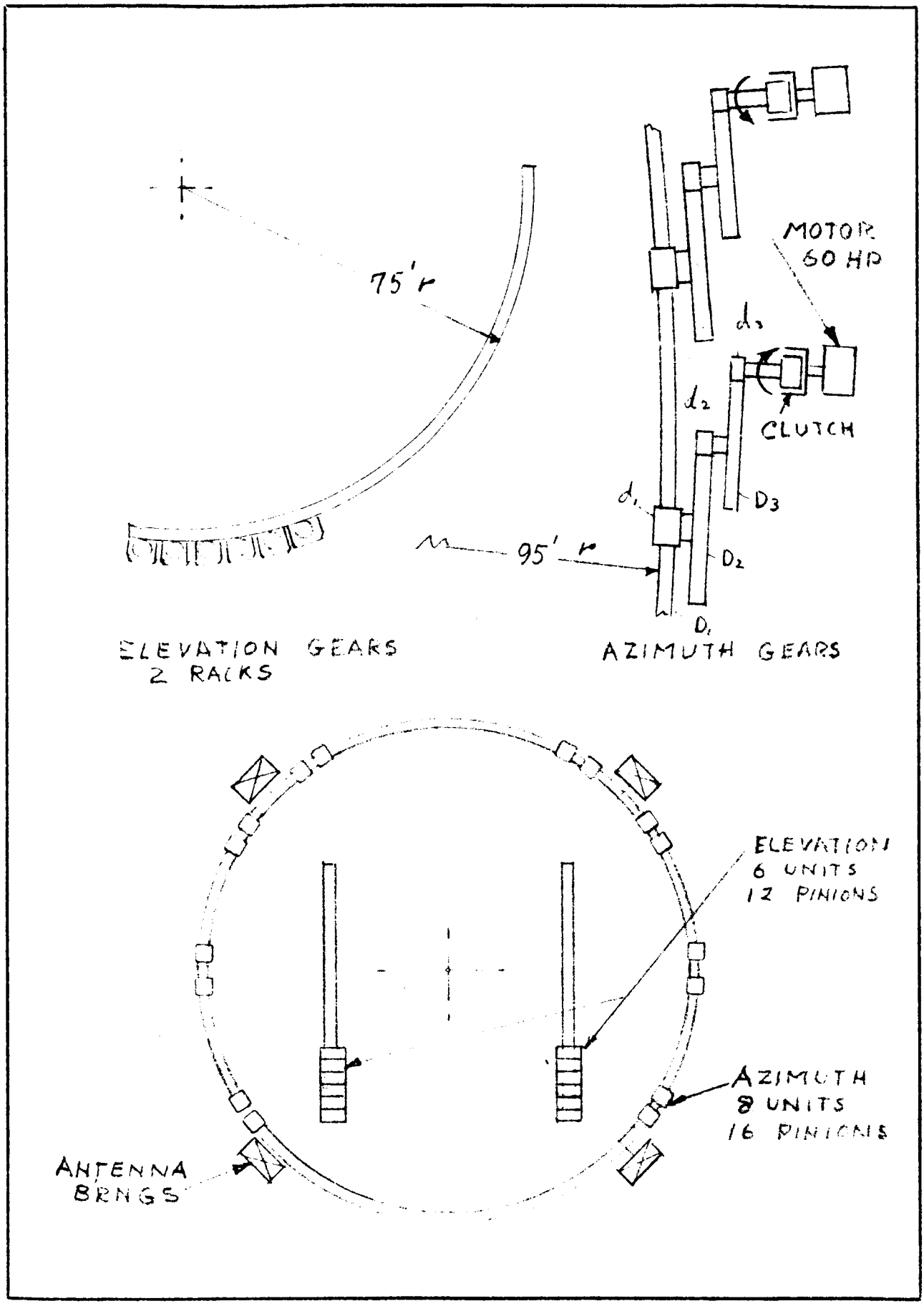

FIG 1

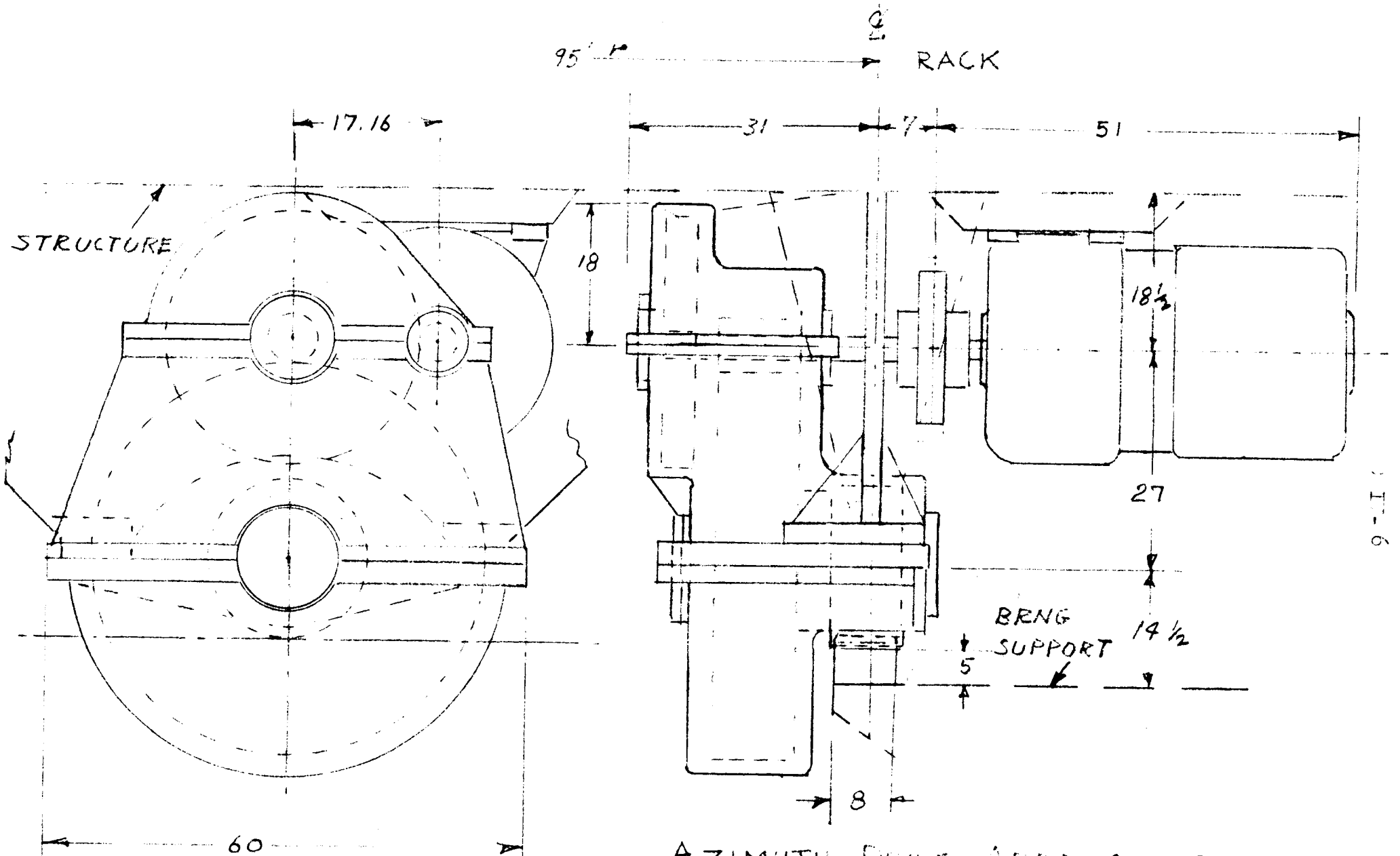

AZIMUTH DRIVE ARRANGEMENT

FIG 2

SNP
5-7-61

SKETCH SHEET
WESTINGHOUSE FORM 2444 D

WESTINGHOUSE ELECTRIC CORPORATION

GEAR DATA

DSIF AZIMUTH GEARING

	d_1	D_1	d_2	D_2	d_3	D_3
R	118.75		8		7.583	
PD	19.20	180 : 2280	6.00	48.00	4.00	30.33
b	2+1.5	8	10.20	10.20	3.75	3.75
RPM	9.232	.083	79.16	98.92	600	79.16
P_d	1.25		4		6	
PA	20° STUB		20° STUB		20° STUB	
N	24	240	24	192	24	192
T	336,000		42,500		5,500	
F	35,000		14,000		2,750	
S_c	47,000		151,400		182,000	

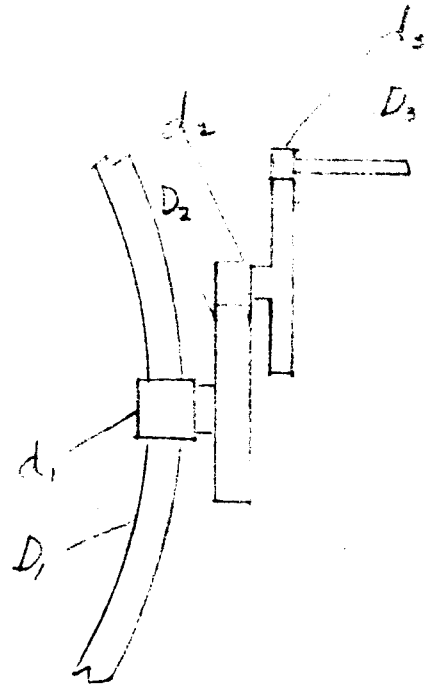

FIG 3

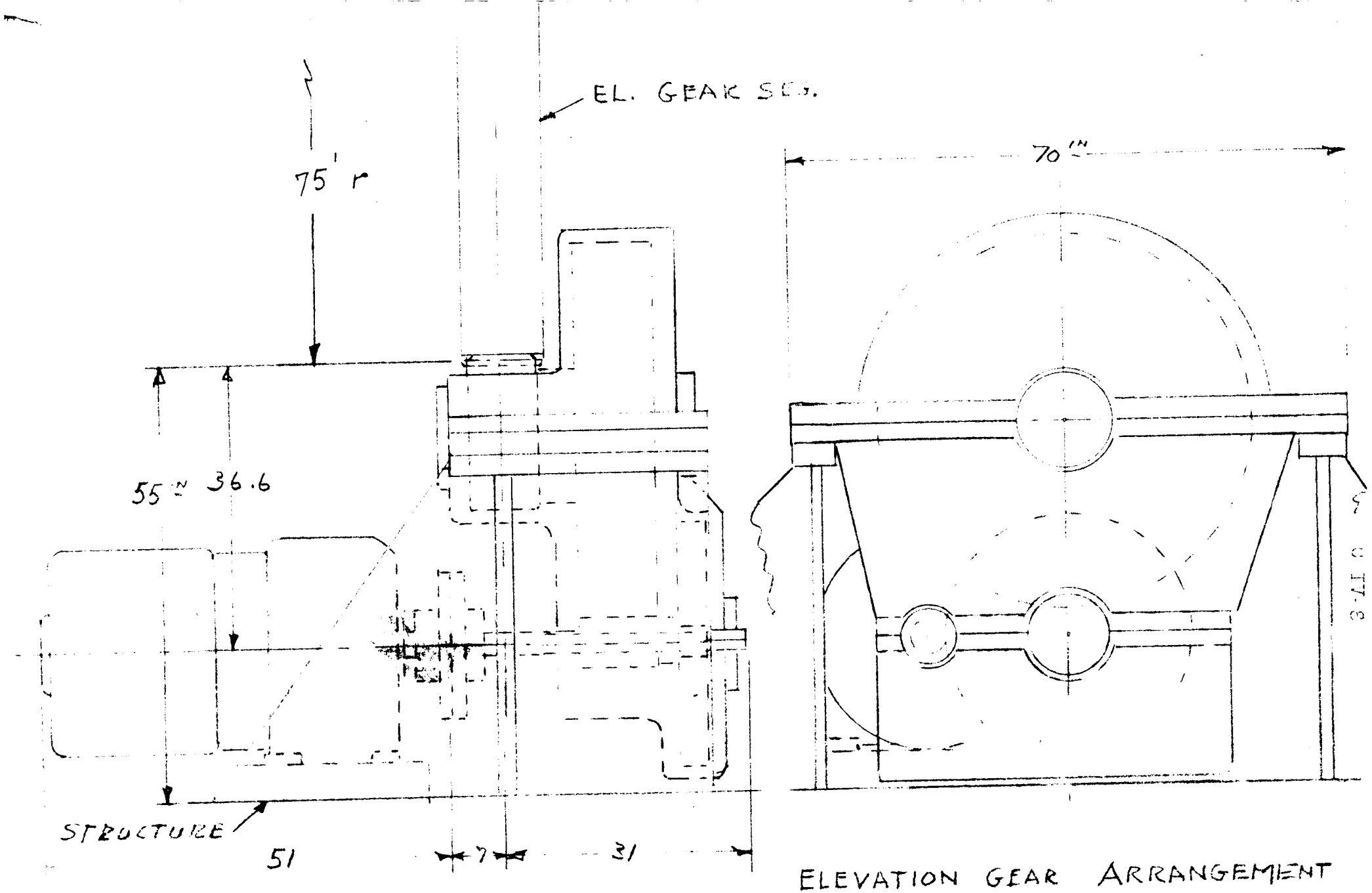
EL. GEAR SEG.
75' r
70"
55" 36.6
STRUCTURE
51
7
31
ELEVATION GEAR ARRANGEMENT
SDP
3-7-61

FIG. 4

F = TAN FORCE

ΣF = SUM OF FORCES

F_T = TOTAL FORCE

FS = FACTOR OF SAFETY

T = TORQUE

T_E = BIAS TORQUE

T_O = ALLOWABLE BENDING LOAD

T_B = ALLOWABLE BENDING LOAD IN REVERSE BENDING

R = RATIO

d_1 = PINION PITCH END

d_3 = " GEAR END

l_d = LIMITING LENGTH

b OR l = FACE LENGTH

Y = LEWIS FORM FACTOR

C = VELOCITY FACTOR (LENGTH)

σ_{yp} = YIELD STRENGTH OF MTL

δ = DEFLECTION - ON PITCH CIRCLE

FIG. 5

GEAR DESIGN - AZIMUTH

$\Sigma F = 21 \times 10^6/95 = 221000$ lbs.

$F = 221000/8 = 27,600$ lbs.

T_G (ENG. [illegible] 35% = [illegible]) = 394 lb ft.
OF COUPLING RATING

$K = 7200$

$T_{KF} = 394 \times 7200 = 2.83 \times 10^6$ lb ft.

F DUE TO $T_G = 2.835 \times 10^6/95 = 29,800$ lbs.

$F_T = 27,600 + 29,$[illegible] $= 57,400$ lbs.

FS FROM GEAR CAPABILITY
BASED ON YIELD STRENGTH

σ_{yp} (YIELD @ 310 BHN [illegible])

$$T_o = \frac{1.6}{m} \cdot \frac{8 \cdot 4.15}{P_d} \left(\frac{\sigma_{yp}}{F.S.} \right) \quad \star$$

$$m = 1 + \frac{.075}{K_f}$$

★ 59.SA9

FIG. 6

WESTINGHOUSE ELECTRIC CORPORATION

$$FS = \frac{1.6 \times 8 \times .415 \quad 120000}{1.622 + 1.25 \quad 57,400} = 6.5$$

BENDING STRESS *

$$S_t = \frac{F \; P_d}{C \; b \; Y}$$

$$(d_1) \quad S_t = \frac{5000 \times 1.25}{.95 \times 2 \times .411} = 14,000$$

$$(d_2) \quad S_t = \frac{14000 \times 4}{.88 \quad 10.2 \quad .411} = 15,180$$

$$(d_3) \quad S_t = \frac{2750 \times 6}{.528 \times 3.75 \quad .411} = 16,200$$

BENDING LOAD ALLOWANCE

$$T_B = \frac{1.6 \; f \; Y \; \sigma_e}{M + P_d} = \frac{1.6 \times 8 \times .415 \times 52000}{\left(14 \cdot \frac{.075 \times 5.13}{.303}\right) \times 1.25} = 149,000$$

* MALEEV & HARTMAN

FIG. 7

MASS MOMENT OF INERTIA OF GEARING

ITEM	MR^2 - LB. IN. SEC^2		
	ABOUT OWN AXIS	RATIO^2	REFERRED TO INPUT PINION
PINION d_3	1.14	1	1.14
GEAR D_3	58.2	$\frac{1}{7.58^2}$	1.02
PINION d_2	1.69	$\frac{1}{2.58^2}$	.03
GEAR D_2	100.80	$\frac{1}{(7.58 \times 4)^2}$	.27
PINION d_1	.58	$\frac{1}{(2.5 \times 2)^2}$	.26
ELEC. CPLS.	13.10	1	13.10
(INCL. FLUID CPLG.)			
TOTAL			15.82
TOTAL (LB. FT. SEC^2)			1.30

FIG. 8

ANGULAR DISPLACEMENT OF PINION d_3 DUE TO TOOTH DEFLECTION

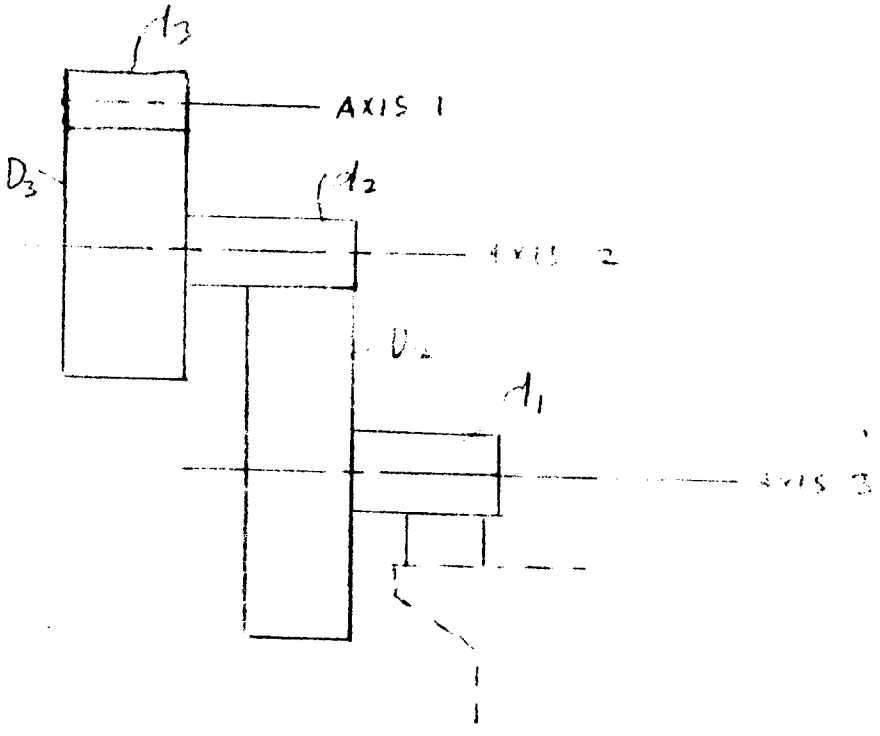

$$\delta_{\text{PITCH LINE}} = \frac{F}{\ell}\left[\frac{E_1 z_1 + E_2 z_2}{(E_1 z_1)(E_2 z_2)}\right], \text{ WHERE } z = \frac{Y}{.761 + 7.25Y}$$

FOR 20 STUB TEETH & $N_1 = 29$, $Y = .415$

AND $z = \frac{.415}{.761 + 7.25(.415)} = .110$

$$\therefore \delta = \frac{F}{\ell}\left[\frac{1}{1.67 \times 10^7}\right]$$

FIG. 9

SKETCH SHEET
WESTINGHOUSE FORM 2444 D

WESTINGHOUSE ELECTRIC CORPORATION

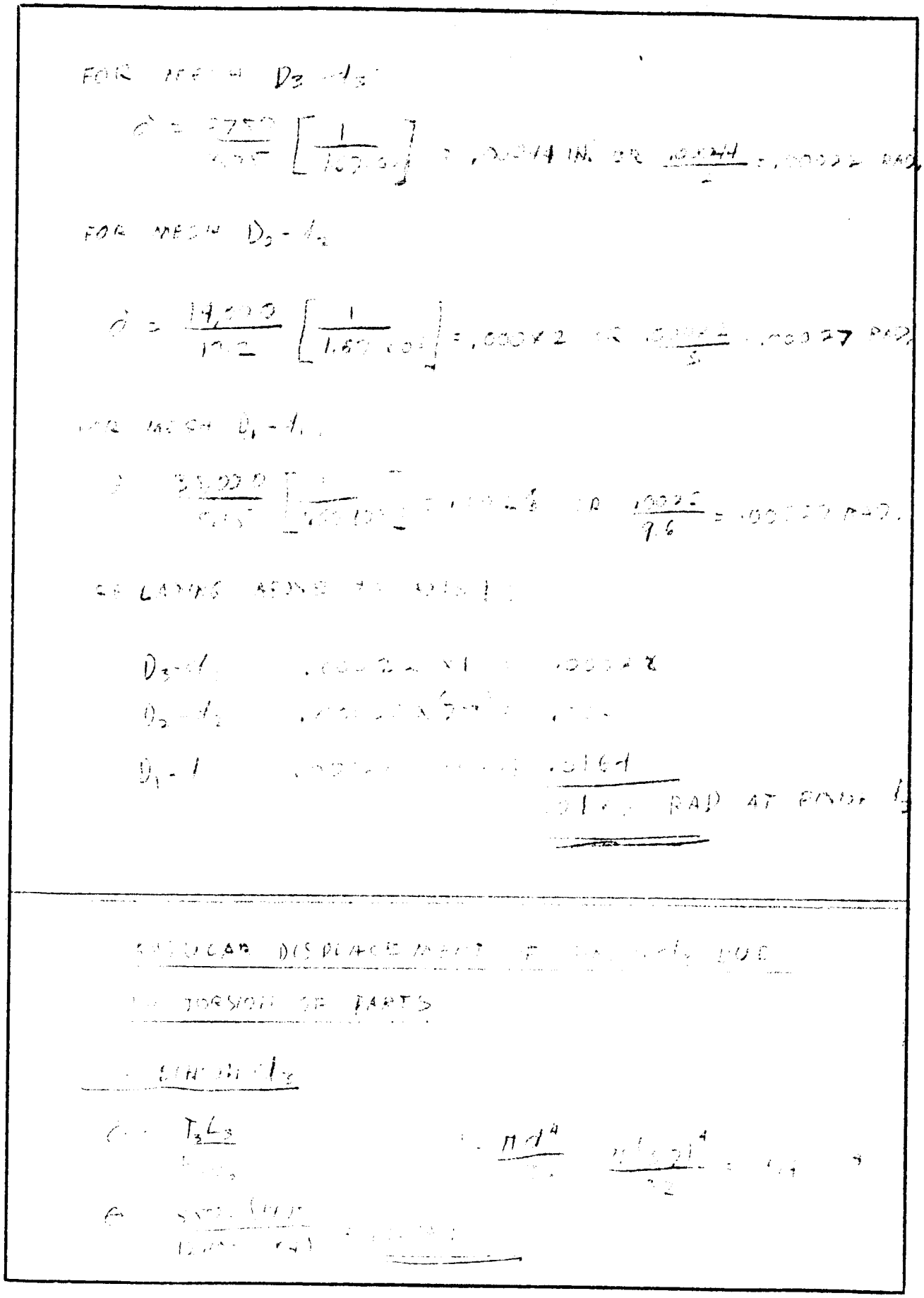

FIG. 10

FOR PINION d_2

$$\theta = \frac{T_2 L_2}{E_s J_2} \qquad J_2 = \frac{\pi d^4}{32} = \frac{\pi (6)^4}{32} = 127 \text{ in}^4$$

$$= \frac{12{,}000 (13.7)}{12.10^6 (127)}$$

$$= .003775 \text{ RAD.}$$

RELATING THIS TO AXIS 1:

$$\theta = .003775 (7.5\text{X}) = .02\text{X}4 \text{ RAD}$$

FOR PINION d_3

$$\theta = \frac{T_1 L_1}{E_s J_1} \qquad J_1 = \frac{\pi d^4}{32}$$

$$= \frac{\pi (1.2)^4}{32}$$

$$= \frac{36{,}000 (13.3)}{12.10^6 (13.30)}$$

$$= .0000279 \text{ RAD}$$

RELATING THIS TO AXIS 1

$$= .0000279 (7.5\text{X}\,\text{X}) = .0169 \text{ RAD}$$

TOTAL θ

.00049
.02X4
.0169
.04579 RAD. AT PINION d_3

FIG. 11

SUMMARY

TOTAL ANGULAR DISPLACEMENT OF PINION d_3 TO PRODUCE 336,000 LB. IN TORQUE AT PINION 1, IS

.0186 RAD. — TOOTH DEFLECTION
.0458 " — SHAFT DEFLECTION
.0644 RAD.

$\therefore$ SPRING CONSTANT

$$K = \frac{T_3}{\theta_3} = \frac{5500}{.0772} = 85{,}000 \text{ LB. IN./RAD}$$

$$= 7100 \text{ LB. FT./RAD.}$$

FIG. 12

D. SERVO DRIVE SYSTEM

I SERVO AND DRIVE SYSTEM

A functional block diagram of the Servo System in accordance with our present concept is shown in Drawing 825-D-919.

The Azimuth Drive is provided by sixteen and the Elevation Drive by twleve Type WCS-215 electromagnetic couplings. One half of this number of couplings will provide rotation in one direction and the other half will provide rotation in the opposite direction about each axis in order to eliminate backlash in the gearing and provide continuous control at zero velocity. The coupling will be modified to have a dry air gap and arranged for closed circulating oil cooling to achieve high reliability. This coupling has a maximum torque rating of 1120 lbs. feet and an inertia of 1.0 ob. ft. sec^2. These are standard design values and design modifications are being considered to improve the torque squared to inertia ratio and minimize the power dissipation. Because of the time factor, it was essential to proceed with the study on the basis of the standard design.

The torque-slip characteristic of the coupling is shown in Figure (1). It is desirable to minimize the maximum slip to limit power dissipation and still provide very nearly maximum torque over the desired operating range of 0-0.25°/second. It was felt that a 50 percent

WESTINGHOUSE ELECTRIC CORPORATION

CURVE NO. _____

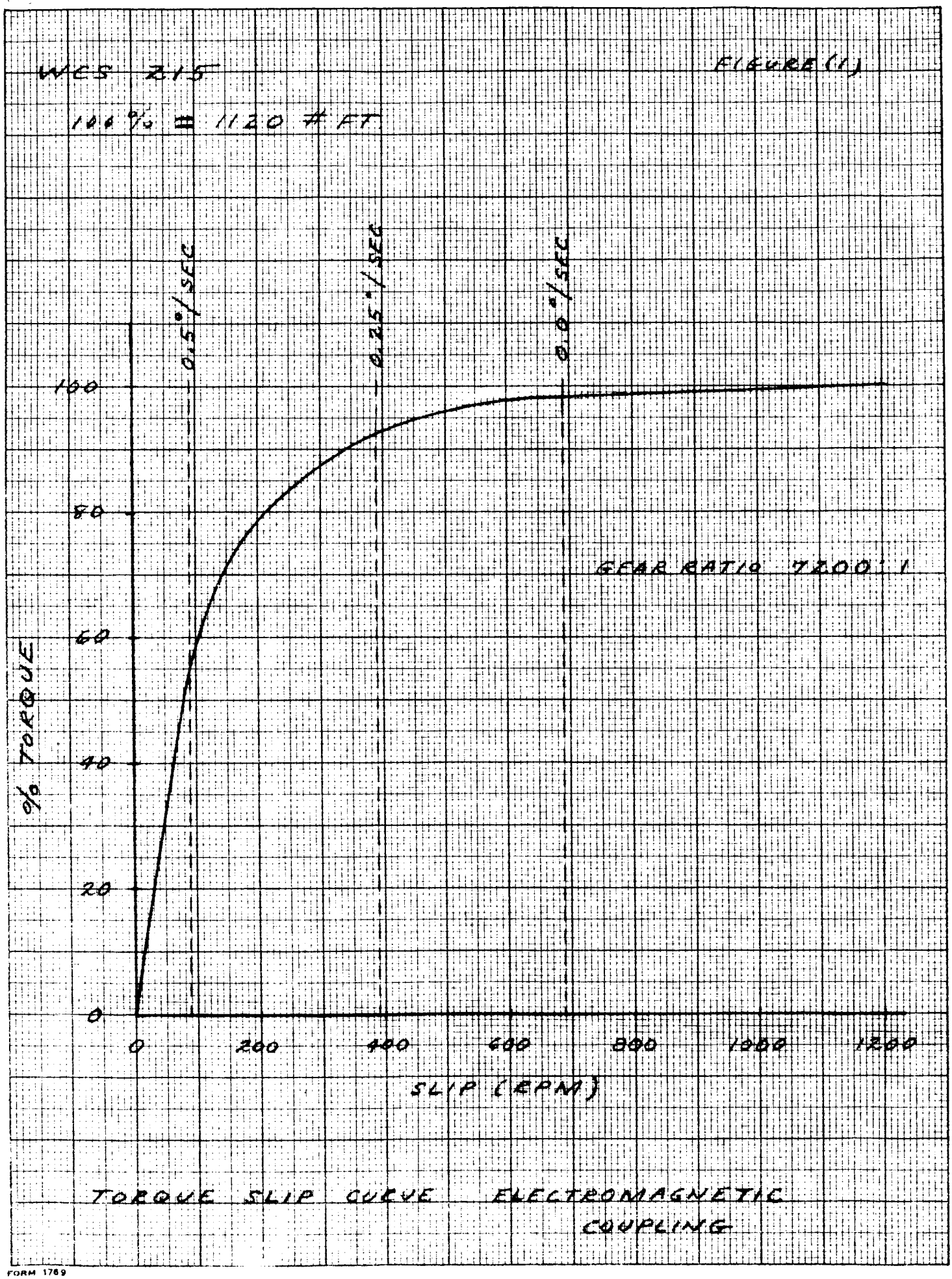

TORQUE SLIP CURVE ELECTROMAGNETIC COUPLING

FORM 1769

SIGNATURE _____ DATE _____ CURVE NO. _____

reduction in maximum torque would be permissible at 0.5°/second as a compromise between velocity range and maximum slip. It should be noted that full reverse torque is still available from the opposite coupling in each drive unit.

It is also desirable to drive the coupling directly from an a-c motor supplied with 60 cycle/second power. As shown in Figure (1), the use of a motor having a synchronous speed of 720 rpm and a gear ratio of 7200:1 between the coupling and the associated antenna axis would achieve these objectives. On the basis of using a 100 hp, 720 rpm, CS-776, driving motor, a preliminary study has shown that with this selection the motor characteristics will have a negligible effect on drive performance.

The maximum torque available to drive the antenna about the azimuth axis at 0.25°/second in either direction is 60×10^6 lb. ft. The total inertia of the antenna including the drive about the azimuth axis is 23×10^8 lb. ft. second^2 so that a torque of 40×10^6 lb. ft. is required to produce the maximum permissible angular acceleration of 1.0°/sec.^{2} about that axis. The maximum wind torque at a wind velocity of 60 mph has been calculated to be 20×10^6 lb. ft. without aerodynamic compensation. With compensation, this can be reduced by at least 50 per cent. Using hydrostatic bearings, the friction torque is negligible.

The maximum torque available to drive the antenna about the elevation axis at 0.25°/second in either direction is 45×10^{6} lb. ft. The total inertia of the antenna, including the drive, about the elevation axis is 12×10^{8} lb. ft. sec^{2} so that a torque of 21×10^{6} lb. ft. is required to produce the maximum angular acceleration of $1^{\circ}/sec.^{2}$ about that axis. The maximum wind torque at a wind velocity of 60 mph has been calculated to be 23×10^{6} lb. ft. without aerodynamic compensation. With compensation, this can be reduced by at least 50 percent. Using hydrostatic bearings, the friction torque is negligible. Thus each drive provides a 200 percent excess torque capacity at an acceleration of $0.2^{\circ}/sec.^{2}$ and a velocity of 0.25°/sec. in a 60 mph wind.

This capability must be balanced against the coupling power dissipation under stall conditions. The torque excitation curve for the WCS-215 coupling is shown in Figure (2). As shown, each of the couplings in a drive unit should be biased at about 35 percent of their rated output to provide a linear combined characteristic and adequate torque for backlash compensation. Under stall conditions, this produces a power dissipation of 55 HP per coupling and a total power dissipation of 1550 HP for the 28 couplings used. The reduction of this power dissipation is one of our current objectives.

The response of an electromagnetic coupling is determined by two time delays, one associated with the excitation field and one with the formation of eddy currents in the coupling drum. Information available concerning these time delays is

quite limited. A coupling is being connected to a laboratory dynamometer to obtain experimental data. Pending the results of this study, it has been assumed that the field delay is 1.0 seconds and the eddy current delay is 0.05 seconds on the basis of general information.

In order to compensate for the field delay, the use of a bistable field current feedback loop is proposed. The field will be excited from a three phase unidirectional converter, Trinistor Controlled Rectifier. The output voltage of the converter can be switched from full positive to full negative by changing the polarity of the input signal and provides a field forcing factor of 500 percent of rated excitation. A unit has been designed and built and is currently being tested. Although RF noise generation has not yet been measured, it has been found necessary to employ RC networks to attenuate the slope of the voltage wavefronts to prevent faulty operation of sensitive electronic equipment in the vicinity of the converter.

Using an operational amplifier as a voltage comparator, a circuit feedback loop bistable frequency of 60 cycles/second can be achieved as indicated by analytical, computer, and experimental studies. The small signal time delay associated with the coupling field is reduced by this means to 0.0167 seconds and full excitation can be developed in 0.068 seconds. The eddy current time delay is outside of this loop.

The gearing is being designed for a natural frequency of the drive of 12 cps with the antenna axis locked. Combined

WESTINGHOUSE ELECTRIC CORPORATION

D-6

CURVE NO.

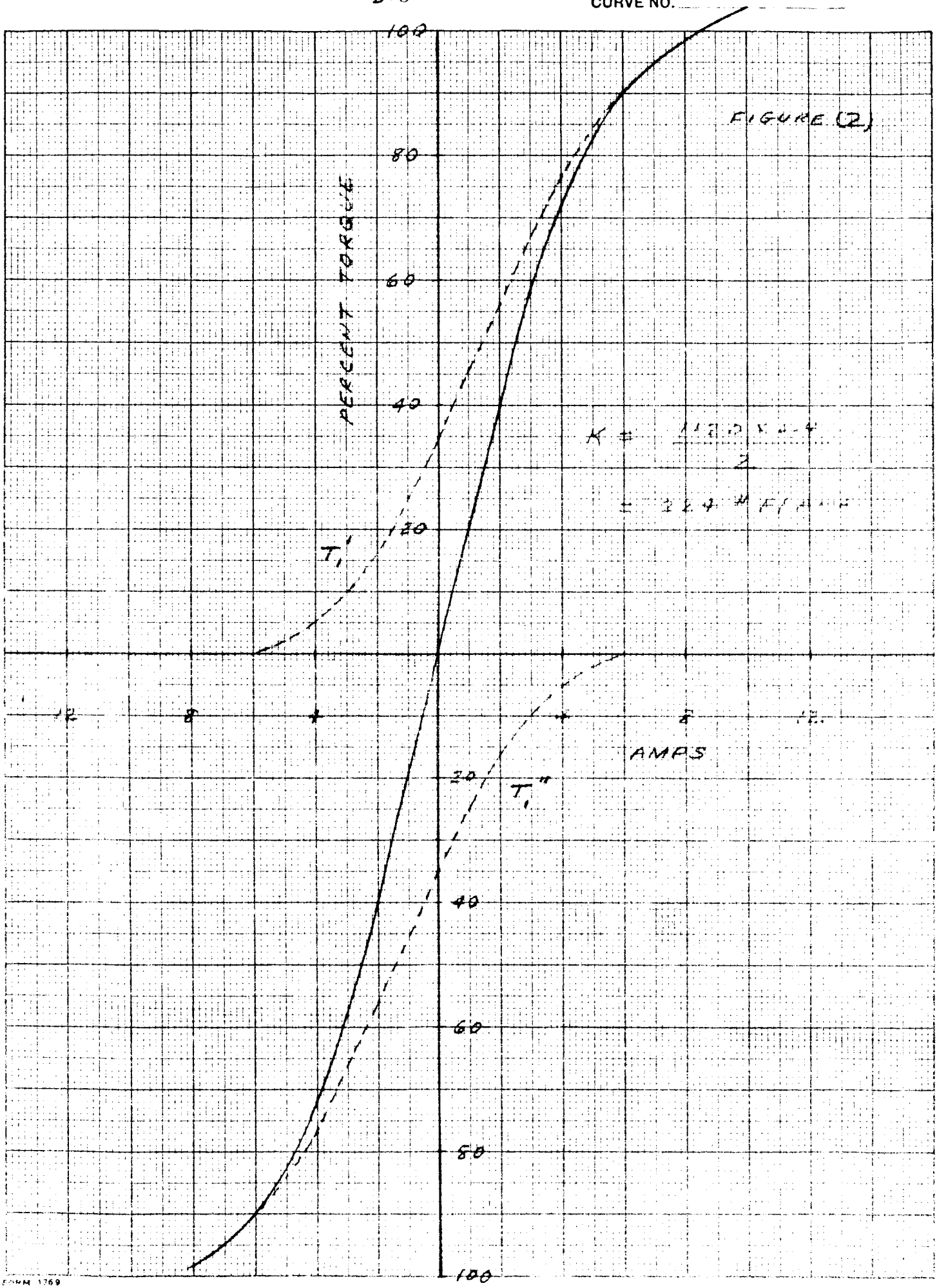

FORM 1769

SIGNATURE DATE CURVE NO.

with the dynamic characteristics of the antenna structure it is possible to incorporate a velocity feedback loop as shown on Dwg. 825D919 having a bandwidth of 2.5 cps and an M_p ratio of 1.0 db. to limit the effect of wind disturbances. At the time of this report, complete computer results on the magnitude of these effects were not available.

The open loop transfer function of the position loop is essentially $(1 + t_{1p}) / (T_{2p})^2$ over the required bandwidth using integral plus proportional control. To achieve minimum positional errors resulting from velocity and acceleration inputs the system is adjusted so that $T_1 = T_2 = (2\pi f_c)^{-1}$, where (f_c) is the system bandwidth. The position signals will be in digital form and the integral plus proportional control will be accomplished by digital means. Required saturation levels of the position and integral loops has been studied for the case of a ramp function input having a scope of $0.20^\circ/sec^2$ and a ceiling of $0.25^\circ/sec.^2$. For a system bandwidth of 0.2 cps, the saturation level of the position level should be 0.1° and the saturation level of the integral loop should be 0.18° seconds. If the bandwidth is reduced to 0.01 cps, the former must be increased by a factor of 20 and the latter by a factor of 400.

The capability of the digital control in this regard can be evaluated as follows:

Let the input error = ϵ counts

The output from the decade divider unit

$f_{o_1} = f_2 \times \frac{\mathcal{E}}{1000}$ $\quad f_2$ = input pulse rate vs decade divider

$f_2 = \frac{f_1}{K_1}$ $\quad f_1$ = X-tal pulse rate

K_1 = Bandwidth setting

The transfer function to the output of the divider =

$$\frac{1}{P} \cdot \frac{f_1}{1000} \cdot \frac{1}{K_1}$$

I

If $f_1 = 1000$ pps

this becomes = $\frac{I}{P} \cdot \frac{I}{K_1}$

K_1 settings are 1, 2, 4, 8 and 16 giving an integrator time constant of 1 - 16 and a bandwidth from 0.16 to 0.01 cps, for example. However, in order to linearize the divider output (the division gives non-uniform output spacing), a further fixed division is introduced of 10-1. To hold the time constant of the device still from 1 - 16, the input pulse rate is increased by 10-1. This gives a crystal frequency of 10 kc/s.

The integration constant = $\frac{c}{1000} \times K_1$ count secs. for any maximum error signal.

A bandwidth of 16 and a counter capacity of 5000 with 1000 bits per degree from the encoder gives 38,000 counts secs. or 80° sec. bandwidth setting of 1 gives 5° sec. The quantization effects of the digital signals is being evaluated.

II. INSTRUMENTATION

Antenna position in terms of azimuth and elevation will be expressed in digital form by using special encoders attached to the antenna position sensing device on the ground reference structure.

All position command signals will be transformed to an equivalent AZ-EL command in digital form.

A digital comparator is provided to generate a digital error signal obtained by comparing the antenna axis position with the digitized position command signal.

The error signal is modified by an adjustable band width control before being transformed to a linear analog error signal which actuates the servo drives on each axis.

We have arrived at this concept after considering many other configurations involving mixed co-ordinate systems and believe it has several definite advantages.

1. Keeping everything inside the loop in AZ-EL co-ordinates greatly simplifies a signal flow and minimizes equipment in critical circuits.
2. The instrument mount on the ground reference structure at the intersection of the antenna axes is considerably simplified and consequently seems more reliable.

Command Signal Generation

All input command functions will be transformed as required to provide a corresponding digital command signal in AZ-EL co-ordinates. A reversible Binary coded decimal counter provides the position command intelligence to the digital comparator for the "Slew", "Manual","Manual Rate", and "Automatic Track" modes of operation.

a. Slew control is obtained by generating pulses at a rate proportional to the desired slew velocity. The slew pulses are injected into the reversible counter so that the counter will count up or down

depending on the direction of slew, and provide a corresponding change in position command.

b. Manual positioning can be achieved by using the slew control to set the antenna at the desired position as determined from a decimal readout of the azimuth and elevation command position contained in the reversible counter.
If desired incremental positioning can be obtained by injecting a slow pulse rate into the reversible counter until the desired position is reached.

c. Automatic Track operation can be achieved by converting the d-c voltage analog of position error to a vairable pulse rate applied to the reversible counter reference. Polarity of the tracking signal determines whether the pulses add to or subtract from the count, and pulse rate would be proportional to amplitude of tracking signal.

d. Manual Rate (aided track) will be obtained by adding an adjustable bias to the pulse rate controlled by the Automatic Tracking signal. If such a bias were set to provide the required tracking rate by itself then the automatic track signal would reduce to zero.

It is presumed that in the slave mode, the commands supplied on the 5 hole punched tape will be in celestial co-ordinates and time. Such a system provides a universal frame of reference and also greatly reduces the amount of information stored on the tape. One set of tape information including Sidereal Hour Angle (SHA) Declination (DECL) and

time is translated by a tape reader and put into memory storage. Tape time identification is compared with G.M.T. and when time identity arrives the information in SHA and DECL, memory is released to serve as a position command for antenna positioning.

Since SHA is in celestial co-ordinates it is necessary to transform SHA to local hour angle (LHA) which is the angle measured west from the local zenith meridian. Such transformation from SHA to LHA is made by using a siderial clock arranged to give a digital expression of local siderial time, where 0 hours occurs when the 0 siderial hour circle is at the local zenith. SHA from the memory and siderial time from the sideral clock are compared in the comparator subtractor to give a digital expression of LHA.

LHA and DECL signals thus obtained are applied to a co-ordinate converter which transforms the LHA-DECL to equivalent signals in AZ-EL co-ordinates which are then used as position command signals.

Means will also be provided for setting SHA and declination from a manual adjustment as well as from the tape.

An adjustable rate pulse generator will permit accurate adjustment of declination rate over the range $\pm 0.0004^{\circ}$ per sec. Likewise pulses will be added to or subtracted from the siderial time at such rates as to permit $\pm$ percent adjustment on the siderial rate.

Scan Function Generation

Elliptical spiral scanning can be attained by electro-mechanical generation of two sine functions expressed in both

analog and digital form. One sine function will be superimposed on the Azimuth command and the other on elevation. Rate of scan will be determined by adjusting frequency. Ellipticity and orientation of the elliptical axis can be controlled by adjustment of the relative amplitudes and phase of the sine generators. Spiral can be obtained by simultaneous amplitude adjustment. Analog output of the scan generator will be superimposed on the manual rate (aided track) and digital output will be superimposed on digital AZ-EL commands derived from Slave or Siderial mode commands.

The sawtooth scan generator may consist of two counters one for each axis. By using reversible counters, counting up may correspond to scan and counting down to slew back.

Adjustable pulse rates applied to the counters determine the scan rate. Adjusting to a preset count can determine the maximum angular excursion of the scan. Adjustment of relative scan rates on the two axes will determine the orientation of the resultant scan pattern.

Co-ordinate Converter

It is the function of the co-ordinate converter to transform digital command signals in LHA and DECL co-ordinated to the equivalent AZ-EL co-ordinates and vice versa.

One possible method of obtaining such co-ordinate conversion is shown on the attached sketch. Figure No. 3. A model of the unit is shown on photo No. ___

A two axis auto collimator attached to an equatorial (HD) mount is aimed at a plane mirror on an AZ-EL instrument mount. Similarly a two axis auto-collimator attached to the AZ-EL

mount is aimed at a plane mirror on the H-D mount. This unit is similar in construction to the dual unit on top of the tower.

The H-D and AZ-EL instrument mounts are so arranged mechanically as to permit continuous tracking of collimators and mirrors over a hemisphere.

Each axis of the two instrument mounts has attached to it a servo drive motor and a precision angle encoder capable of 0.001^{o} resolution. When a command signal in LHA and DECL co-ordinates is applied to the H-D instrument mount, instrument servos drive the two axes of the mount to such a position that the axis angles as measured by the encoders match the command.

As the H-D mount moves, the auto-collimator on the AZ-EL mount generates error signals which are fed into the servo drives on the two axes of the AZ-EL mount. The AZ-EL mount therefore, follows the H-D mount very closely and encoders on the mount axis provide digital angle signals in AZ-EL co-ordinates.

The auto collimators are capable of detecting angular errors of less than 1 second of arc and it is expected that corresponding accuracy of follow-up can be obtained.

The process of transforming from AZ-EL to LHA-DECL co-ordinates is exactly the same in the reverse sense.

Further study is now being made to provide quantative answers to the following problem areas encountered in this co-ordinate converter.

a. What is the effect of the apparent degradation in gain and response which occurs at the Zenith and polar regions?

b. What practical limitations exist in regard to providing instrument servos using the autocollimator error signal

considering that overall error should be limited to the region of 1-2 arc seconds at maximum operating velocity and acceleration of the antenna?

c..Other methods of co-ordinate conversions are being studied.

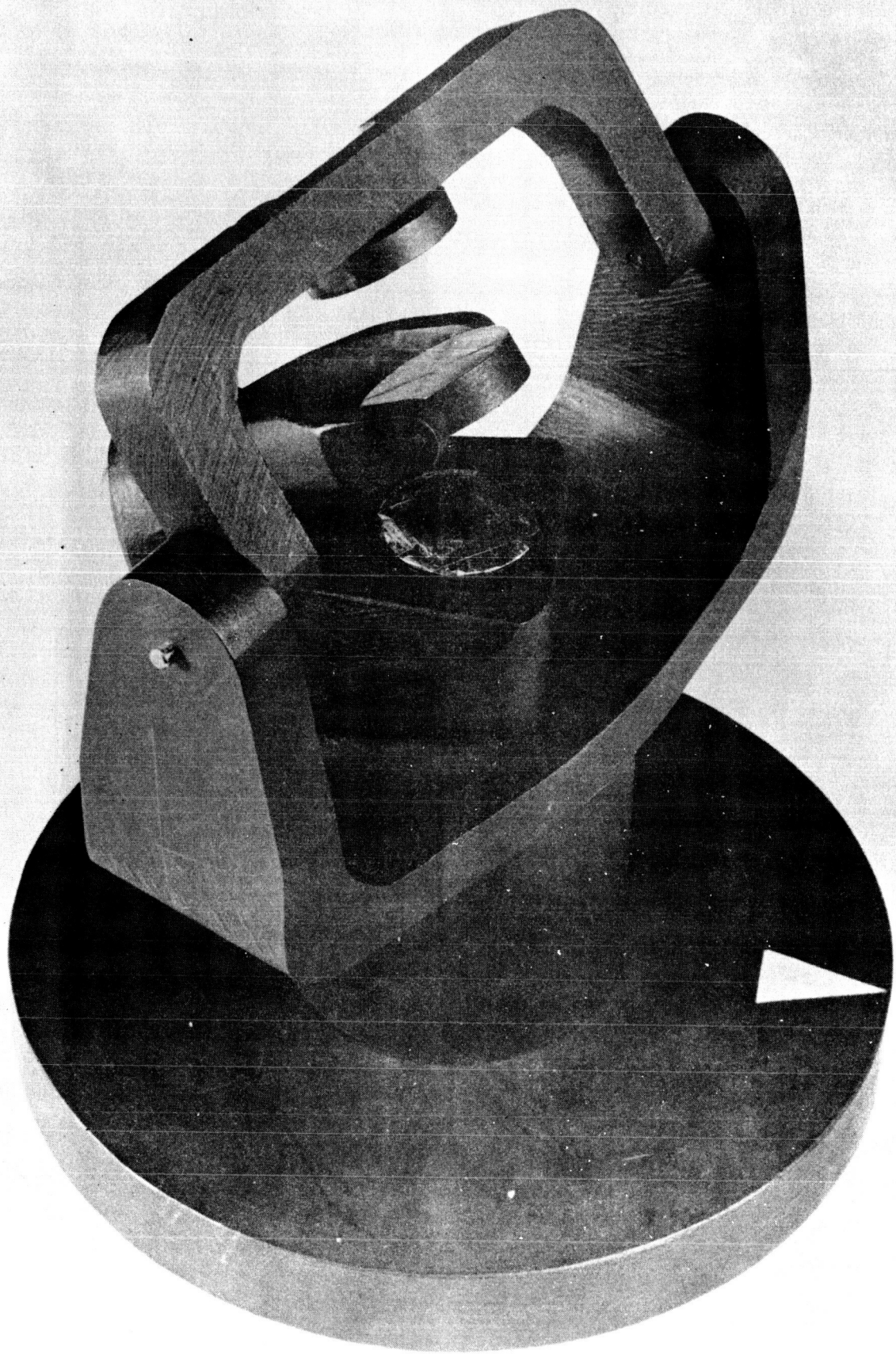

DRAWING
SH. NO. 1 OF 1 SUB -

REVERSIBLE COORDINATE CONVERTER

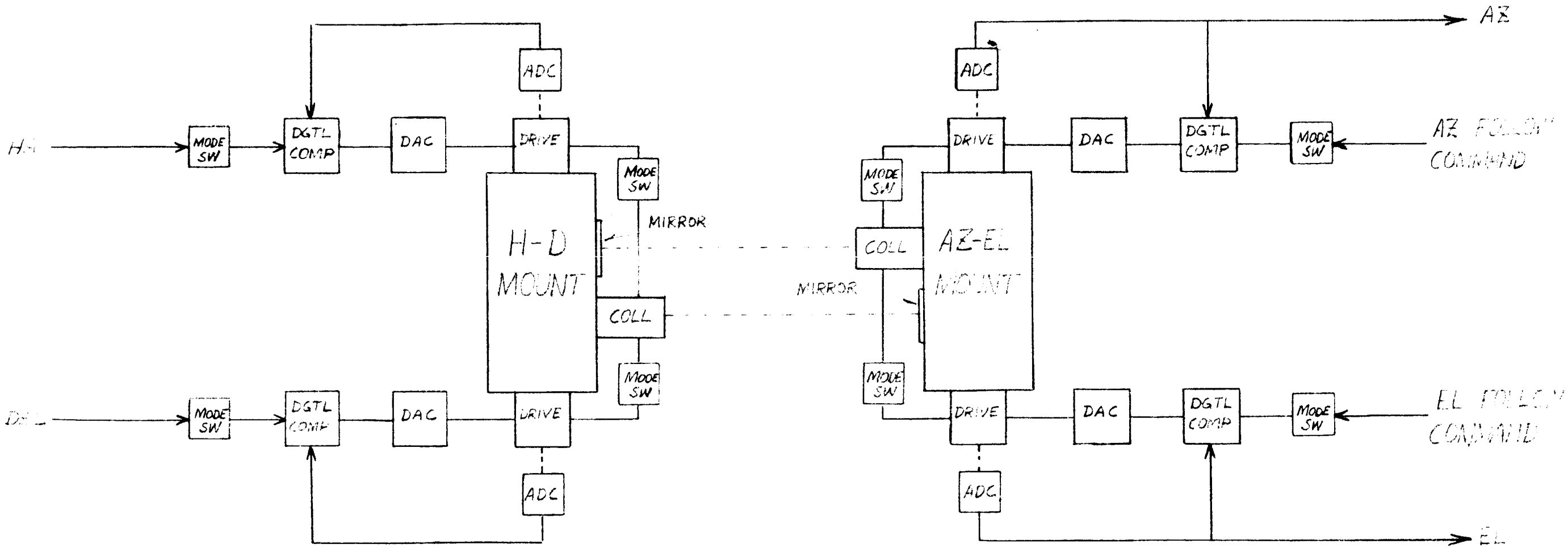

FIGURE NO. 3

WESTINGHOUSE ELECTRIC CORPORATION DIV. & PLANT LOCATION CONTROL DEPT BUFFALO DIVISIONS, BUFFALO, N.Y. U.S.A.

S.O.	APPLICATION	DRAFTSMAN	DATE	SHEETS	SHEET NO.	SUB	DRAWING
	J.P.L. 240' ANTENNA	[illegible]	3-[illegible]	1	1	-	

651